

University of Nevada, Reno

# **Development of Novel Proton Exchange Membranes**

A thesis submitted in partial fulfillment of the requirements

for the degree of Master of Science in

Chemical Engineering

by

Anasuya Adibhatla

Dr. Alan Fuchs / Thesis Advisor

December, 2009



University of Nevada, Reno  
Statewide • Worldwide

THE GRADUATE SCHOOL

We recommend that the thesis  
prepared under our supervision by

**ANASUYA ADIBHATLA**

entitled

**Development Of Novel Proton Exchange Membranes**

be accepted in partial fulfillment of the  
requirements for the degree of

**MASTER OF SCIENCE**

Dr. Alan Fuchs, Advisor

Dr. Vaidyanathan R. Subramanian, Committee Member

Dr. Cahit Evrensel, Graduate School Representative

Marsha H. Read, Ph. D., Associate Dean, Graduate School

December, 2009

## *ABSTRACT*

Proton Exchange Membrane (PEM) was developed for the use in PEM fuel cells.

Membranes were cast from various polymers and composite membranes were prepared with heteropoly acid (HPA) particles. Studies were conducted on various polymers and their possible application in fuel cells. Proton conductivity and other characterization techniques were carried out for the polymeric membranes.

For high temperature operation of fuel cells novel high temperature stable polymers were developed and characterized. It was found that the new polymer based systems increased the overall performance of the system. Single membrane tests were carried out to study the performance of the fuel cell.

## *ACKNOWLEDGEMENTS*

I would like to extend my gratitude towards my Master's thesis advisor Dr. Alan Fuchs for his able and fatherly guidance without which I would never have been able to finish this work. I thank him for his patience, his wealth of knowledge that he shared with me, for his optimism that inspired me and for his belief in me. I respect his diligence and his devotion towards work that has motivated me to work harder.

I am thankful to US Department of Energy, NREL, for financially supporting this project and giving me a chance to add a little to the research in this area.

I thank Dr. Cahit Eversel and Dr. Ravi Subramanian for serving as my committee and my lab mates and friends for their support.

I also appreciate Dr. Jeffery Lacombe for lending his tensile testing instrument without which it would have been difficult to reach my goal. Dr. Coronella has helped me use his instruments during the course of this project that helped me a lot and I appreciate him for this.

I would like to thank the staff at Lawrence Berkley National Labs, Dr. Svec and his group, for their association with us and for sharing their instruments with us for our characterization. My special thanks to Ms. Rebekah Woosley for testing my samples at the UNR agriculture Department.

Last, but not the least I would like to thank all the faculty and staff at the UNR Chemical Engineering and Material Science Department for their support and their guidance that has enabled me to finish my work in this department.

*DEDICATION*

To my parents, my family that has supported me and motivated me to pursue my goals  
and for their patience.

## *Table of Contents*

Abstract.....	i
Acknowledgement.....	ii, iii
Chapter I - Introduction .....	1
1.1 Background and motivation.....	1
1.2 Fuel cell- Types and application.....	1
1.2.1 PEMFC.....	2
1.2.2 Direct Methanol Fuel cells.....	4
1.2.3 Alkaline Fuel Cells.....	6
1.2.4 Phosphoric Acid Fuel Cell.....	7
1.2.5 Molten Carbonate Fuel Cells .....	8
1.2.6 Solid Oxide Fuel Cells.....	9
1.3 Proton Exchange Membrane Fuel Cells and its components .....	10
Chapter II - Literature Review	
2.1 Proton Transport .....	16
2.2 Composite Membranes and Nafion®.....	18
2.3 Inorganic Proton Conductors .....	20
2.4 Sulfonation .....	23
2.5 Novel polymers.....	25
Chapter III - Experiments and Characterization	
(A) Experimental .....	29
3.1 Materials.....	35
3.2 Synthesis of composite membrane .....	35
3.3 Synthesis of sulfonated polymer.....	35
3.3.1 Synthesis of sulfonated polymer.....	35
3.3.2 Sulfonation using acetyl sulfate .....	36
3.4 Sulfonation of polysulfone .....	37
3.5 Synthesis of polymer from monomers .....	38
3.5.1 Synthesis of polysulfone .....	38

3.5.2 Synthesis of polyether sulfone quinoxaline .....	40
(B) Characterization .....	44
3.6 Differential Scanning Calorimeter (DSC).....	44
3.7 Ion Exchange Capacity (IEC).....	47
3.8 Matrix Assisted Laser Desorption Ionization Mass Spectroscopy (MALDI-MS).....	49
3.9 Electrochemical Impedance spectroscopy (EIS).....	55
3.10 Gel Permeation Chromatography (GPC).....	59
3.11 Thermogravimetric Analyzer (TGA).....	60
3.12 Single Membrane Test Cell.....	62
Chapter IV - Results	
4.1 Preparation of composite membranes .....	66
4.2 Sulfonation conductivity and ion exchange measurements .....	67
4.3 MALDI –MS .....	82
4.4 Gel Permeation chromatography (GPC).....	94
4.5 Single Membrane fuel cell test.....	96
4.6 TGA .....	99
Conclusions .....	104
Future Work .....	106
References .....	110
Appendix .....	113



## *List of Tables*

Table 1: Components and roles in PEMFC .....	11
Table 2: Commercial PEM membranes .....	14
Table 3: List of chemicals used, source and chemical structure .....	30
Table 4: Specifications of Cam-Ten Tensile load testing device .....	32
Table 5: Details of Pyris DSC.....	45
Table 6: List of common MALDI-MS matrices [sigma Aldrich].....	53
Table 7: Summary of results .....	80
Table 8: Results obtained from GPC .....	96

## List of Figures

Figure 1: Schematic figure of PEMFC and zoomed view of MEA (From: <i>Fuel cells-Green Power</i> , information brochure by U.S. Dept. of Energy) .....	3
Figure 2: Picture of DMFC [5] .....	6
Figure 3 : Representation of PAFC [5].....	7
Figure 4: Molten Carbonate fuel cell [5] .....	8
Figure 5: Solid Oxide fuel cell [5] .....	9
Figure 6: Components of PEMFC [8].....	11
Figure 7: Keggin type structure of HPA [27] .....	20
Figure 8: Dawson Structure of HPA [27] .....	21
Figure 9: Sulfonation using acetyl sulfate [29].....	24
Figure 10: Untreated polysulfone and sulfonated PSf [33] .....	25
Figure 11: Synthesis of cross-linked polymer [39].....	27
Figure 12: Com-Ten tensile testing device [41] .....	32
Figure 13: Rectangular blocks attached to fabricate MEA .....	33
Figure 14: Com Ten tensile testing device used to make MEA .....	34

Figure 15: Sulfonation using chlorosulfonic acid [42] .....	36
Figure 16: Sulfonation of PES acetyl sulfate [43] .....	37
Figure 17: Synthesis of polysulfone [48].....	39
Figure 18: Synthesis of polyether sulfone quinoxaline.....	41
Figure 19: Synthesis of polyether sulfone quinoxaline Type II.....	42
Figure 20: Reactor setup for polymer synthesis .....	43
Figure 21: Differential Scanning Calorimeter (DSC) [43] .....	46
Figure 22: Conductivity cell for EIS measurements [47] .....	55
Figure 23: EIS potentiostat[48].....	56
Figure 24: Typical EIS plot [48].....	57
Figure 25: Electric circuit representation of Nyquist plot [48].....	58
Figure 26: Representation of TGA [50].....	60
Figure 27: Scribner fuel cell testing stand 850e.....	61
Figure 28: A single membrane fuel cell.....	63
Figure 29: Fuel cell opened and monopolar plate view .....	64
Figure 30: Losses in a typical polarization plot [51]. .....	65

Figure 31: Nyquist plot of pure Kapton.....	68
Figure 32: EIS plot of 3.4 % HPA and Kapton composite membrane .....	69
Figure 33:Nquist plot of PES- 70wt% HPMo .....	71
Figure 34: Picture of SPES- 50% SiWA.....	72
Figure 35: EIS plot of PES- 50% SiWA.....	73
Figure 36: Nyquist plot of Sulfonated PES (SPES).....	74
Figure 37: Nyquist plot of SPES with 20mL CSA .....	75
Figure 38: EIS plot of 40% PBI-PES- 60wt% SiWA.....	77
Figure 39: EIS plot of poly ether sulfone quinoxaline.....	78
Figure 40: EIS plot of acid doped polyether sulfone quinoxaline .....	78
Figure 41: EIS plot of 20% PESQ- SPEEK-50% SiWA .....	80
Figure 42: Spectra of dithranol matrix.....	82
Figure 43: Mass spectra of HABA matrix .....	83
Figure 44: : PSf- tested with dithranol spectra.....	84
Figure 45: : PSf - $\alpha$ - cyannocinnamic acid spectra .....	85
Figure 46: Psf- $\alpha$ -cinnamic acid spectra .....	86

Figure 47: Chemical structure of PSf [13].....	87
Figure 48: Linear mode spectra of commercial PSf .....	87
Figure 49: Synthesis of polyether sulfone quinoxaline type I .....	88
Figure 50: Mass spectra of PESQ Type I.....	89
Figure 51: Synthesis of polyether sulfone quinoxaline type II.....	90
Figure 52: Polyquinoxaline co-polymer in dithranol matrix spectra .....	91
Figure 53: Synthesis of polyether sulfone quinoxaline type III.....	92
Figure 54: Mass spectra of polyether sulfone quinoxaline type III .....	93
Figure 55: GPC spectra for commercial polysulfonee.....	94
Figure 56: GPC spectra of polyether sulfone quinoxaline.....	95
Figure 57: A sample MEA.....	96
Figure 58: Polarization curve obtained from SPEEK- 50% PWA membrane at 50 <sup>0</sup> C.....	97
Figure 59: Polarization curve of 40% PESQ- 38% SPEEK and 42% HPW .....	98
Figure 60: TGA of pure PES .....	99
Figure 61: TGA plot of SPES .....	100
Figure 62: TGA plot of composite PES - 50wt % SiWA .....	101

Figure 63: TGA plot obtained for SPES-50wt% HPA .....	102
Figure 64: TGA of polyether sulfone quinoxaline type I .....	103
Figure 65: Sulfonated polyether sulfone quinoxaline.....	107
Figure 66: Sulfonated polysulfone.....	108

## *CHAPTER I*

### *INTRODUCTION*

#### *1.1 GENERAL BACKGROUND AND MOTIVATION*

A fuel cell is an electrochemical device that converts the chemical energy of hydrogen and oxygen to electrical and heat energies. These were first discovered by William Grove in 1850's. In recent years, membranes and the device have seen many improvements. Fuel cells are now being developed now for automobile applications, for portable devices and residential power.

Current commercial membranes are faced with few drawbacks of lower performance at higher temperature. In this thesis, novel composite membranes for fuel cells have been developed. Composite heteropoly acid membranes with novel polymers have been synthesized which provide advantages for fuel cells membranes.

#### *1.2 FUEL CELLS- TYPES AND APPLICATIONS*

Electrical energy from renewable resources involved the use of fuel cells for energy storage. Hydrogen is an excellent energy carrier because it can be transferred over long distances efficiently.

There are various types of fuel cells classified by operating temperature. They are also classified on the basis of the fuel used, the ions transferred and the electrolyte used. Based on these classifications, the reactions that take place in the fuel cell differ. As a

result, this classification affects the application of specific fuel cell. Each fuel cell has its own advantages and limitations. Various types of fuel cells are described below.

### 1.2.1 **Proton Exchange Membrane (PEM) Fuel Cell:**

The development of proton exchange membranes was the focus of this research.. Proton Exchange Membrane fuel cells use an ionomeric membrane to act as an electrolyte between the anode and cathode. A membrane replaces the liquid electrolyte in a conventional battery. PEM fuel cells use a solid membrane with porous carbon electrodes<sup>[1]</sup>. The main fuel for this fuel cell is hydrogen and oxygen. Air can also be used as a fuel for this fuel cell. Electrochemical reactions take place on the anode and cathode of the fuel cell to generate protons and water.



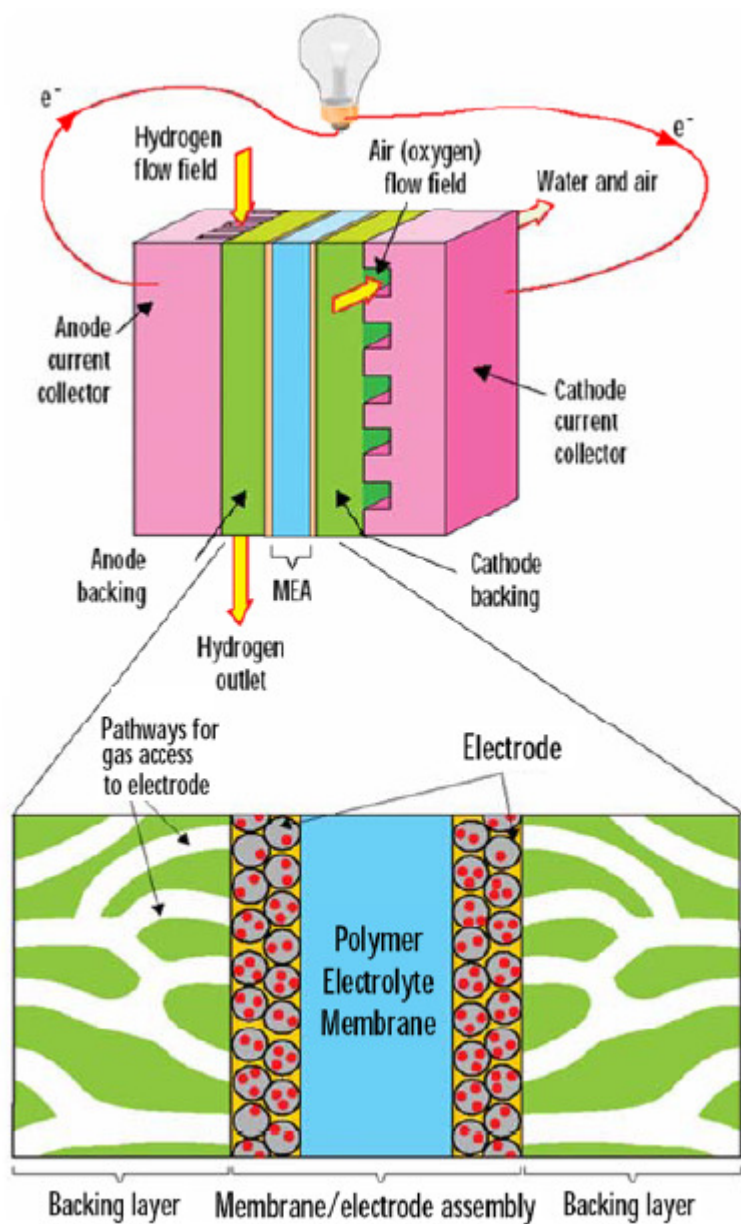


Figure 1: Schematic figure of PEMFC and zoomed view of MEA (From: *Fuel cells- Green Power*, information brochure by U.S. Dept. of Energy)

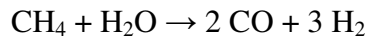
The electrode for this fuel cell is platinum and ruthenium metals supported on carbon. This mixture is either coated or pressed on the membrane on either side to result in a Membrane Electrode Assembly (MEA). The other parts of the MEA include a gas diffusion layer (GDL) and a binder which will be discussed later.

A general diagram of the PEMFC is shown in **Figure 1**. The PEMFC operate at relatively low temperatures. The usual range that these operate in is 60-90<sup>0</sup> C. This low temperature allows a quick start-up and better durability for the overall system<sup>[3]</sup>. However, the use of platinum increases the cost of the fuel cell. The catalyst is also highly sensitive to carbon monoxide, which is present in the hydrogen. The carbon monoxide gets adsorbed on the surface of catalyst, reducing its overall capacity. Hence, the catalyst needs to be replaced periodically, increasing financial aspect of the fuel cell maintenance. Research is being done on ways to reduce this catalyst poisoning by either looking at other possible catalysts or by changing the operating conditions.

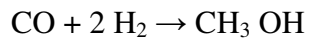
### **1.2.2 Direct Methanol Fuel Cells:**

While most of the fuel cells are powered by hydrogen, the DMFCs are powered by methanol. Methanol, also called wood alcohol, is the lowest molecular weight compound in the class of alcohols. It can be synthesized from methane. Its utilizes a two step reaction, one of them produces synthesis gas from methane and the second step includes reaction of the synthesis gas under certain conditions to result in methanol.

At moderate pressures of about 4 MPa and high temperature around 850<sup>0</sup> C, the methane reacts with steam to produce synthesis gas, syn gas [4].

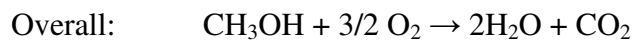
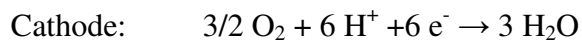
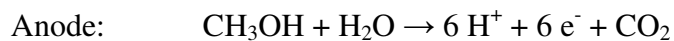


In the second step, this synthesis gas is reacted on appropriate catalyst by the following reaction to result in methanol <sup>[4]</sup>.



This methanol can either be used directly or can be reformed in the fuel cell before use.

Methanol is fed directly to the anode. The following reactions take place in a DMFC <sup>[4]</sup>:



The DMFCs do not have significant storage problems since methanol is safe and easy to handle and transport. DMFCs are well suited to power portable devices like hand held devices and laptops.

### 1.2.3 Alkaline Fuel Cells:

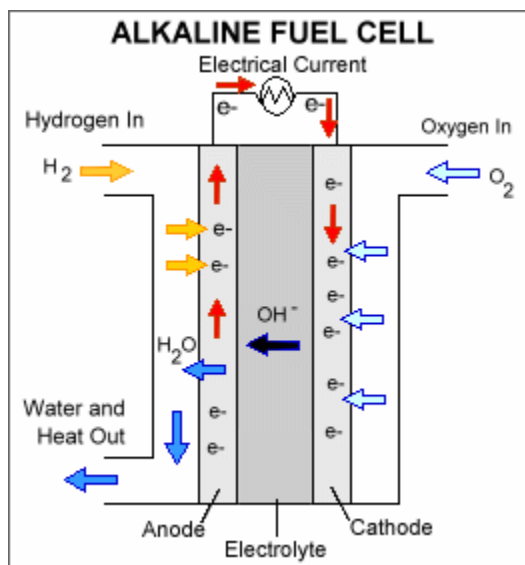


Figure 2: Picture of DMFC [5]

Alkaline fuel cells were one of the first to be used and found their application in the US spacecrafts. It uses a dilute solution of potassium hydroxide in water as electrolyte. Typically, an alkaline fuel cell operates from 100<sup>0</sup> C to 250<sup>0</sup> C. They are highly susceptible to poisoning due to carbon dioxide; hence, the feed fuel has to be highly pure when it is to be used in the fuel cells [5].

### 1.2.4 Phosphoric acid fuel cells:

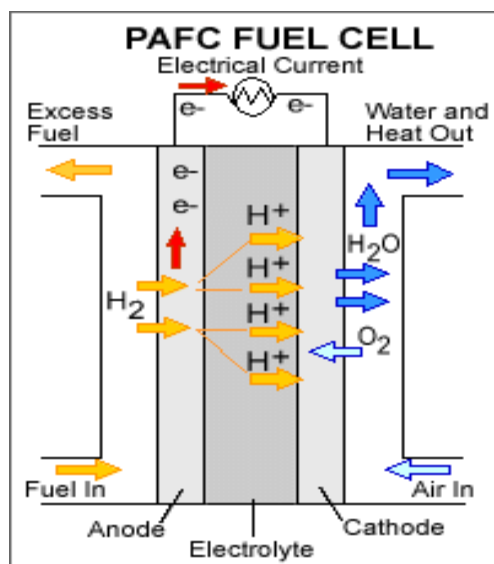


Figure 3 : Representation of PAFC [5].

Phosphoric acid (PA) fuel cells are operated with phosphoric acid as electrolyte. The acid is bound in carbon- matrix and carbon electrodes. It is the one of the first fuel cells and is the first to be used commercially. This is mainly used as a power source for stationary applications. But, a few PA fuel cells have also been used to power buses. PAFCs are tolerant of impurities in fossil fuels. They are 85% efficient when both electricity and heat are being generated. When only electricity is generated, their efficiency reduces to 37- 42%<sup>[5]</sup>. These are heavy and large as compared few other fuel cells like PEMFC and hence are also expensive. They also use platinum as catalyst adding more to the cost.

### 1.2.5 Molten Carbonate Fuel Cells:

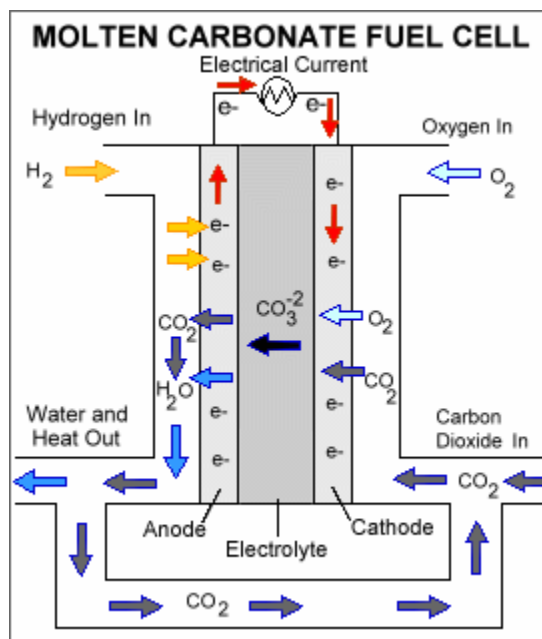


Figure 4: Molten Carbonate fuel cell [5]

Molten carbonate (MC) fuel cells presently work for coal and natural gas powered power generators. They are also being used in military operations. They are high temperature fuel cells that use a molten carbonate salt mixture suspended in porous ceramic as an electrolyte. Because of the high operating temperature, precious metal catalysts are used and they have lower risk of poisoning. MCFCs can reach up to 60% efficiency and when the waste heat is captured and reused, the efficiency is as high as 85%. However, the primary disadvantage of MCFCs is their durability<sup>[6]</sup>. At that high temperature at which the fuel cell operates, the corrosive electrolyte accelerates corrosion and parts break down. Research is being done to reduce the corrosion by using alternate electrolyte or corrosion resistant components.

### 1.2.6 Solid oxide fuel cells:

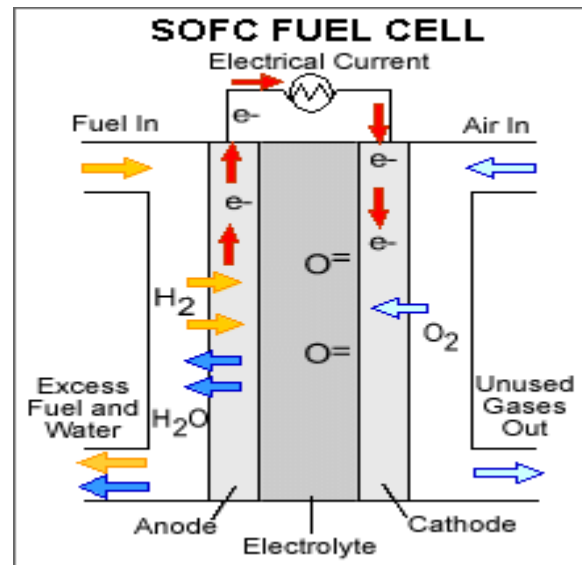
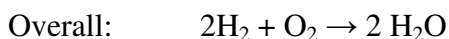
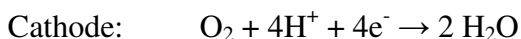


Figure 5: Solid Oxide fuel cell [5]

SOFCs use a hard, non-porous ceramic compound as electrolyte. SOFCs are nearly 50-60% efficient in converting the fuel to electricity. These operate at very high temperature of nearly 1000<sup>0</sup>C [5]. This removes the need for a precious catalyst and thereby reduces the cost of the overall unit. SOFCs are also sulfur resistant, can tolerate higher sulfur than any other fuel cell. However, the high temperature operation also brings a disadvantage of slow start –up of the device. It also needs sufficient thermal shielding to retain heat which adds cost and another factor for safety concern. Research is being conducted now to lower the operating temperature so that these can be use in domestic purposes.

### 1.3 PROTON EXCHANGE MEMBRANE FUEL CELLS AND ITS COMPONENTS

The following reactions take place on the anode and the cathode of the fuel cell <sup>[7]</sup>.



The major advantages of using PEMFC are its scalability and its friendliness towards environment. It can be seen in the overall cell reaction that water is the only byproduct. The fuel is hydrogen on one side and oxygen on the other side. The hydrogen enters on the anode and comes in contact with platinum catalyst on the anode. It splits into proton and electrons. The proton diffuses into the membrane (electrolyte) to the other side, the cathode. Oxygen combines with the electrons that travel through the outer circuit and the protons to form water on the cathode.

For a fuel cell assembly, there are many parts that combine together to make it a cell and to carry out the reactions. These are shown in **Figure 6**. This Figure shows various parts that make a fuel cell device in a sequential manner in which they are assembled.



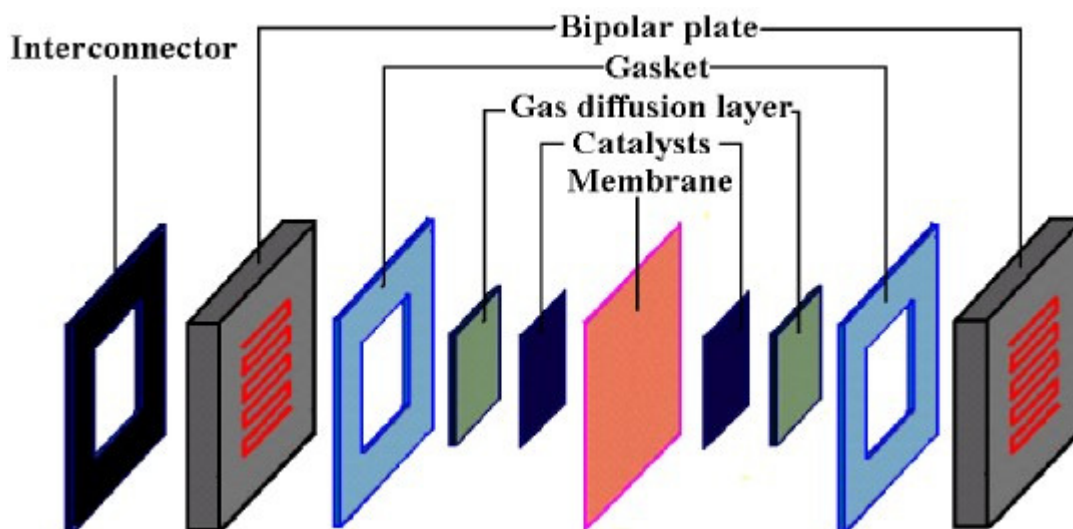


Figure 6: Components of PEMFC [8]

A PEMFC consists of the following parts and their roles are mentioned below in the **Table 1**.

Table 1: Components and roles in PEMFC

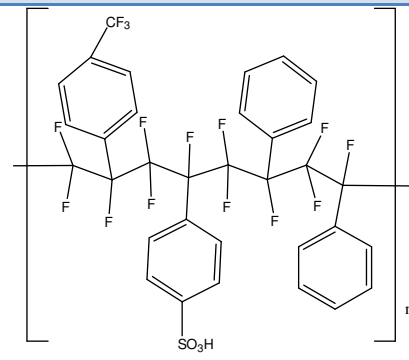
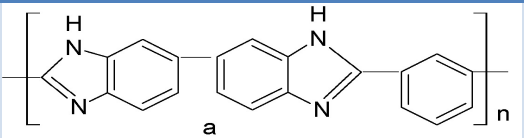
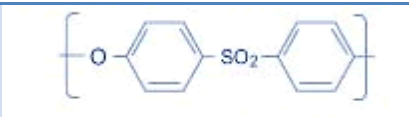
Parts	Material	Contribution in the fuel cell
<b>End plates</b>	Copper ( plated with gold)	These define the fuel cell and hold all the components between them. They are plated with gold to avoid oxidation.
<b>Interconnector</b>	Copper (plated with gold)	In a fuel cell as a stack, this acts as a connector between two adjacent fuel cells
<b>Bipolar plates</b>	Graphite	Bipolar plates are the one of the most important

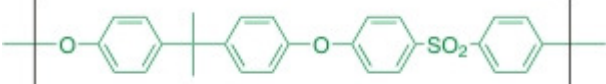
		components in the fuel cells. It has flow channels of a definite geometry engraved in it. It is the carrier of the fuel in the cell. The gas flows in the channels and reacts on the catalyst. On the cathode, this also acts as a carrier for the water that is being formed. In a stack of fuel cell, flow channels are carved on either side.
<b>Gas diffusion layer (GDL)</b>	Carbon cloth or carbon paper	This provides a layer of gas distribution uniformly over the catalyst area. It is a highly porous cloth through which the gases diffuse through and spread over the catalyst. It also provides a structural layer of stability for the membrane electrode assembly (MEA).
<b>Gasket</b>	Silicone polymer	It is a window frame shaped silicone gasket that is placed between the bipolar plates and the MEA. It acts as a support layer for the MEA from being destroyed by the stress of the entire assembly.
<b>Catalyst</b>	Platinum metal	Platinum is used as catalyst on

		<p>whose surface hydrogen and oxygen react. It is either sprayed or coated on the membrane surface with a binder (polymer solution) and carbon Vulcan. It is also mixed with metals like Ruthenium to reduce the cost. Generally <math>1\text{g/cm}^2</math> of catalyst is added to each side of the membrane.</p>
<p><b>Proton Exchange Membrane</b></p>	<p>Polymer (aliphatic or aromatic)</p>	<p>This is electrolyte of the fuel cell. It is fabricated from various types of polymer solutions. Most widely used polymer membrane is Nafion® manufactured by DuPont. Few other polymers are available commercially manufactured by various companies. Most of them are aliphatic in nature and are fluorinated.</p>

The **Table 2** below lists the various types of commercially available PEMs and their structures.

Table 2: Commercial PEM membranes

Polymer	Type	Structure
<b>Nafion®</b> <b>DuPont</b> <sup>[9]</sup>	Per fluorinated	$\left[ \begin{array}{c} \text{F}_2 \quad \text{F}_2 \\   \quad   \\ \text{---C---C---} \\   \quad   \\ \text{F}_2 \quad \text{F} \end{array} \right]_m \left[ \begin{array}{c} \text{F}_2 \quad \text{F} \\   \quad   \\ \text{---C---C---} \\   \quad   \\ \text{F}_2 \quad \text{F} \end{array} \right]_n$ $\left[ \begin{array}{c} \text{O---C---C---} \\   \quad   \\ \text{F}_2 \quad \text{F} \\ \text{CF}_3 \end{array} \right]_x \text{O---} \left[ \begin{array}{c} \text{F}_2 \\   \\ \text{---C---} \\   \\ \text{F}_2 \end{array} \right]_y \text{---SO}_3\text{H}$
<b>BAM-3G</b> <b>3M</b> <sup>[9]</sup>	Per fluorinated	
<b>Hyflon</b> <sup>[10]</sup>	Fluorinated	$\text{---}(\text{CF}_2\text{---CF})_x\text{---}(\text{CF}_2\text{---CF}_2)_n\text{---}$ $\quad \quad \quad  $ $\quad \quad \quad \text{OCF}_2\text{CF}_2\text{SO}_2\text{F}$
<b>Polybenzimidazole</b> <b>(PBI) Celanese</b> <sup>[11]</sup>	Aromatic	
<b>Polyvinyl</b> <b>difluoride</b> <b>(PVDF)</b> <sup>[12]</sup>		$\left[ \begin{array}{c} \text{F} \quad \text{H} \\   \quad   \\ \text{---C---C---} \\   \quad   \\ \text{F} \quad \text{H} \end{array} \right]_n$ <p>PVDF</p>
<b>Polyether</b> <b>sulfone</b> <sup>[13]</sup>	Aromatic	

<b>Polysulfone</b> <sup>[13]</sup>	Aromatic	
------------------------------------	----------	--

## *CHAPTER II*

### *LITERATURE REVIEW*

Vast research is being done in the field of PEMFC, including development of membranes, designing the fuel cells, optimization of catalyst and the electrochemical aspects of reactions. This literature review emphasizes mainly the membrane development, sulfonation and proton conductivity improvement. This literature review also includes the uses and other aspects of inorganic proton conductors and their applications in various parts of the fuel cells. Apart from these, some parts of the literature review will also address the development of new polymers for PEM applications and their properties.

#### **2.1 PROTON TRANSPORT**

A polymer in PEMFC takes place of a liquid electrolyte, making the fuel cell easier to handle and portable. A proton conducting membranes are applied to electrochemical sensors and electrochromic devices. Proton conductivity of a membrane relies mostly on the water mobility through the membrane [14].

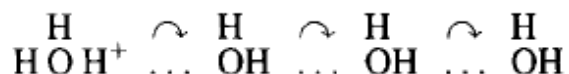
The importance of water transport and mobility is directly associated to the proton conductivity. The inherent protonic charge carriers are solvated by mainly water, oxo-acid anions (e.g., in  $\text{CsHSO}_4$ ) or oxo-acids like phosphoric acid, heterocycles or oxide ions. These help in proton conduction by forming a protonic charge over them. In some cases they also generate protonic charge by self dissociation e.g., phosphoric acid and

imidazole group to some extent [15]. This is achieved by soaking the membranes in Bronsted Acid or base.

For better proton conduction, presence of a strong hydrogen bond is also required. But, for long range proton conduction, breakage and reformation of bonds take place. This is called vehicular transport for proton conduction. Another type of proton transport mechanism occurs that is called Grotthus mechanism. In this type of transport, the proton attached temporarily to a negative charged entity in the polymer chain and then hops to another negative ion site and so forth. This way proton propagates through the membrane. This type of phenomena is observed when sulfonic acid groups exist in the polymer chain.

In a study of basic biopolymer as proton exchange membrane for fuel cell systems by Salgado J.R , where they tested biopolymer (chitosan- oxide compoubs) as prospective fuel cell membranes mentioned about the Grotthus mechanism on the oxide. The conduction takes place takes place between adjacent  $\text{OH}^-$  and  $\text{O}_2^-$  groups rather than diffusion [16]. This type of transport can be slower depending in the distance that the proton has to travel by this mechanism as compared to vehicular.

Proton mobility in water is abnormally high <sup>[1]</sup>. At room temperature this is found to be about five times that of potassium ion <sup>[2]</sup>. This is attributed to Grotthus mechanism of transport. One possible representation of this is given by Bernel and Fowler <sup>[4]</sup>, who suggested that the proton hops from a  $\text{H}_3\text{O}^+$  to a freely rotating nearest  $\text{H}_2\text{O}$ . Its pictorial representation can be given as:



It is also predicted that proton mobility increases with the size of hydrogen-bonded cluster.

## **2.2 COMPOSITE MEMBRANES AND NAFION**

Nafion® is a perfluorosulfonic acid polymer that is structurally proton conductive. Nafion consists of three regions; a) polytetrafluoroethylene (PTFE) b) side chains of –O--CF<sub>2</sub>--CF--O--CF<sub>2</sub>--CF<sub>2</sub>-- which helps in connecting the molecular backbone to the third region of the Nafion® membrane, that is, c) ion clusters consisting of sulfonic acid ions. When the membrane is hydrated, the hydrogen ions attach to the water molecule and move to sulfonic acid groups <sup>[17]</sup>. Thus, the hydrophobic PTFE backbone structure provides structural stability to Nafion® and to other PFSA membranes. The fact that the fluorine atom is connected to the same carbon atom as the sulfonic acid group is attached to, makes the sulfonic acid act like super acid and boosts the conductivity by a lot. Because of the hydrophobic and hydrophilic interactions between PTFE and sulfonic acid groups in PFSA membranes, the proton conduction increases. When the membrane is hydrated, the phase separation increases and the hydrophobic part increase the mechanical stability even when the water is present. The hydrophilic part increases the proton conductivity further when hydrated.

It was observed by <sup>[17]</sup> that in composite membranes, a hybrid transport occurs because of the fact the inorganic component helps with the Grotthus transport.



[18] carried out DMFC tests with Nafion® membranes and compared it to composite membranes made from Nafion® and silica. When acidic silica was added to the polymer, the proton conductivity was observed to increase. Methanol was also observed to decrease probably because of the fact that the methanol flow was blocked by the inorganic particles.

Nafion® was found to exhibit low conductivity beyond 80°C. Composite membranes have been synthesized using sulfated Zirconia (SZrO<sub>2</sub>) that has been proved to increase the proton conductivity of Nafion®. Some of the membranes prepared with this treated zirconia have showed an increase in the performance as well. Hara and Miyayama determined the conductivity of the sulfated zirconia to be about  $2.1 \times 10^{-1}$  S/cm. The IEC was observed to increase as the amount of S-ZrO<sub>2</sub> added increased<sup>[19]</sup>. However, this membrane was tested for IEC by soaking it in NaCl but it might be possible that ZrO<sub>2</sub> may be washed into water increasing the IEC and hence increasing the IEC of the sample tested<sup>[20]</sup>. Similar results were obtained by<sup>[21]</sup> where they prepared Nafion®- ZrO<sub>2</sub> composite membranes and observed that the membranes were stable even over 200°C.

Tests were conducted on Nafion®- Polybenzimidazole (PBI) composite membrane<sup>[20]</sup>. This membrane was acid doped in 85% phosphoric acid. These membranes were tested for conductivity and in fuel cell for its performance. It was found that the membrane performance was increased by a 55% during the tests<sup>[22]</sup>. Nafion® - silicon dioxide and PWA were synthesized as a composite membrane by<sup>[23]</sup>. This was done in order to improve the performance of the Nafion® based membranes.

### **2.3 Inorganic Proton Conductors:**

Inorganic proton conductors are added to a polymer to make a composite membrane to enhance the properties of the polymer to be used as a PEM. Some of the common IPCs are hygroscopic oxides like silica,  $\text{TiO}_2$ ,  $\text{ZrO}_2$  and  $\text{Al}_2\text{O}_3$ , Clays like “Fuller’s earth”, Zeolites, mineral acids like  $\text{HCl}$ ,  $\text{H}_2\text{SO}_4$ , etc., hydrogen cesium sulfates and phosphates, heteropolyacids, etc.<sup>[24]</sup>.

Heteropolyacids belong to a class of inorganic proton conductors, called polyoxometallates. These are clusters of tungsten, molybdenum or vanadium and uranium oxides. These possess a central atom in a cage like structure made by tungsten or molybdenum, oxygen octahedra. This is shown in **Figure 7** below.

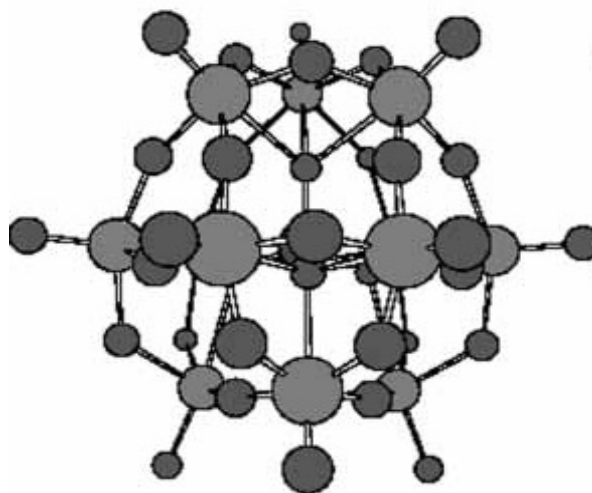


**Figure 7: Keggin type structure of HPA [27]**

This is a common representation of Keggin type of structure that heteropolyacids, like  $\text{H}_3\text{PW}_{12}\text{O}_{40}$ , exhibit. The Dawson structure that is shown by HPAs like  $\text{H}_6\text{P}_2\text{W}_{18}\text{O}_{62}$  is shown in **Figure 8**. It is a common ball and stick representation of atoms to show a chemical structure.

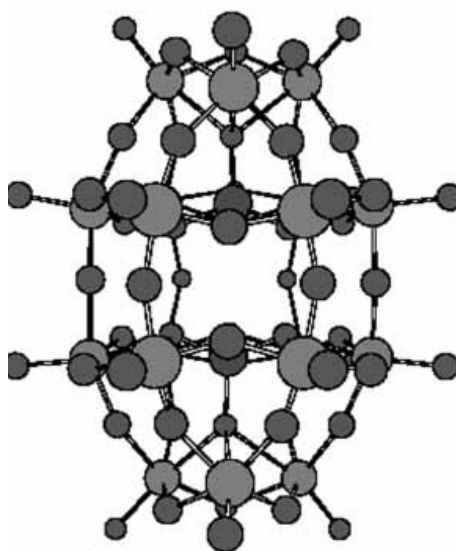


**Figure 8: Dawson Structure of HPA [27]**

There are more than these common structures that occur for HPAs. These are found to have very high proton conductivity at room temperature,  $> 0.1 \text{ S/cm}$  and the bonds are thermally stable  $> 200^\circ\text{C}$  [27].

Nafion® was made as a composite membrane with types of heteropolyacids. Additives like phosphotungstic acid, silicotungstic acid, phosphomolybdic acid and silicomolybdic acid were investigated and the membrane performance was tested between  $80^\circ\text{C}$  to

120<sup>0</sup>C. The tests were carried out at various humidity levels, allowing a simple mechanism to describe the proton transport for this system. According to them, transport of proton takes place in these composite membranes due to phase separation that occurs in Nafion®. Vehicular transport takes place, with the vehicle as water molecules that diffuse through the membrane. They proposed that for proton transport to occur, there are two types of resistances that occur,  $R_d$  (resistance to vehicular transport) and  $R_h$  (resistance to hopping transport). Thus, for a membrane at 100% humidity, the resistance is low, increasing the overall conductivity. The role of HPA in this is found to decrease the  $R_h$  value at high temperatures and low humidity. It is also suggested that the size of additives, when in nanometer levels enhance the conductivity further <sup>[25]</sup>.

The published works by John A. Turner and Andrew M. Herring were carefully studied during the course of this literature review. Their work has been briefly mentioned in this section. Their work is a major contributor to the HPA research.

Herring. A.M. et al, have studied heteropoly acids as a possible electrocatalyst material for fuel cells. They used HPA based on vanadium and molybdenum as a catalyst material for the oxidation and reduction respectively. Very small, but stable loadings of heteropoly acids  $[\text{PMo}_{(12-n)}\text{V}_n\text{O}_{40}]^{(3+2)-}$  ( $n= 0-3$ ) were used. It was observed that these materials could also be used as electrocatalysts when large quantities can be added to the gas diffusion layer support. They observed an increase in the current at potentials lower than the anode. It was observed that there exist significant activation losses at the anode. For these catalysts the losses due to the anode overpotential are actually lower than the redox losses <sup>[26]</sup>.

Thin pellets of HPA and composite membranes of 1:1 (w/w) of HPA and polyvinylidenedifluoride- hexafluoropropylene have been investigated by [27]. They proved in their work that the high proton conductivities of HPA can be used to enhance the proton conductivity of the PEM without any external humidification. HP<sub>2</sub>W<sub>18</sub> showed moderate activity at 120<sup>0</sup>C with a little humidification. However, their membranes suffered from issues such as porosity.

#### **2.4 Sulfonation:**

Sulfonation is a process of enhancing the proton conductivity of a polymer by attaching covalently bond sulfonic acid group, HSO<sub>4</sub><sup>-</sup> to the chain. Noshay and Robeson developed a mild sulfonation method for the commercial bisphenol-A based poly (ether sulfone). They carried out the sulfonation using a combination of 2:1 of sulfur trioxide and triethyl phosphate complex. The resulting polymer was neutralized by sodium methoxide [28].

The sulfonation of poly (ether imide) was carried out by using acetyl sulfate as a sulfonating agent. Acetic anhydride was reacted with sulfuric acid resulting in acetyl sulfate and acetic acid. When this acetyl sulfate was reacted with the polymer, it resulted in sulfonated poly (ether imide). The mechanism proposed by them is given in **Figure 9**:

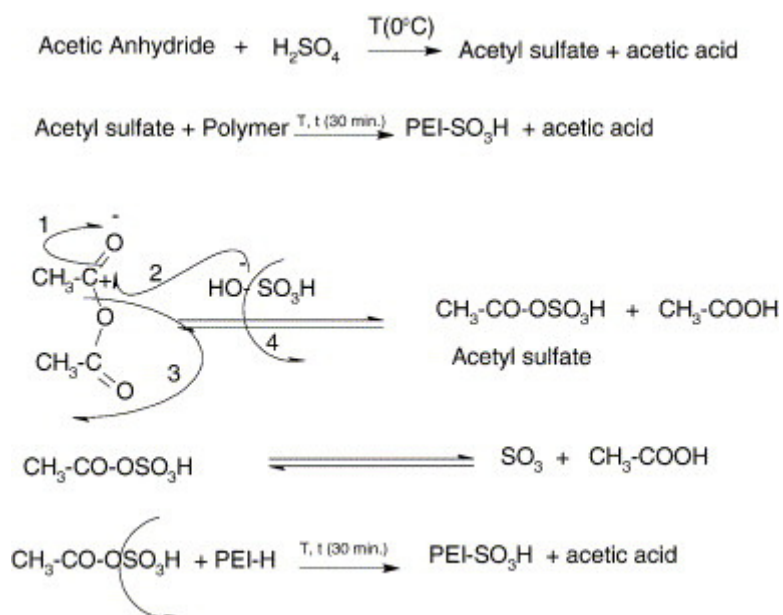


**Figure 9: Sulfonation using acetyl sulfate [29]**

They show that the sulfonation reaction is reversible in nature, hence, care should be taken while reaction is carried out to make sure that the reactions conditions are proper [29].

There are three major sulfonating agents; chlorosulfonic acid, oleum and  $\text{SO}_3$  and its complexes. Sulfonation of polyether sulfone was performed by chlorosulfonic acid as a sulfonating agent. Degree of sulfonation and IEC was determined for the sulfonated polymer. HNMR confirmed that the polyether sulfone was sulfonated [30]. PEEK and PES were sulfonated by using sulfonating agent as sulfuric acid and fuming sulfuric acid [31]. High degrees of sulfonation of PES were achieved when sulfur trioxide was used as sulfonating agent. They found that SPEEK was easier to sulfonate and these could be used for water electrolysis. R. Nolte et al sulfonated polyether sulfone and polysulfone by using chlorosulfonic acid. Polymer was dissolved in dichloroethane before adding

chlorosulfonic acid. Another process was suggested to sulfonate polymers based on sulfur trioxide<sup>[32]</sup>. Tabulation of various methods of sulfonation of polysulfone and also stating the advantages and disadvantages of each sulfonating agent was also performed<sup>[33]</sup>.

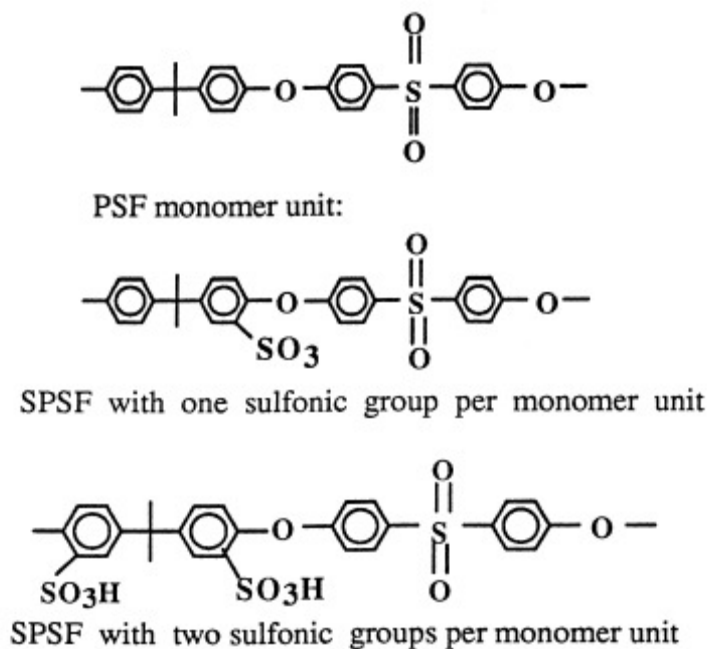


Figure 10: Untreated polysulfone and sulfonated PSf [33]

## 2.5 Novel polymers:

Novel polymers are being developed for use as PEM. The main factors that give impetus towards development of the novel polymers are the high temperature stability, better proton conduction and lower humidity.

High temperature operation under anhydrous conditions of fuel cell has many advantages. At high temperatures, the kinetics at the catalyst is faster as compared to lower temperatures. Carbon monoxide tolerance over platinum catalyst improves at high

temperatures. Higher energy is obtained and need of external humidification is eliminated [34].

Proton conducting membranes were prepared based on blends with PBI by [35]. PBI was blended with a novel polymer based on polyether sulfone containing pyridine unit. The synthesis was based on polycondensation reaction of polymerization. Copolymers were prepared based on polyether sulfone and pyridine. When this polymer was blended with PBI resulted in better glass transition and mechanical stability. These membranes were acid doped and tested at high temperature for conductivity. The conductivities were in the order of  $10^{-2}$  S/cm.

Similar work was carried out by N. Gourdoupi et al who worked on a similar polymer and performed the characterization of the polymer. They studied a similar reaction with the change in the monomers and cast membranes from the polymer. These membranes were acid doped too and were tested for their proton conductivity at high temperatures. Conductivities in the order of  $10^{-2}$  S/cm were observed for doping levels of 200 wt% [36].

Novel biphenol- based wholly aromatic poly (arylene ether sulfone) contains sulfonate groups. This polymer is synthesized by following the polycondensation reaction scheme. They have proposed this polymer as a candidate for PEMs. Potassium carbonate was used as a base catalyst in the reaction that acts as a base to the formation of HF during the reaction and also catalyses the reaction. The films obtained were found to have good proton conductivity and good mechanical stability [37].



A new class of monomers, bis(phthalazinone)s were synthesized and were reacted with a variety of aryl halides to obtain a polycondensation polymer. The polymer was found to have good Tg after they were copolymerized with polyether sulfones. The polymers were all found to be stable even over 400<sup>0</sup>C [38].

Also, it was interesting to find that novel crosslinked sulfonated polyether sulfones were synthesized from allyl terminated telechelic sulfones polymers with a bisazide. The reaction scheme is shown in the **Figure 11** below:

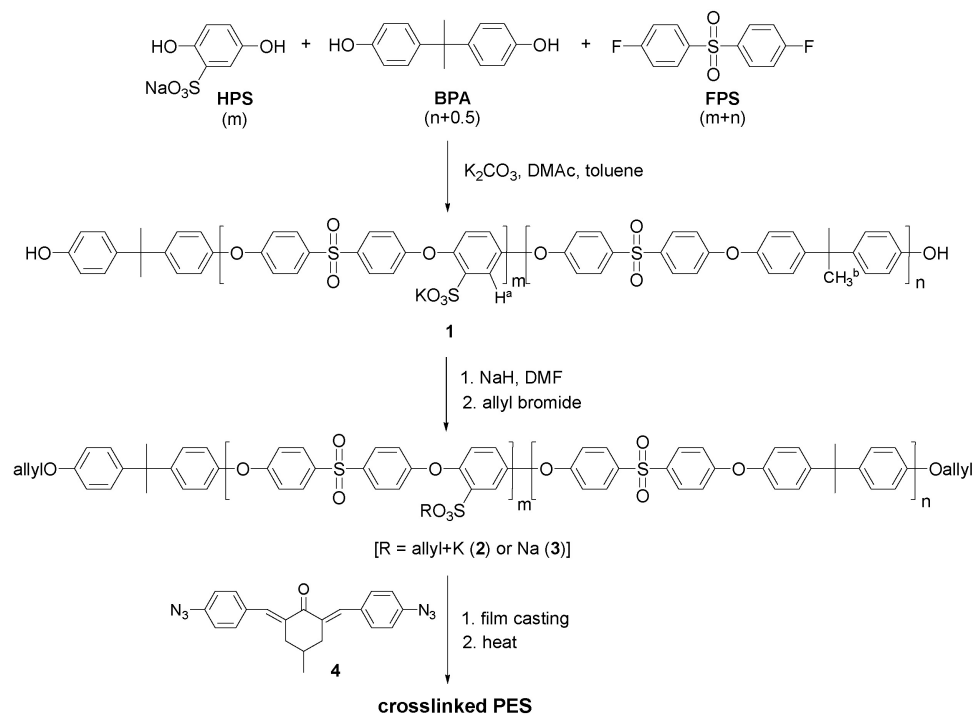


**Figure 11: Synthesis of cross-linked polymer [39].**

It was found that the cross linked polymer had a uniform distribution of hydrophilic part and a controlled hydrophobic part, which was reduced by sulfonated cross linking to the

polyether chain. These membranes presented good protonic conductivity along with impressive mechanical stability <sup>[40]</sup>.

## *CHAPTER III*

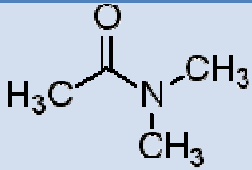
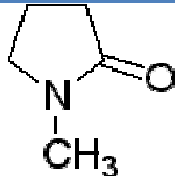
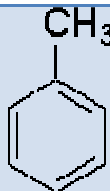
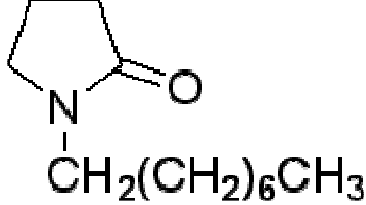
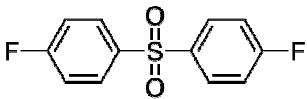
### *Experiments and characterization*

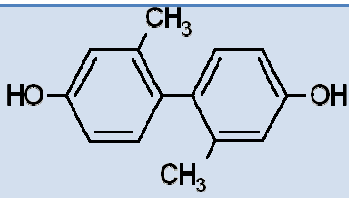
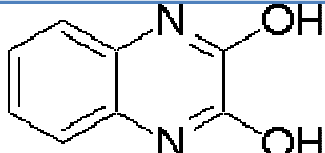
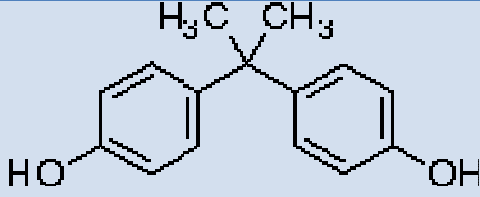
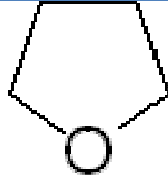
#### **(A) EXPERIMENTAL**

##### **3.1 MATERIALS:**

Polyether sulfone (PES) and polysulfone(PSf) were kindly provided by Solvay chemicals, USA. Kapton® was purchased from Sigma Aldrich Chemical Co. Dimethyl acetamide (DMAc) with a boiling point of 165<sup>0</sup>C and N-methyl pyrrolidone (NMP) of boiling point of 202<sup>0</sup>C, were purchased from (Aldrich Chemical Company Ltd.). Toluene (anhydrous) was purchased from Aldrich Chemical Company Ltd. Silicotungstic acid (HSiW) ( $\geq 99.9\%$  trace metals basis), phosphotungstic acid (HPW) ( $\geq 99.9\%$  trace metals basis), silicomolybdic acid (HSiMo) ( $\geq 99.9\%$  trace metals basis) and phosphomolybdic acid (HPMo) ( $\geq 99.9\%$  trace metals basis) were purchased from Sigma Aldrich. Concentrated sulfuric acid (95%), chlorosulfonic acid, phosphoric acid (85%) and fuming sulfuric acid (20% free SO<sub>3</sub>) were purchased from Sigma Aldrich. The chemicals are listed in **Table 3** with their chemical structure and source.

Table 3: List of chemicals used, source and chemical structure

Chemical	Source	Chemical Structure
Dimethyl acetamide	Sigma Aldrich	
N-methyl pyrrolidinone or 1-Methyl-2-pyrrolidinone	Sigma Aldrich	
Toluene	Sigma Aldrich	
N- octyl- pyrrolidone	Sigma Aldrich	
Silicotungstic acid	Sigma Aldrich	$H_4[Si(W_3O_{10})_4] \cdot x H_2O$
Phosphotungstic acid	Sigma Aldrich	$12WO_3 \cdot H_3PO_4 \cdot xH_2O$
Silicomolybdic acid	Sigma Aldrich	$H_4SiO_4 \cdot 12MoO_3 \cdot x H_2O$
Phosphomolybdic acid	Sigma Aldrich	$12MoO_3 \cdot H_3PO_4 \cdot xH_2O$
Sulfuric acid (98%)	Sigma Aldrich	$H_2SO_4$
Chlorosulfonic acid	Sigma Aldrich	$ClHSO_3$
Fuming sulfuric acid	Sigma Aldrich	$H_2SO_4 \cdot (SO_3)_x$
Bis(4-fluorophenyl) sulfone	Sigma Aldrich	

2,2'-dimethyl-[1,1'-biphenyl]-4,4'-diol	Sigma Aldrich	
2,3-Dihydroxyquinoxaline	Sigma Aldrich	
Bisphenol- A	Sigma Aldrich	
Tetrahydrofuran	Sigma Aldrich	
Acetone	UNR Chemistry Store	
Methanol	UNR Chemistry Store	
Ethanol	UNR Chemistry Store	

Fabrication of MEA was performed by using the Gas Diffusion Electrode; AvCarb E-TEK ELAT ® GDE HT 140 EW, Gas Diffusion Layer; Avcarb 1071HCB, Platinum catalyst which is a mixture of Ruthenium and Platinum HP 50% Pt:Ru on Vulcan XC-

72 and Carbon Black Vulcan XC- 72R, were purchased from Fuel Cell Store. A general purpose tensile and compression testing stand belongs to Antor Series manufactured by Com-Ten Industries was used to prepare MEAs. A 1000 lb load cell was used on the 95 D series. Its specifications are given in **Table 4**.

**Table 4: Specifications of Com-Ten Tensile load testing device**

Maximum capacity	5000 lb
Digital force output	Lb, kg, N, g, oz
Accuracy	0.5 % full scale
Resolution	1/10000 full scale
Speed accuracy	+/- 2.0% of reading

To the device, additional fittings made from aluminum in shape of blocks were attached. This is shown in the **Figure 12**. The membrane is placed between the blocks and GDEs



**Figure 12: Com-Ten tensile testing device [41]**

are placed on the either side and carefully oriented. A cartridge heater is fixed into each aluminum block that is connected to a variac. By changing the voltage, heating could be achieved to the blocks and they are moved closer to each other. The membrane between the blocks gets compressed at a high temperature and the GDE gets hot pressed on it. This is represented in **Figure 13 and Figure 14**.

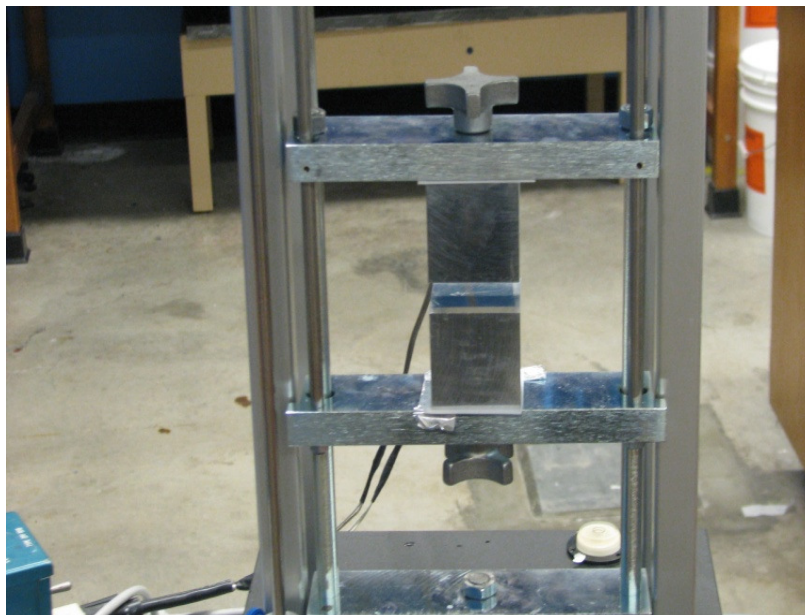


**Figure 13: Rectangular blocks attached to fabricate MEA**



**Figure 14: Com Ten tensile testing device used to make MEA**



### **3.2 SYNTHESIS OF COMPOSITE MEMBRANE**

5g of PES was dissolved in 40mL of dimethyl acetamide solvent at slightly elevated temperature ( $\sim 50^{\circ}\text{C}$ ). The solution was well mixed continuously by means of a magnetic stirrer. 7.5 g of phosphotungstic acid was added to the solution. The solution was allowed to mix well at  $60^{\circ}\text{C}$  for about 3 hours. Teflon mold was preheated in the oven at  $70^{\circ}\text{C}$  in the vacuum oven. After the phosphotungstic acid was well mixed, the solution was poured in the mold and heated in the vacuum oven at  $70^{\circ}\text{C}$  until completely dry. It usually takes 8-9 hours to dry completely. The membrane is then characterized. All the reagents were used as received without any further purification.

### **3.3 SYNTHESIS OF SULFONATED POLYMER**

There are four different ways of sulfonating the polymer. Three of them were used to test for sulfonation. Sulfonation was carried out by using acetyl sulfate, chlorosulfonic acid and fuming sulfuric acid.

#### ***3.3.1 Sulfonation by chlorosulfonic acid:***

5 g of PES was dissolved in 50 mL of 98% sulfuric acid at room temperature under constant stirring. After the polymer was completely dissolved in the sulfuric acid, the temperature of the solution was decreased to lower than  $0^{\circ}\text{C}$ . This temperature was maintained till the end of reaction. 40mL of chlorosulfonic acid was slowly added dropwise in the reaction vessel under constant mixing. After the addition of the acid, the reaction mixture at low temperature was

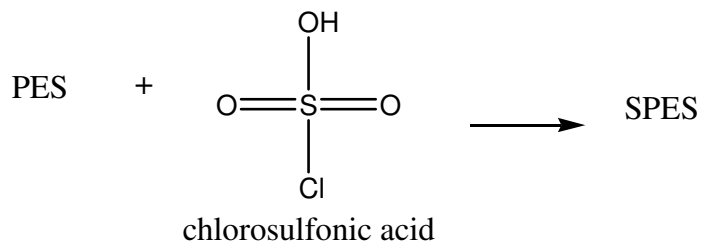


**Figure 15: Sulfonation using chlorosulfonic acid [42]**

allowed to mix for 5 hours. **Figure 15** shows the reaction mechanism of chlorosulfonic acid with PES.

The polymer after being reacted for 5 hours was poured into cold deionized water. This isolated the polymer in water from the sulfuric acid and hydrochloric acid. The polymer is filtered from the water by using a funnel under vacuum. The polymer is washed with water a number of times till the polymer is neutralized. The pH is tested by using a pH paper. The polymer is neutralized till the pH of polymer matches the pH of the DI water that is used to neutralize the polymer.

### ***3.3.2 Sulfonation using acetyl sulfate:***

Acetyl sulfate was freshly prepared before use at  $-7^{\circ}\text{C}$  and the polymer solution was added. The reaction was carried out for 3 hours before isolating SPES in ethanol. Figure 1 represents the sulfonation reaction of PES. PES was dissolved in sulfuric acid and allowed to form a homogeneous solution. The temperature was reduced to  $0^{\circ}\text{C}$  using an ice bath. Chlorosulfonic acid was added drop wise slowly into the solution. The reaction was allowed to proceed for 3 hours before SPES was isolated in ice cold water. The lower temperature was maintained to avoid cross linking and decomposition of the

polymer chain which usually occurs at temperatures higher than 200<sup>0</sup>C. The polymer was then washed until neutral and subsequently dried. This has been represented in **Figure**

**16.**

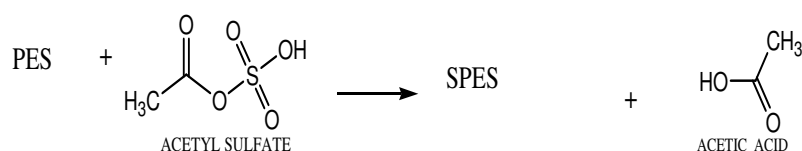
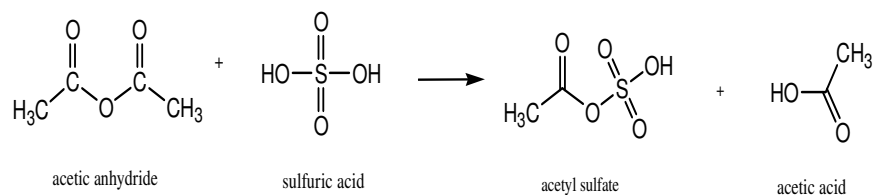
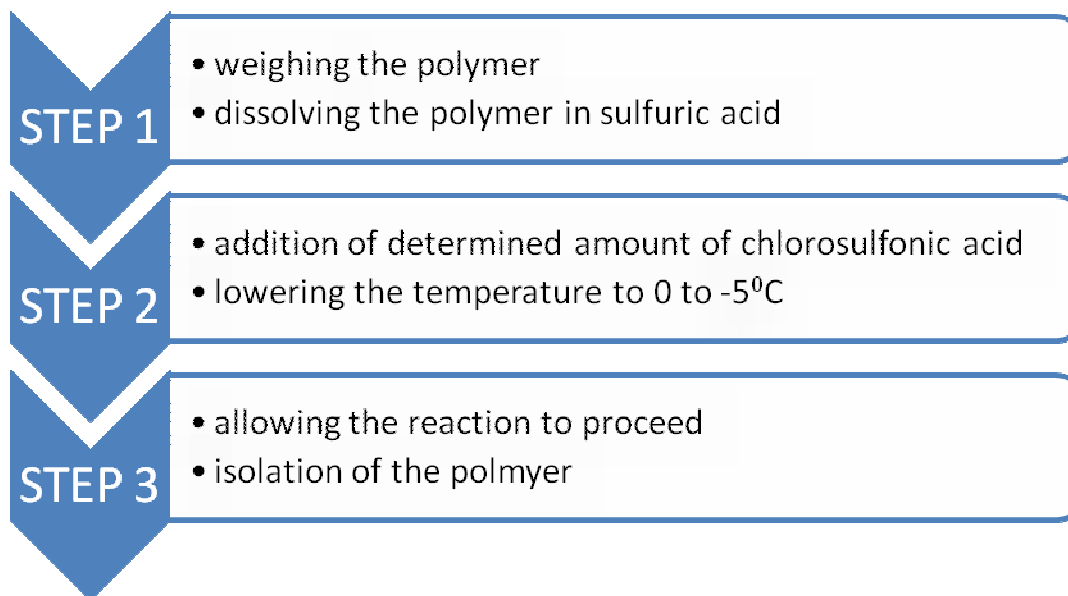


**Figure 16: Sulfonation of PES acetyl sulfate [43]**

### **3.4 SULFONATION OF POLYSULFONE:**

5 grams of PSf was dissolved in 40mL tetrahydrofuran until it resulted in a homogeneous solution. Chlorosulfonic acid was added carefully drop wise at lower temperature. The reaction was allowed to continue for 5 hours. Later, the sulfonated polymer was poured slowly in methanol. This isolated the polymer from the acid solution. The polymer was washed several times and neutralized. The pH was measured and made equal with the deionized water used. The polymer was then dried in vacuum oven at 50<sup>0</sup>C for overnight.



### **3.5 SYNTHESIS OF POLYMERS FROM MONOMERS**

#### **3.5.1 Synthesis of polysulfone**

Polysulfone was synthesized by two methods. The monomers were reacted in presence of solvents DMAc and toluene and potassium carbonate. The reaction scheme is shown in figure below. Pre-weighed and dried monomers were added to a 3-neck reactor connected to a mechanical stirrer. Thermocouple was attached to the reactor and was connected to a temperature controller that heated the heating mantle in which the reactor was placed. A condenser was connected to the reactor vessel to reflux the solvent. Nitrogen inlet was attached to another neck of the reactor that purged the reactor with nitrogen. The reaction setup is shown in **Figure 20**.

The polymer that was formed after the reaction was cooled, dissolved in THF and then later isolated in cold DI water.

Another method that was used to synthesize polysulfone was to react the monomers in presence of potassium carbonate in inert atmosphere in absence of solvent.

Stoichiometric amounts of monomers were added to a 3 neck reactor connected to thermocouple, condenser and a nitrogen inlet. The temperature was initially maintained at 80°C and then later increased to 150°C. The monomers reacted at that temperature and the temperature was maintained at 150°C for 24 hours. This is shown in **Figure 17**. After the polymer was formed, the solid mass was allowed to cool down to room temperature

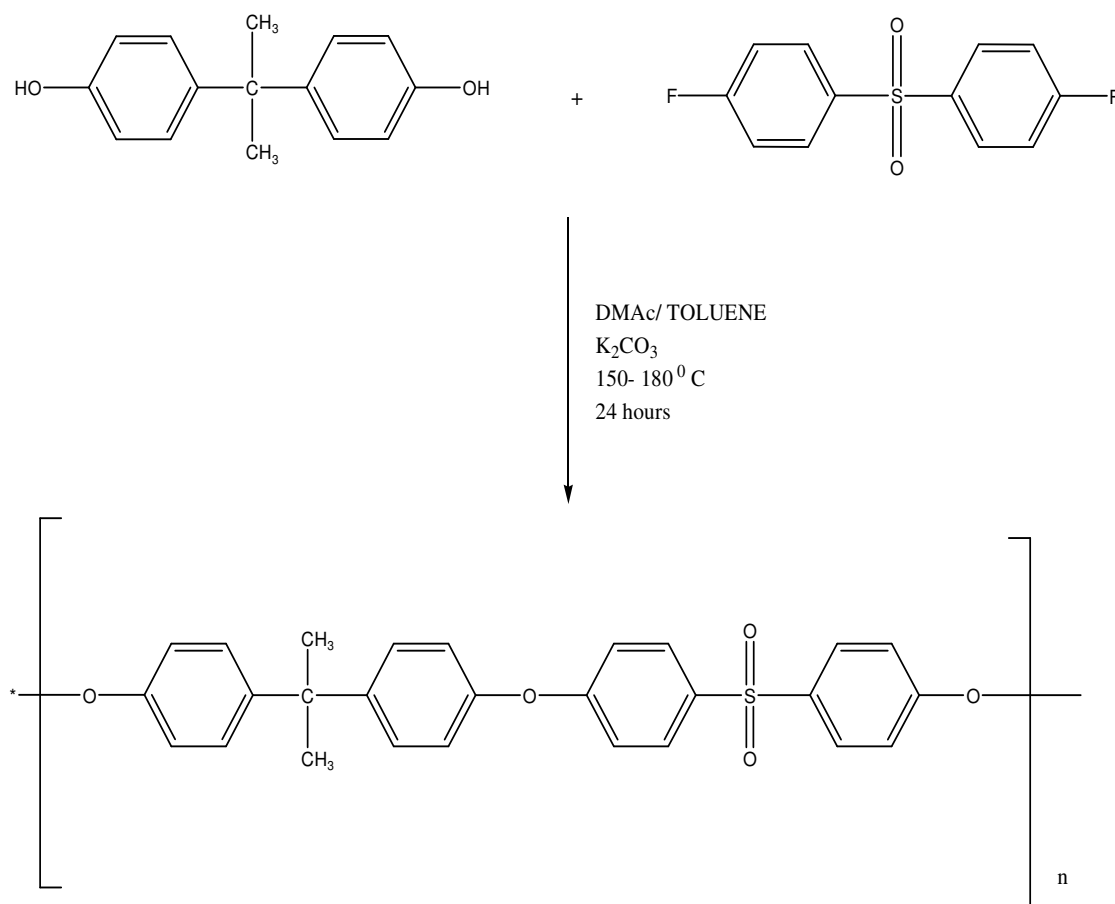


**Figure 17: Synthesis of polysulfone [48]**

and to it THF was added. The solid mass was dissolved in THF at slightly elevated temperature. The polymer was isolated in cold DI water and was dried in vacuum oven.

### **3.5.2 Synthesis of polyether sulfone quinoxaline**

The synthesis of new polymers was based on the general approach of nucleophilic substitution polymerization. Two dihydroxy group containing aromatic monomers were reacted with a dihalide containing monomer to yield a copolymer with hydrogen fluoride as a byproduct. The general reaction scheme is shown in the **Figure 18**.

Potassium carbonate is added as a base catalyst to neutralize the reaction as well as to catalyze it. Cesium carbonate can also be used to for the same purpose and results in better homogeneity in terms of polymer synthesis [50]. It is also proven that the use of cesium carbonate is extremely helpful when high molecular weight polymers are desired. [50].

A reactor vessel attached to a mechanical stirrer system with a trap and condenser was used. Bisphenol- A (10mmol, 2.868g), fluorophenyl sulfone (20mmol, 5.136g), dihydroxyquinoxaline (10mmol, 1.654 g) and  $K_2CO_3$  (26.67mmol, 3.722g) were added to the reactor. 40mL of DMAc and 20 mL of toluene were added as solvents. The reactants were allowed to mix at 110 – 120° C. The water was azeotropically removed using toluene, from the reaction mixture by removing toluene from the system. The temperature was then increased to 165 – 170° C and the reaction was allowed to run for 24 hours.

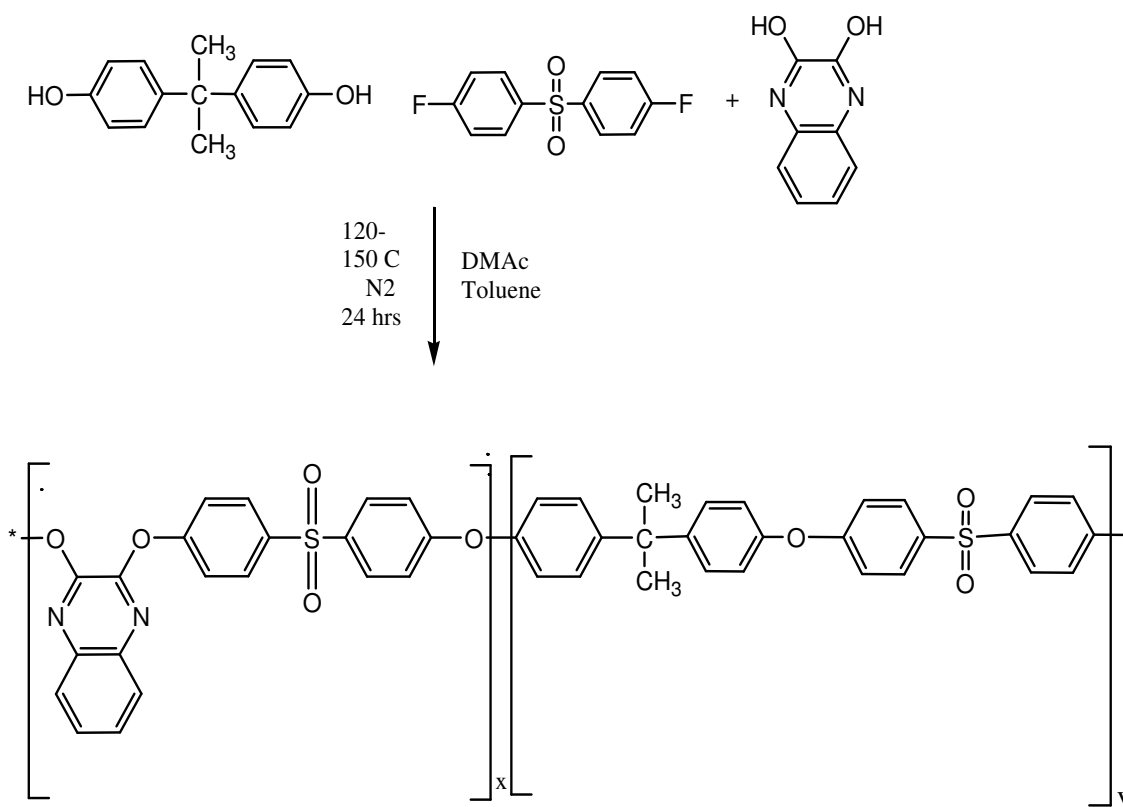


**Figure 18: Synthesis of polyether sulfone quinoxaline**

Similarly, reactions were carried out between other monomers that possessed dihydroxy groups and fluorophenyl sulfone. These reactions resulted in various copolymers of polyether sulfone and homopolymers. The reaction scheme in **Figure 19** shows reaction that was carried out.

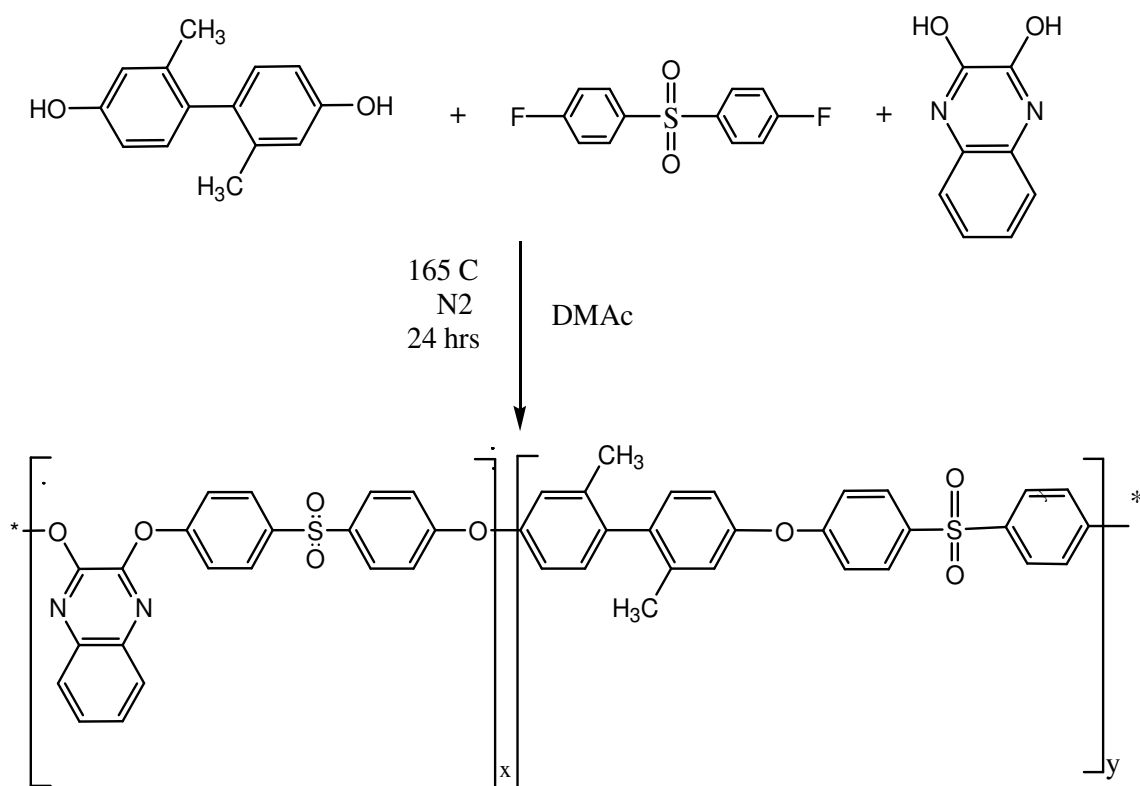


**Figure 19: Synthesis of polyether sulfone quinoxaline Type II**

The reaction setup is shown in the **Figure 20**. A mixer is attached to a 3-neck reaction vessel and to it are also connected, nitrogen gas purge, a thermocouple and a condenser. The thermocouple attached to the reactor, control the temperature by connecting it to a controller attached to the heating mantle.



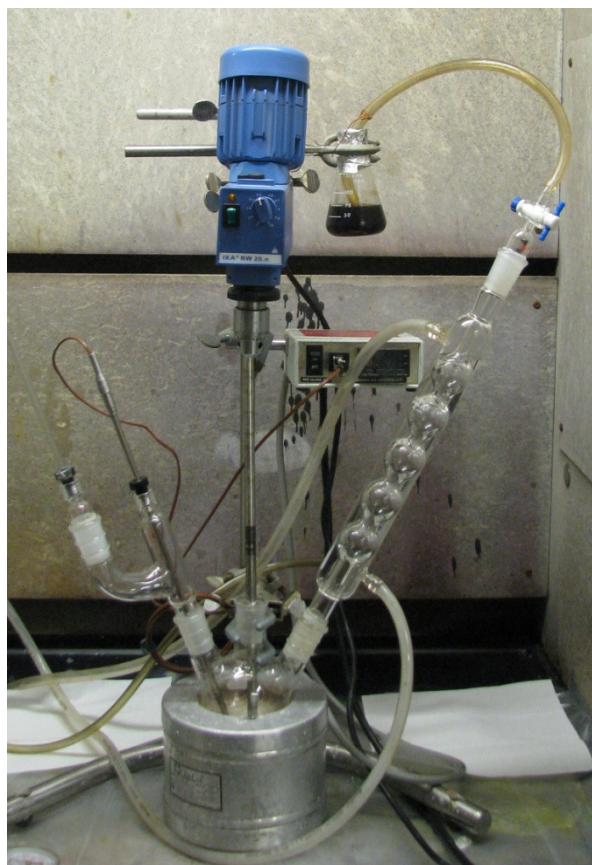


**Figure 20: Reactor setup for polymer synthesis**

## **(B) CHARACTERIZATION**

After synthesizing the membrane, characterization is carried out. The most common methods of characterization are the determination glass transition temperature,  $T_g$ . This is done by the use of Differential Scanning Calorimetry (DSC), sulfonation extent by ion exchange capacity, molecular weight determination by MALDI and Gel permeation Chromatography, tests for proton conductivity and performance in terms of current and voltage relationship.

### **Differential Scanning Calorimetry (DSC)**

Depending on the temperature, the polymer molecules undergo a transition in state and in structure. Three states are well recognized for polymers: Melt state, glassy state and crystalline state. The major transition temperatures in the polymers are melt temperature  $T_m$  and glass transition temperature,  $T_g$ .  $T_g$  is a temperature below which free rotations cease because of the energy barriers offered by the intermolecular forces.  $T_g$  is usually related to stiffening temperature of the polymers<sup>[50]</sup>. Melting is a transition which occurs in crystalline polymers. Melting happens when the polymer chains fall out of their crystal structures, and become a disordered liquid<sup>[50]</sup>. The glass transition is a transition which happens to amorphous polymers; that is, polymers whose chains are not arranged in ordered crystals, even though they are in the solid state.

But even crystalline polymers will have some amorphous portion. This portion usually makes up 40-70% of the polymer sample. This is why the same sample of a polymer can have both a glass transition temperature and a melting temperature. The amorphous portion undergoes the glass transition only, and the crystalline portion undergoes melting only. DSC enables us to study the heating- cooling affects on the polymer and allows us to investigate the polymer in its native state. Since the heating – cooling is carried out at constant pressure, the heat flow is equivalent to the enthalpy change [40].

$$\left(\frac{dq}{dt}\right)_p = \frac{dH}{dt}$$

The calorimeter consists of a sample holder and a holder for reference. High temperature operation is ensured by the fact that both the holders are made of platinum. Each holder has individual heaters. When current flows, the sample gets heated. Both the holders are maintained at constant temperature. The schematic of the DCS is shown in **Figure 21**.

The specifications of the Perkin Elmer DCS are shown in **Table 5** <sup>[43]</sup>:

**Table 5: Details of Pyris DSC**

Range of temperature	-170 <sup>0</sup> C to 750 <sup>0</sup> C
Sensitivity	0.2 μW
Dynamic range	0.2 μW to 800 mW
Calorimetry	
Accuracy	Better than +/- 1.0 %

Precision	Better than +/- 1.0 %
Temperature	
Accuracy	Better than +/- 0.1 %
Precision	Better than +/- 0.01 %
Scan rate	
Heating	0.01 <sup>0</sup> C up to 500 <sup>0</sup> C/ min
Cooling	0.01 <sup>0</sup> C up to 500 <sup>0</sup> C/ min

The DCS instrument that is used in the lab is supplied by Perkin- Elmer and is of the model Pyris-1. Sample and reference pans are used in the DSC. A furnace is connected to

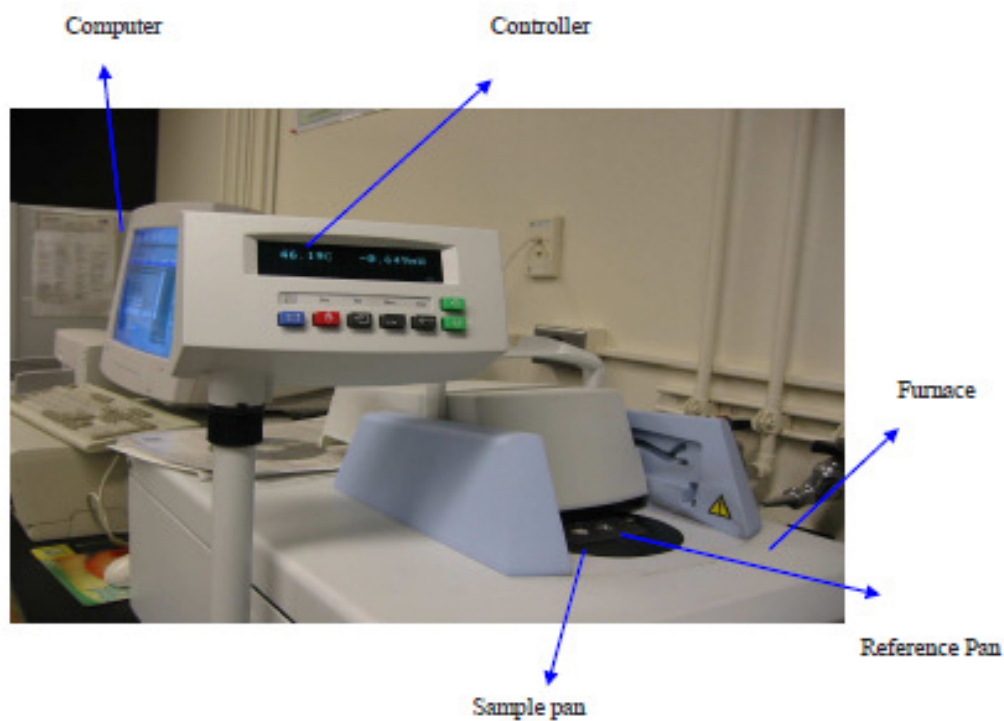


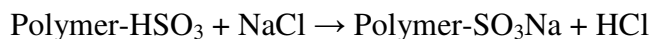
Figure 21: Differential Scanning Calorimeter (DSC) [43]

to the stage on which the pans and the heating or the cooling rates are controlled. The difference between the sample pan and the reference pan is measured.

### **3.6 ION EXCHANGE CAPACITY (IEC):**

The ion exchange capacity of a polymer is calculated after it has been sulfonated. It indicates the number of milli-equivalents of ions in 1g of dry polymer. It is a measure of degree of sulfonation of a polymer. The sulfonic acid groups are covalently attached to the polymer chain and decreases the overall polymer pH of the polymer. The higher the degree of sulfonation, higher is the IEC and vice versa. Higher IEC of a polymer should increase its conductivity.

IEC of a polymer was determined by soaking a known weight of the polymer in 2 M NaCl solution for 20 hours. The polymer was then filtered. The solution that was left was tested for the IEC.



Thus the sulfonic acid groups exchange their ions with the Na ion in the solution, making the polymer neutral in nature and the solution acidic.

This ion exchanged solution was titrated against 0.1 M NaOH solution using phenolphthalein indicator. The phenolphthalein indicator was prepared by adding powder phenolphthalein in ethanol and water mixture.

The DI water has a pH range of about 5-6 due to the fact that as soon as the water comes in contact with air, the carbon dioxide in air reacts with the ions to form carbonic acid, and to account for it, blank titration with DI water was carried out prior to the acid- base titration.

The IEC was calculated by the formula:

$$IEC \left( \frac{meq}{g} \right) = \frac{V(NaOH) \times N(NaOH)}{\text{weight of dry polymer (g)}}$$

where,

V (NaOH) is the volume in mL of base in the burette (titer value), and

N is the normality of the NaOH solution

By substituting the values, the value of the IEC can be determined. From this the value of the degree of sulfonation can be determined. It is given by:

$$DS = \frac{120 \times IEC}{1000 + 120 \times IEC - 200 \times IEC}$$

Where DS is the degree of sulfonation.

### **3.7 MATRIX- ASSISTED LASER DESORPTION IONIZATION – MASS SPECTROSCOPY**

The MALDI that was used at UNR was Applied Biosystems 4700 Proteomics Analyzer (Applied Biosystems, CA). MALDI TOF/TOF mass spectrometer was equipped with linear and reflector modes. The software used was: 4000 Series Explorer v 3.6

For a polymer, molar mass plays a very important role in determining the polymer properties like mechanical behavior, melt temperature and viscosity of melts. The width of molar mass distribution depends on the polymerization process, mechanism and kinetics. Depending on the polymerization process, the macromolecules can be cyclical, cross-linked, copolymers and can have various functional groups.

The molecular mass of the polymer can be determined. An average number can be determined, and these are defined in terms of molar mass, corresponding number and concentration. The number average molar mass of a polymer is given by<sup>[46]</sup>:

$$M_n = (\sum n_i M_i) / \sum n_i$$

The weight average molar mass is given by:

$$M_w = \frac{\sum_i (M_i^2 \cdot n_i)}{\sum_i (M_i \cdot n_i)}$$

$M_w$  is determined from the methods that are sensitive to weight of molecules like sedimentation or light scattering.

Another molar mass average that is of importance is measured from viscosity measurements. It is given by <sup>[46]</sup>:

$$M_v = \left[ \frac{\sum_i (M_i^a \cdot w_i)}{\sum_i (w_i)} \right]^{\frac{1}{a}}$$

Here 'a' is obtained from Mark- Houwink relationship. Its value ranges from 0.5 – 1 depending on the structure of molecules.

A measure of the width of the distribution of polymers molar mass is called the polydispersity index given by

$$Q = \frac{M_w}{M_n}$$

The value of Q is 1 for monodisperse samples. These are those polymers that have same mass for all the molecules. Many polycondensation products show a value of 2.



Mass spectroscopy separates ions based on their mass and charge. The mass spectrometers measures two parameters that are used for characterization of mass resolution and sensitivity<sup>[46]</sup>. Mass resolution describes ability of a mass spectrometer to separate ions of adjacent mass numbers. Sensitivity is determined by the minimum amount of sample that is consumed by the instrument to produce a useful signal. The first step in measurement by mass spectrometers is that the ions need to be generated from the sample. The type of ionization is dependent on the type of sample.

Ions are formed by the removal or addition of an electron giving a radical cation  $M^+$  or anion  $M^-$ . Here,  $M$  denotes the molecular species to be ionized,  $e^-$  denotes an electron and  $X$  denotes a proton or  $Na^-$ ,  $Li^-$ ,  $K^-$  or  $Ag^-$  atom.

After ionization, the ions are separated according to their  $m/Z$  ratio value. Analyzers are high vacuum regions where ions are oscillating electromagnetic fields. Ions of different mass, velocity and charge can be collected and separately using these fields.

The time of flight analyzer is one of the most widely used mass analyzer for pulsed ion sources for MALDI MS. The TOF mass analyzer makes use of the fact that mass- to – charge ratio of an ion can be determined by measuring the velocity after accelerating it to a defined kinetic energy. The basic equations for kinetic and electrostatic energies are given by<sup>[46]</sup>:

$$\frac{m \cdot V^2}{2} = z \cdot e \cdot U$$

Where

$V$  = ion velocity

$M$  = mass

$Z$  = number of charges

$U$  = acceleration voltage

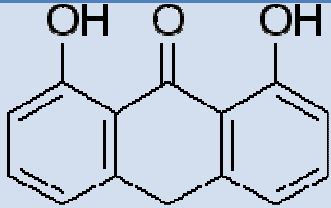
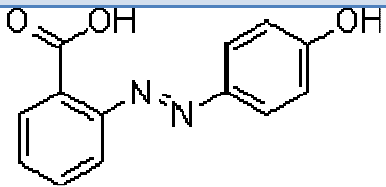
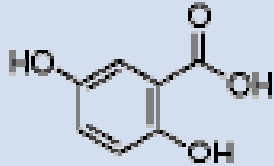
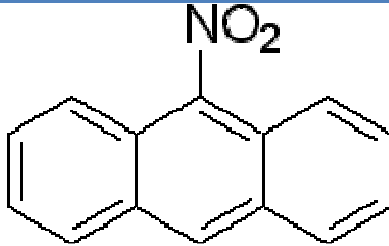
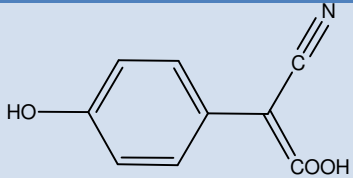
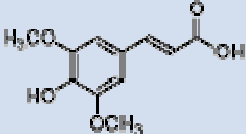
From this relation it can be observed that smaller ions at a constant kinetic energy will travel faster than the more bulky ones. A detector measures the time-of-flight of particles. Detection of ions and their analysis is the next step after the ions have been separated and generated.

Short pulses of laser in combination to possibility to focus to small spot sizes result in ion generation comparable to as point source in space and time. These are ideal conditions for TOF analysis.

### **Matrices and sample preparation <sup>[46]</sup>:**

Matrices and preparation techniques can be performed in numerous ways. Depending on the sample, its acidity, its aromatic nature and many other factors, the matrix and the sample preparation method may vary. If a cationized analyte is to be used, a matrix should be chosen that does not compete with the sample for cations. In case the analyte is aromatic in nature, then AgTFA and Cu(II)Cl<sub>2</sub> is the preferred cationizing agent. The table below gives a brief list of the most widely used matrices and their structure.

Table 6: List of common MALDI-MS matrices [sigma Aldrich]

Matrix	Molecular weight	Structure
Dithranol	226.23	
2-(4-Hydroxyphenylazo)benzoic acid - HABA	242.23	
2, 5 – Dihydroxybenzoic acid – DHB	154.13	
9- nitroanthracene (NA)	223.23	
$\alpha$ -cyano- 4- hydroxyl cinnamic acid - CCA	189.17	
Sinapinic acid – SA	224.21	

Sample preparation is an important step in MALDI especially for synthetic polymers. No standard protocol has been developed for polymers and it's mainly trial and error. In general, the matrix and sample preparation should serve 3 propose: a) co-crystallization with analyte with large molar excess to prevent cluster formation of analyte molecules; b) strong absorption of laser light in the matrix with subsequent energy transfer to analyte, and c) achieving ionization of the analyte.

The most widespread method of sample preparation is the dried droplet method. Specific amounts of analyte and matrix are dissolved in a suitable solvent. Small amount of cationizing agent are added to it. The solution is mixed in the ratio of 10:10:1 for polymer, matrix and cationizing agent respectively and then agitated. A drop of this solution is spotted on the MALDI plate. The sample is allowed to dry and then introduced to the ion source of the spectrometer.

### **Sample Preparation:**

The general sample preparation method is to dissolve the polymer in THF. The matrix used was 10mg/ mL matrix in THF and 10 mg/mL of silver trifluoroacetate was used as a cationizing agent. The sample was prepared by mixing the matrix, AgTFA and sample in 10:1:1 ratio prior to spotting on the MALDI target. 0.5  $\mu$ L of sample was spotted on the target. Spectra of plain matrix were also obtained to compare with polymer spectra.

### **3.8 ELECTROCHEMICAL IMPEDANCE SPECTROSCOPY (EIS):**

This technique is used to determine the proton conductivity of a membrane by an in-plane measurement. BekkTech conductivity cell was used to place the sample and to measure the conductivity of the sample. **Figure 22** shows the BekkTech conductivity cell. It contains four platinum electrodes. These electrodes are connected to the potentiostat /impedance analyzer using alligator clips. The potentiostat was purchased from Princeton Applied Research and its model number is PARSTAT 2273. The EIS is capable of testing a sample from 10 $\mu$ Hz to 1MHz. 2A current can be applied with a 100V. It possesses 10<sup>13</sup> Ohms input impedance.

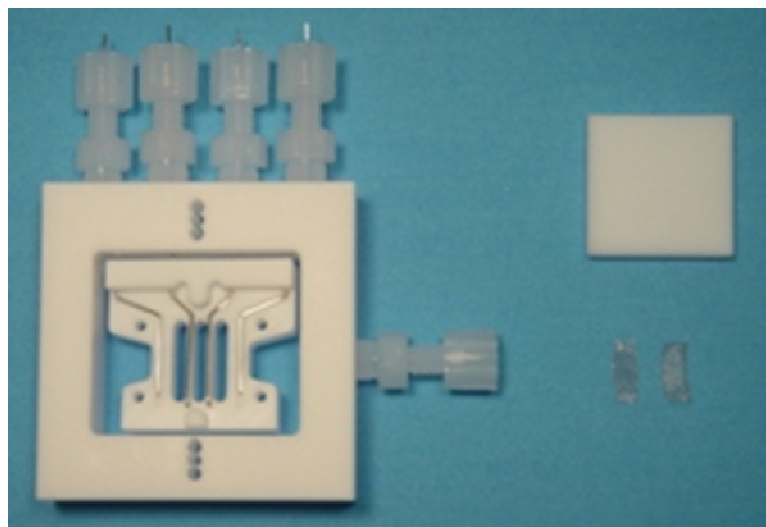


**Figure 22: Conductivity cell for EIS measurements [47]**

The electrochemical potentiostat is synchronized to a computer that has the PARSTAT software, Power Suite, installed. This software has a capability to measure Bode plots and Nyquist plots. This software can also be used to model the Nyquist plots obtained.



Figure 23: EIS potentiostat[48]

Electrochemical impedance is measured by applying an AC potential to the electrochemical cell and measuring the current through the cell. Electrochemical impedance is normally measured by applying a small excitation signal. This is done so that the cell's response is pseudo-linear. In a linear system, the current response to a sinusoidal potential will be sinusoidal at the same frequency but shifted in phase [48].

The excitation signal is expressed as a function of time, has a form,

$$E(t) = E_0 \sin(\omega t)$$

The expression for  $Z(\omega)$  is composed of a real and an imaginary part. If the real part is plotted on the X-axis and the imaginary part is plotted on the Y-axis of a chart, we get a

“Nyquist plot”. The points on Y-axis are negative and each Nyquist point on the plot is the impedance at one frequency.

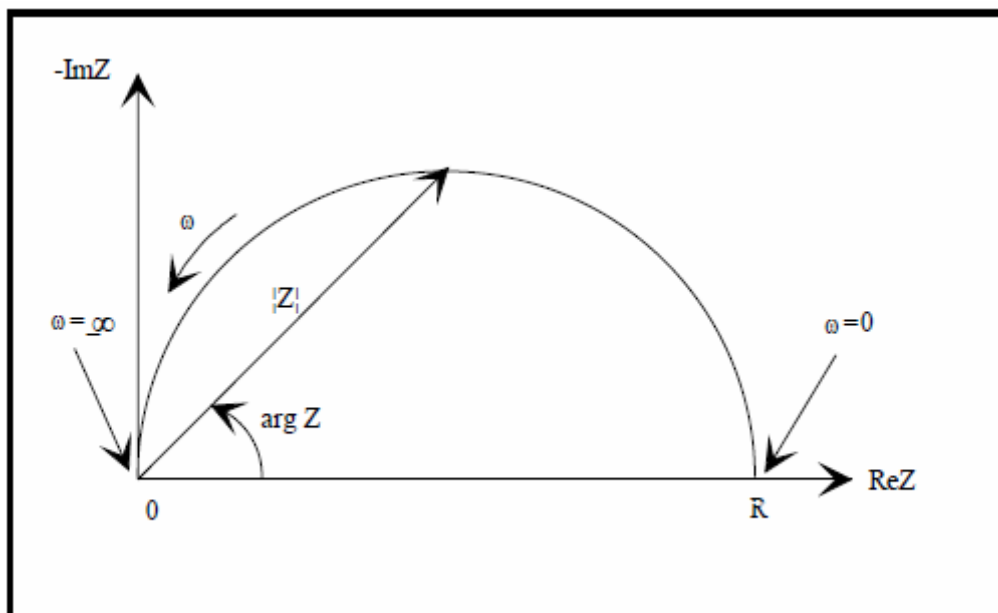


Figure 24: Typical EIS plot [48]

The Nyquist plot impedance can be represented as a vector of the length  $|Z|$ . The angle between this vector and the X-axis is called the “phase angle”. The circuit in **Figure 25** resulted in the Nyquist plot above. Every Nyquist plot is generated from an electrical circuit.

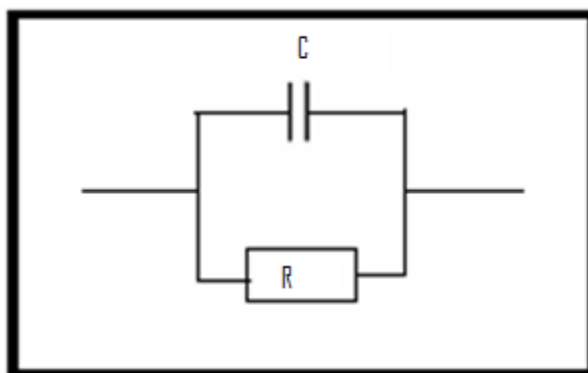


Figure 25: Electric circuit representation of Nyquist plot [48]

Membranes were cut into small pieces and placed in the conductivity cell. The upper Teflon block was screwed tight on the conductivity cell and it was connected to the electrochemical testing device. The dimensions of the membrane were measured and the conductivity was measured in 100% humidity at room temperature. The Nyquist plot gave the resistance values and the reciprocal of that resulted in conductivity. The conductivity can be calculated by the following equation:

$$\sigma = \frac{l}{t * w * R}$$

Here,  $\sigma$  = conductivity in S/cm

t = thickness of the membranes in cm

w = width of the membrane in cm, and

R = resistance of membrane in k $\Omega$ .



### **3.9 GEL PERMEATION CHROMATOGRAPHY (GPC):**

GPC is one of the most popular methods of molecular weight determination of polymers. The separation is driven by the hydrodynamic properties of the molecules. The polymer is dissolved in a suitable solvent and passed through a column that is filled with porous particles. Higher molar mass particles are the easiest to pass through the column and hence elute first. The molecules with lower molar mass will penetrate into the pores and hence will elute later.

GPC was carried out at the Organic and Macromolecular Synthesis Facility in Molecular Foundry located at Lawrence Berkeley National Laboratory, Berkeley, CA. The GPC columns were fabricated by Viscotek. GPC was used to determine the molecular weight of the polymers and their polydispersity index (PDI).

Gel Permeation Chromatography (GPC), also known as Size Exclusion Chromatography (SEC), is a chromatographic technique that employs specialized columns to separate natural and synthetic polymers, biopolymers and nanoparticles on the basis of size<sup>[49]</sup>. When the GPC separation is coupled with advanced detectors such as light scattering, viscometer and concentration detectors, it will provide a distribution of absolute molecular weight, molecular size, and intrinsic viscosity as well as information on macromolecular structure, conformation aggregation and branching.

**Sample preparation:** The polymers were dissolved in THF. About 1 mL of the solution was pipette using a micro pipette. The solution was filtered with 0.45 $\mu$  m PTFE filter

before placing the sample solution in the vials. The GPC columns were standardized using polystyrene standards. The GPC is coupled with light scattering detectors that generated distribution curves.

### **3.10 Thermogravimetric Analyzer (TGA):**

Thermogravimetric analysis of the composite membranes was carried out to investigate the thermal behavior of the membrane after the polymer has been sulfonated and combined with HPAs. TGA provides quantitative measurement of mass change in materials associated with transition and thermal degradation [50]

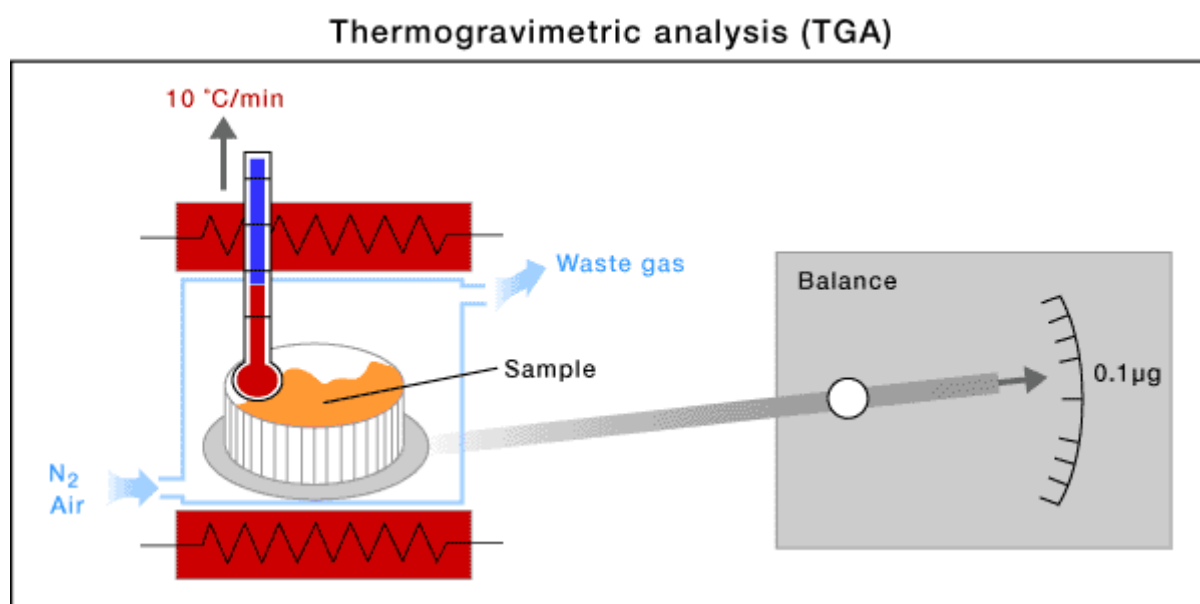


**Figure 26: Representation of TGA [50]**

In a TGA, the sample is placed on a pan made of platinum. Analysis is done based on weight of the sample and its loss with increase of temperature over time. The heating is

done in the absence of air for the samples that are prone to oxidation, which is generally the case with polymers. The heating is done in a nitrogen atmosphere that flows at a rate of 50 mL/min. Perkin Elmer TGA- 7- Thermogravimetric analyzer (Waltham, MA) is used to analyze the moisture content and thermal stability. Samples were first heated up at the rate of  $10^{\circ}\text{C}$  to  $105^{\circ}\text{C}$  and held there for 10 mins. Then increased to  $900^{\circ}\text{C}$  at the rate of  $50^{\circ}\text{C}$  and held there for 60 min. Mass change that takes place at  $105^{\circ}\text{C}$  corresponds to moisture.

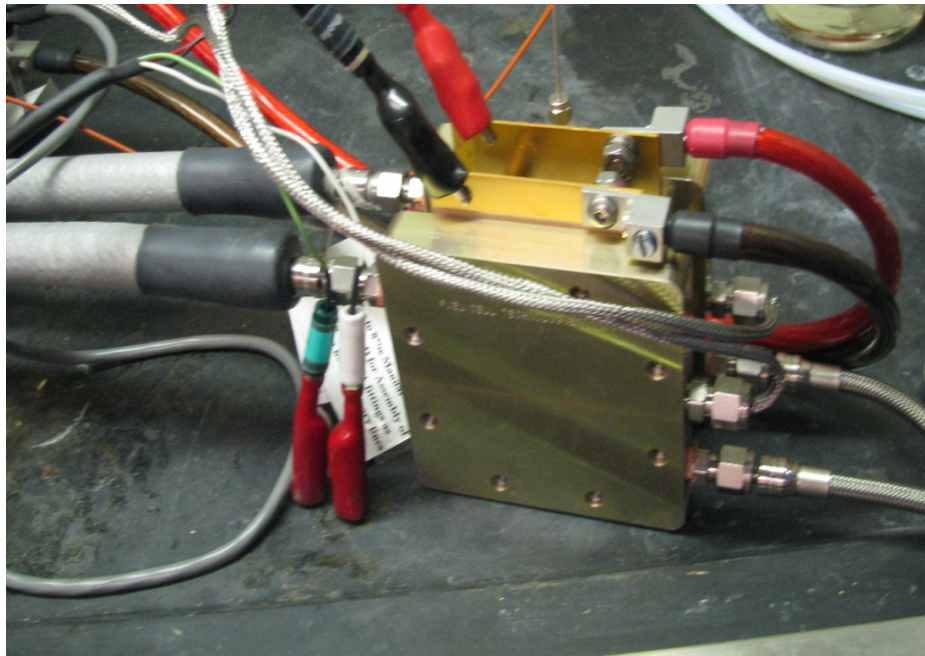
### 3.11 Single Membrane Test Cell:



Figure 27: Scribner fuel cell testing stand 850e

A single membrane was tested on Single membrane testing device manufactured by Scriber Associates. It is shown in **Figure 27**. This device has a humidifier that can operate up to  $120^{\circ}\text{C}$ . It is suitable for upto  $50\text{cm}^2$  and small stacks apart from single

membrane tests. It has both anode and cathode humidifier. The presence of mass flow meters at the anode and cathode enables us to control the flow-rate control of inlet gases. It has a built-in impedance analyzer that enables the measurement of proton conductivity at higher temperatures. Multi-gas selector at anode and cathode can be used to study the affect of various gases on the catalyst.



**Figure 28: A single membrane fuel cell**

After the MEA is fabricated, it is placed in the fuel cell. The fuel cell is attached to the anode and cathode flows are shown in the **Figure 28**. Then the gas flow is started and load is applied on the fuel cell. The monopolar plates are shown in **Figure 29** below.

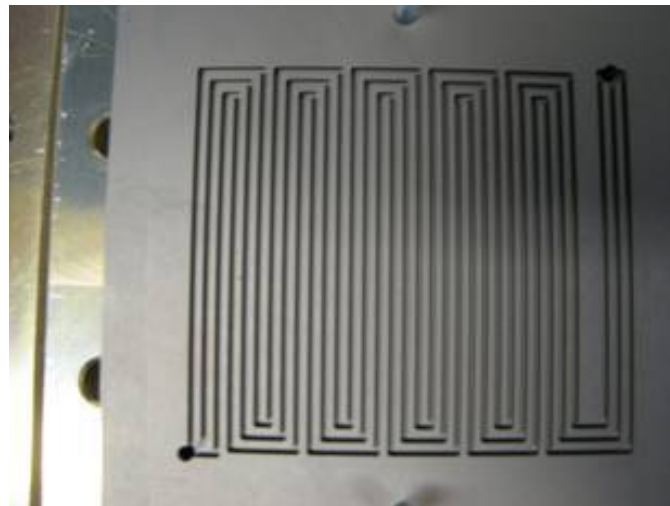
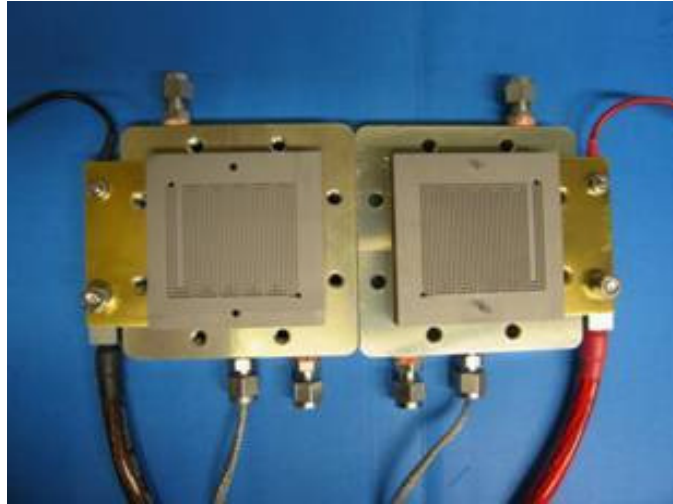


**Figure 29: Fuel cell opened and monopolar plate view**

The polarization curve is a graphical representation of the voltage- current relation for the membrane. The ideal standard potential of a fuel cell in which hydrogen reacts with oxygen is 1.229 V with liquid water as product. And when gaseous water is produced, the potential is 1.18V <sup>[51]</sup>. this is the oxidation potential of the hydrogen. However, there are numerous irreversibilities in a fuel cell that decrease the equilibrium cell potential. The losses are from three sources: a) activation polarization, b) ohmic polarization, and c) concentration potential <sup>[51]</sup>.

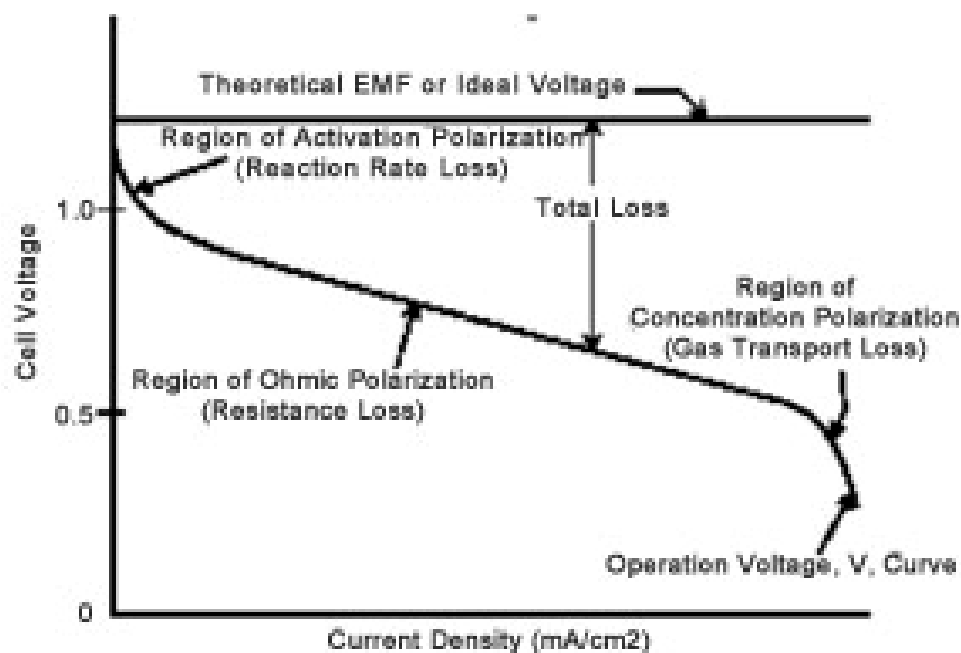


Figure 30: Losses in a typical polarization plot [51].

Activation polarization is present when the rate of electrochemical reaction is controlled by slow kinetics. At lower rate of the reaction, the losses will be higher. The activation losses are most predominant at low current densities [51]. Ohmic losses occur because of the resistance of the membrane to protons. Thus, these losses are proportional to the conductivity of the membrane. These can be reduced by increasing the membrane conductivity and by decreasing the electrode separation<sup>[51]</sup>. Concentration polarization is caused due to inability of the material to maintain a constant concentration of the gases. In other words, concentration gradient causes a loss in the overall performance [51].

## *CHAPTER IV*

### *Results and discussions*

#### **4.1 PREPARATION OF COMPOSITE MEMBRANES**

Initial composite membranes were prepared by the addition of HPA to commercially available polyimide, Kapton ®. This was a good polymer to use since it was a good film former and was aromatic in nature. By virtue of its aromaticity, it could withstand moderate temperatures.

While preparing the composite membranes from HPA and SPES, few problems were encountered including formation of bubbles and non-homogeneous films. These initial problems might have been due to improper mixing, sudden heating in the oven and presence of air trapped in the solution while casting the film. Vacuum was used to get rid of the bubbles and the membranes were heated at low temperatures for a constant heating rate and not sudden heating. After these problems were solved, homogenous films were obtained.

Composite membranes were prepared by adding different types and amounts of HPA to the polymer matrix. Amongst the HPAs, silicotungstic acid was found to be most conductive. However, its addition to the polymer was limited. When more than 50% of SiWA was added to the system, the film that was obtained was non-homogenous and resulted in the formation of small white clusters throughout. This was believed to be the



saturation limit of SiWA and the white clusters were because of the crystallization of SiWA due to exceeding saturations. PWA was found to be suitable up to 60 wt% that resulted in homogenous films and considerable amount of conductivity.

#### **4.2 Sulfonation, conductivity and ion exchange measurements**

The extent of sulfonation of polymer was determined by Ion Exchange Capacity (IEC) measurement. The conductivity of the polymer samples and composite membranes were obtained from EIS measurements. It was observed as expected, that the conductivity increased with increase in IEC values.

Sulfonation of PES was first carried out by using acetyl sulfate. After the process of sulfonation, IEC of the polymer was measured. It was found to be about 0.1 meq/gm. For better IEC numbers, sulfonation was carried out by chlorosulfonic acid. Fuming sulfuric acid was used to test for sulfonation. This resulted in the polymer becoming soluble in water and hence the polymer was hard to isolate.

Various amounts of chlorosulfonic acid were added to the reaction mixture during sulfonation. The increase in amount of chlorosulfonic acid increased the overall conductivity. Acid doping was performed by soaking the membranes in 85%  $\text{H}_3\text{PO}_4$ . It also resulted in a significant increase in conductivity.

A pure Kapton® sample was cast as a membrane and the conductivity was measured. It

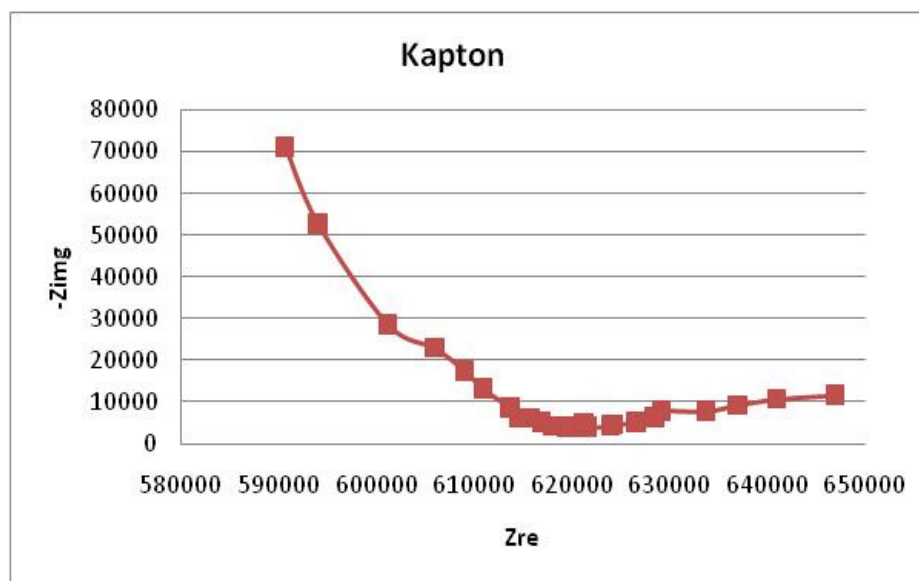
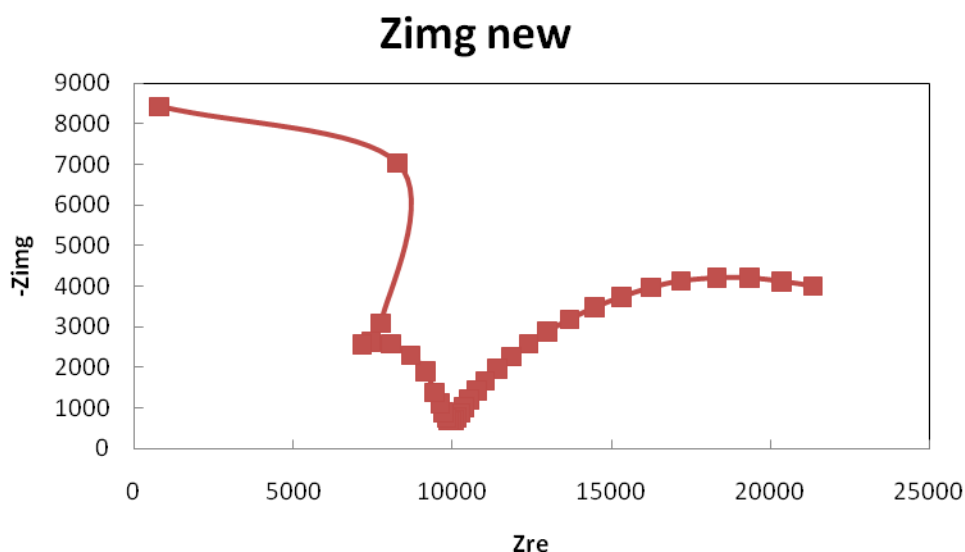


Figure 31: Nyquist plot of pure Kapton

was found to be  $3 \times 10^{-6}$  S/cm. It is shown in figure below.

An EIS spectrum for 3% HPA is shown in Figure below. The frequency was varied from 1 Hz to 1 MHz during the experiment. A potential of 200 mV was applied during the experiment. The shape of this curve indicates that the higher frequency data are due to the capacitive behavior of the material. The lower frequency data are caused by the inductive property of the material. These results indicate that acid doping significantly improved the conductivity of the polyimide membrane. When 3.4% HPA was added the conductivity of the composite acid doped polyimide membrane increased slightly above the acid doped polyimide membrane.



**Figure 32: EIS plot of 3.4 % HPA and Kapton composite membrane**

The pure polyimide membrane demonstrated a conductivity of  $3.2 \times 10^{-6}$  S/cm, while the acid doped polyimide, on the other had showed a conductivity of  $1.7 \times 10^{-3}$  S/cm. This showed that by acid doping the conductivity of the membrane increased substantially.

This is due to temporary adherence of sulfonic acid groups to the polymer surface.

When, 3.4 wt % of HPA particles were added to the polymer matrix, the conductivity of the membrane was found to be  $5.3 \times 10^{-5}$  S/cm. And when that membrane was acid doped, the conductivity increased to  $2.5 \times 10^{-3}$  S/cm. These values proved the effect of HPA and acid doping on the membranes.

Polyimides have been extensively studied in literature for various applications including fuel cell membranes. The main advantages of polyimide that we found are that is an excellent film former. However, polyimide films were brittle and when HPA was added, the broke more easily. The highest HPA content that could be added was around 5 wt %.

This limited the overall conductivity to lower limits. The mechanical stability of Kapton® was also found to be less at high temperatures.

Polysulfone and polyether sulfone were found to be good film formers as well as were stable at high temperature. Literature shows that polyether sulfone has a  $T_g$  of over  $220^{\circ}\text{C}$  [ref]. This encouraged the use of PES and PSf to make composite membranes.

The pure PES membrane was made and tested for conductivity. The EIS plot is attached in the Appendix A2. The conductivity was found to be  $3.2 \times 10^{-5}$  S/cm. The lowest value of the  $-Z_{\text{img}}$  is taken as point of real resistance. The conductivity is calculated by using that value of real resistance.

70 wt % of phosphomolybdic acid was added to PES to make a membrane. The EIS plot of this membrane is showed in Figure 33 below. All the membrane samples were tested three times for repeatability. A composite membrane was made from PES and 70% HPW and the EIS data is shown in the Appendix A-2.

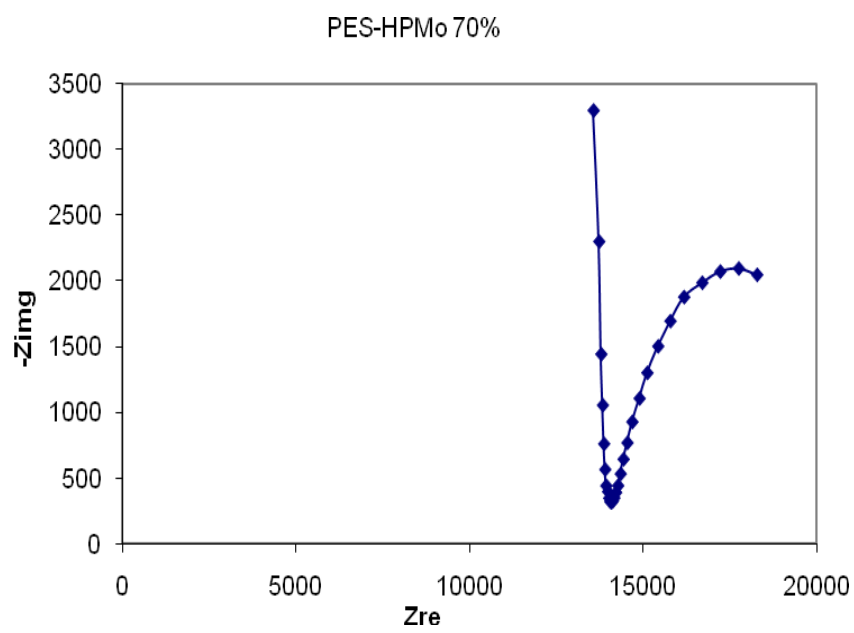


Figure 33: Nyquist plot of PES- 70wt% HPMo

The thickness of the membrane was about 0.358mm and the width of the sample was about 12.16mm. The conductivity was found to be  $5.1 \times 10^{-2}$  S/cm. 50 wt % of SiWA was added to PES to make a composite membrane. This membrane was very non-



**Figure 34: Picture of SPES- 50% SiWA**

homogenous and large clusters of HPA along with holes were observed. This is due to the saturation limit of the HPA amount in the membrane. The membrane was attempted to be prepared several times. A same phenomenon was observed all the times and hence a conclusion was drawn that the membrane cannot hold more than 50 wt % of SiWA, resulting in crystallization. This membrane is shown in **Figure 34**.

The EIS plot is shown in Figure below.

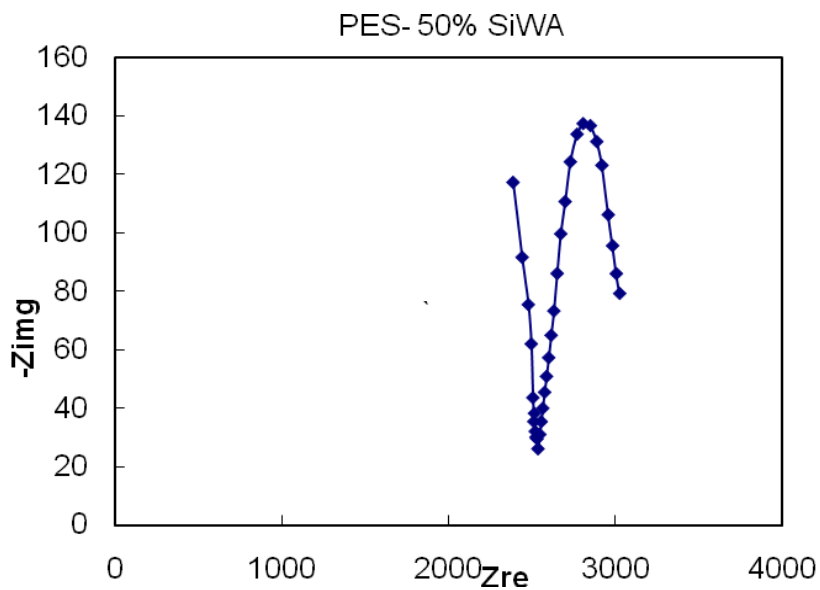
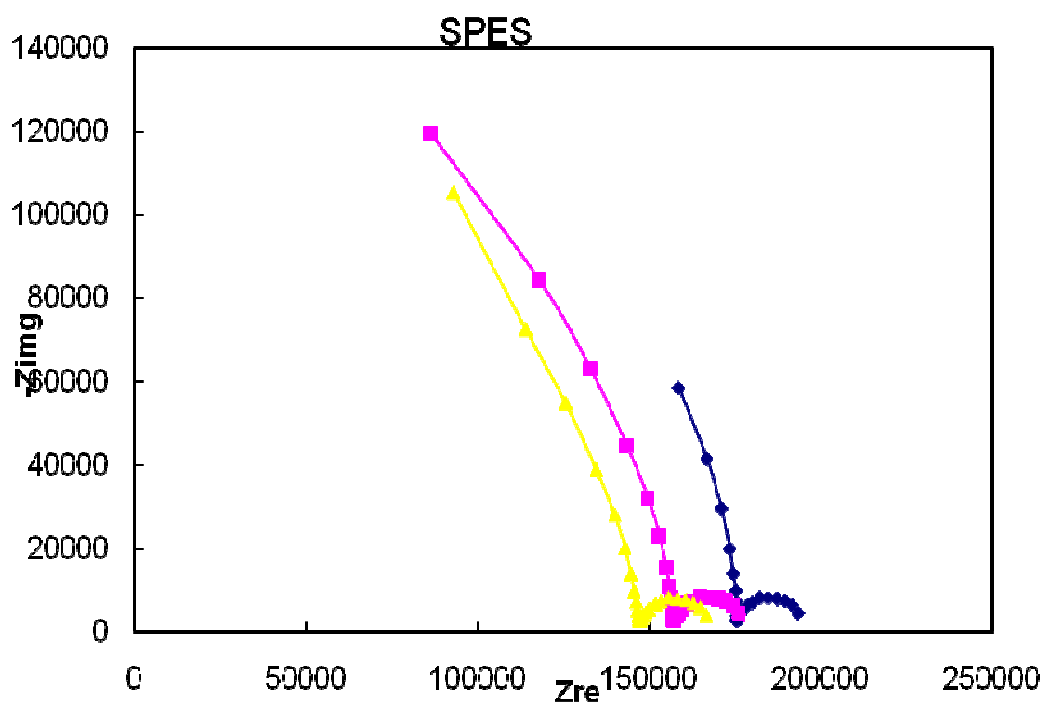


Figure 35: EIS plot of PES- 50% SiWA

This membrane showed a conductivity of  $4.3 \times 10^{-3}$  S/cm.

The polymer was then sulfonated by addition of chlorosulfonic acid. SPES membranes were tested for conductivity by changing the amount of chlorosulfonic acid to the polymer. Also, composite membranes were prepared that were tested for conductivity as well.

Initial results that were obtained for sulfonation using chlorosulfonic acid resulted in a conductivity of  $1.3 \times 10^{-4}$  S/cm. The Nyquist plot for this membrane is shown in the **Figure 36** below. The sample is tested thrice to test for repeatability.



**Figure 36: Nyquist plot of Sulfonated PES (SPES)**

One of the SPES batches was sulfonated with 10 mL of chlorosulfonic acid. Its EIS plot is shown in the **Appendix A-2**. This displayed a conductivity of  $6.9 \times 10^{-4}$  S/cm. The IEC of this membrane was found to be 0.5 meq/gm.

When the amount of chlorosulfonic acid increased to 15 mL the conductivity increased to  $8.1 \times 10^{-4}$  S/cm. The IEC of the membrane was found to be 0.55 meq/mL. The Nyquist plot for this is shown in **Appendix A-2**.



Three curves show three runs that were performed over the membrane to check for its repeatability. The average value of the conductivities was considered to be the final conductivity number.

The amount of chlorosulfonic acid was further increased to 20 mL and the same procedure was followed for calculating the final conductivity of the membrane. The IEC was determined to be 0.67 meq/mL. The Nyquist plot is shown in **Figure 37**.

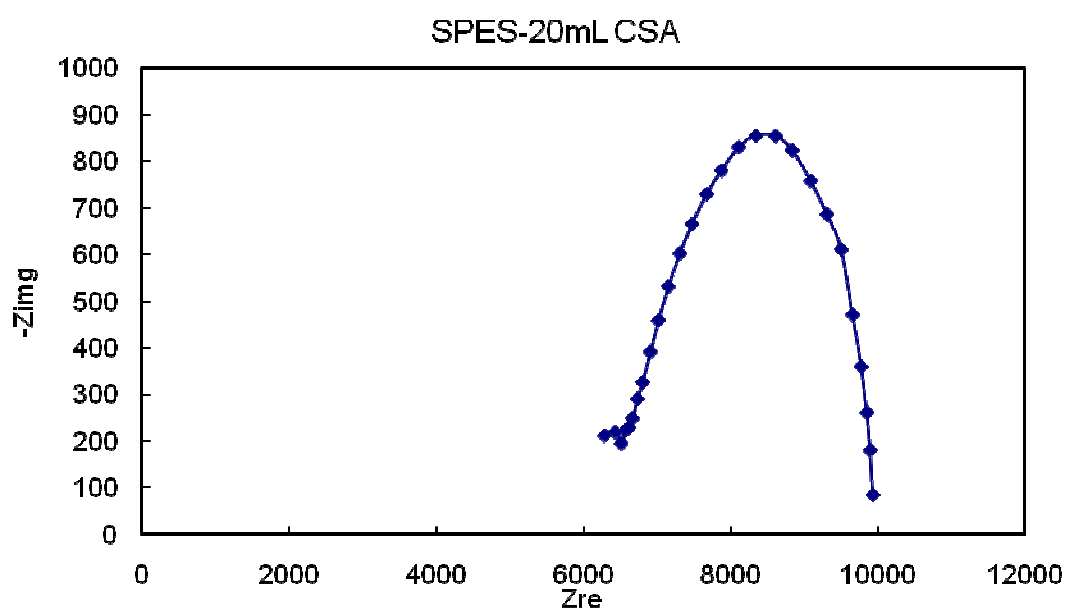


**Figure 37: Nyquist plot of SPES with 20mL CSA**

The conductivity of this membrane was found to be  $3.6 \times 10^{-3}$  S/cm.

The amount of chlorosulfonic acid was further increased and IEC numbers of 0.95 and 1.23 were obtained. The EIS plots are shown in the **Appendix A-2** for these polymers.

The conductivity that was observed for SPES with 0.95 meq/gm of IES was  $2.3 \times 10^{-2}$  S/cm and that with 1.23 meq/gm IEC, it was  $2.5 \times 10^{-2}$  S/cm.

SPES was mixed with 30 wt % of SiWA and cast as a membrane. This membrane was tested for its conductivity and was found to be  $6.1 \times 10^{-3}$  S/cm. this is shown in the EIS plot in the **Appendix A-2**. Composite membrane was also made with 60 wt % of PWA. This membrane displayed a conductivity of  $1.7 \times 10^{-2}$  S/cm. It can be observed that the EIS plot consists of two curves that look similar to semicircles. Electrochemically, it is possible that the circuit consists of a resistor and a capacitor in parallel to each other and further in series with another resistor and capacitor couple that is in parallel to each other. Each semicircle represents a couple of R and C that are in parallel with each other.

Polysulfone was sulfonated by the process mentioned earlier and was made a composite membrane with 30% SiWA. This resulted in a conductivity of  $2.1 \times 10^{-3}$  S/cm.

PBI is found to be a good proton conductor and also is high temperature resistant. The PBI powders that were obtained were blended with PES and SPES. This was done because the SPES and PES were good film formers and the addition of PBI was expected to increase the overall temperature stability and conductivity. To PES, 40 wt % of PBI was added. To this solution, 60 wt % SiWA was added. The conductivity of the membrane was determined to be  $2.8 \times 10^{-2}$  S/cm. The EIS plot of this is shown in **Figure 38**.

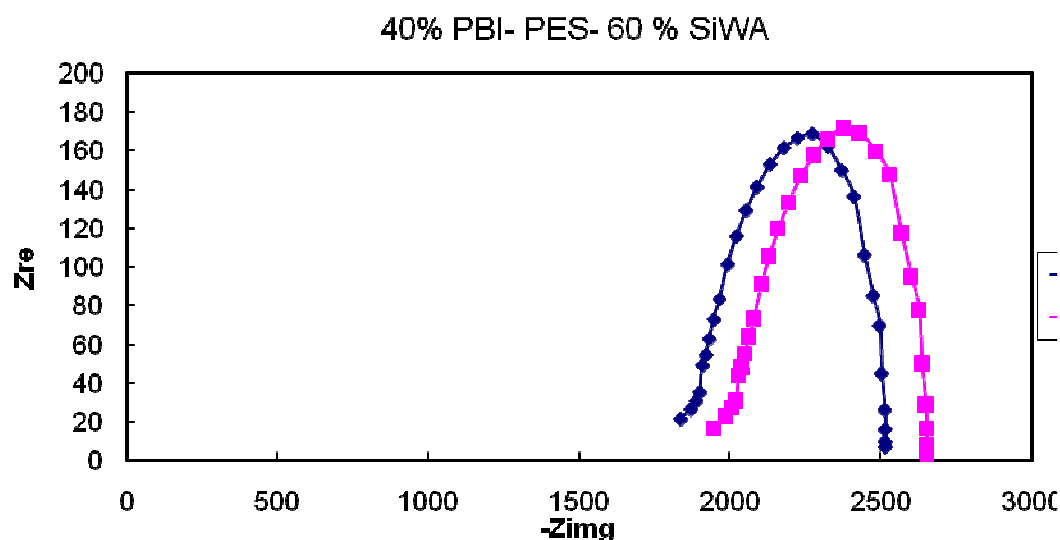


Figure 38: EIS plot of 40% PBI-PES- 60wt% SiWA

A 40 % SiWA blended composite membrane was synthesized with PES and PBI. The membrane was acid doped and was found to have a conductivity of  $2.1 \times 10^{-2}$  S/cm. The membranes results before and after acid doped were obtained.. The conductivity of the membrane before acid doping was  $4.4 \times 10^{-4}$  S/cm. the conductivity improved after acid doping it in 85 % phosphoric acid to  $4.3 \times 10^{-3}$  S/cm. The EIS plot is attached in the **Appendix A-2**.

Polyether sulfone quinoxaline was synthesized and cast as a film. This membrane was tested for conductivity before and after and acid doping. Since the polymer was difficult to resynthesize, just one membrane was tested at first. This is because of the experimental difficulties encountered during the polymerization process.

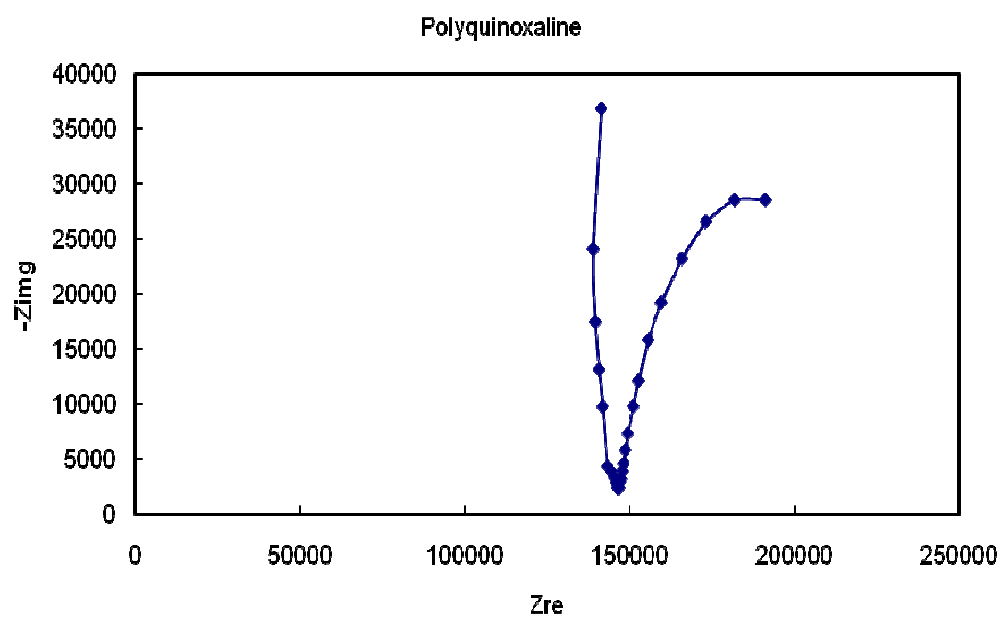


Figure 39: EIS plot of poly ether sulfone quinoxaline

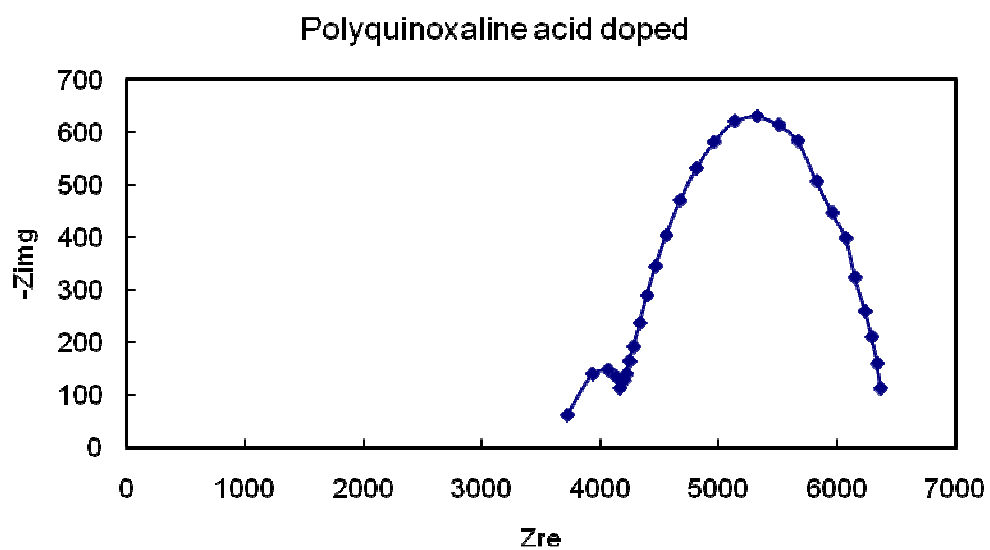
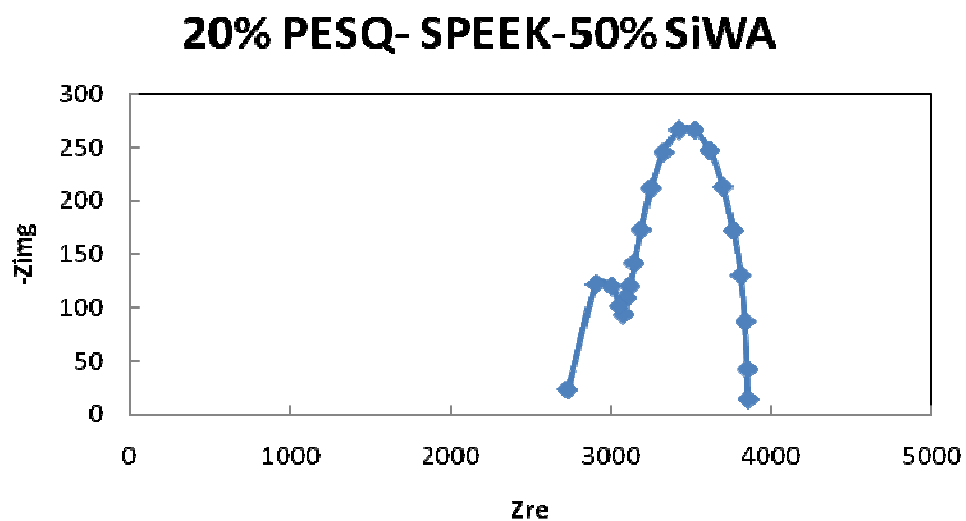


Figure 40: EIS plot of acid doped polyether sulfone quinoxaline

Sulfonated PEEK was synthesized as mentioned in the procedure earlier. This polymer was cast into a film and was also mixed with HPA to composite membranes. The conductivity of SPEEK-50 wt % HPW was found to be  $1.5 \times 10^{-2}$  S/cm.

Membranes were cast with pure polyether sulfone quinoxaline, but the membrane was highly brittle and was attached to the Teflon mold. On an attempt to scrape the membrane, from the mold, the membrane would break in small pieces. This is because of average molecular weight of the polymer was lower than the commercial polymers that yield a film. It was in an intermediate molecular weight polymer that would form film over the mold, but would not result in a proper membrane by itself. Because of this fact, the polymer was blended with SPEEK to make a blended membrane.

20 wt % Polyether sulfone quinoxaline was blended with SPEEK and made a composite with 50 % HPW. This membrane was tested for conductivity and was found to be  $6.4 \times 10^{-2}$  S/cm. The conductivity of the blended membranes with polyether sulfone quinoxaline was found to be higher than that for SPEEK- 50% HPW composite membrane. The membrane conductivity of the SPEEK-50 wt % HPW was found to be  $1.5 \times 10^{-2}$  S/cm. This increase in conductivity can be attributed to the presence of HPA particles and to nitrogen groups in the polyether sulfone quinoxaline structure. The presence of lone pair of electrons will help in better conduction of protons. The Nyquist plot is shown in the **Figure 41**.



**Figure 41: EIS plot of 20% PESQ- SPEEK-50% SiWA**

Composite membrane with 32% SPEEK, 40% PESQ and 48% HPW was synthesized. This membrane was tested for its performance. The results are reported in the section on polarization curves.

The results are tabulated in the **Table7** below:

**Table 7: Summary of results**

<i>Polymer</i>	<i>Conductivity (S/cm)</i>
<i>PES (pure)</i>	$3.2 \times 10^{-5}$
<i>PSf (pure)</i>	$8.1 \times 10^{-5}$
<i>SPES (0.67)</i>	$3.6 \times 10^{-3}$
<i>SPES (1.23)</i>	$2.5 \times 10^{-2}$
<i>SPES- 60% PWA</i>	$1.7 \times 10^{-2}$

<i>70 wt % PMA- PES</i>	$1.8 \times 10^{-3}$
<i>60% PWA-PES</i>	$0.8 \times 10^{-3}$
<i>50% SiWA (non-coated)- PES</i>	$4.3 \times 10^{-3}$
<i>60% PWA- PES- PBI (10% of PES) acid doped</i>	$6.7 \times 10^{-3}$
<i>40% SiWA – PES- PBI(10% of PES) acid doped</i>	$1.4 \times 10^{-3}$
<i>60% PWA – PES- PBI (40% of PES) acid doped</i>	$2.78 \times 10^{-2}$
<i>PES- PES (sulfonated monomer)- 60% PWA</i>	$1.0 \times 10^{-2}$
<i>3.4 % PWA- Polyimide- acid doped</i>	$2.5 \times 10^{-3}$
<i>SPEEK sulfonated using H<sub>2</sub>SO<sub>4</sub></i>	$6.0 \times 10^{-3}$
<i>SPEEK – 50% SiWA</i>	$1.5 \times 10^{-2}$
<i>PES- polyether sulfone quinoxaline</i>	$9.6 \times 10^{-3}$
<i>SPEEK- polyether sulfone quinoxaline (20%) – 50 % HPW</i>	$4.8 \times 10^{-2}$

### 4.3 Matrix Assisted Laser Desorption Ionization – MS

MALDI at UNR was carried out using dithranol,  $\alpha$ - cyanocinnamic acid and HABA as matrices. Spectra were obtained for various polymer samples of polysulfone and polyether sulfone quinoxaline at varying mass ranges. Some of the results are shown in Figures 42-54 below.

#### *Plain dithranol matrix*

Applied Biosystems 4700 Proteomics Analyzer 7007

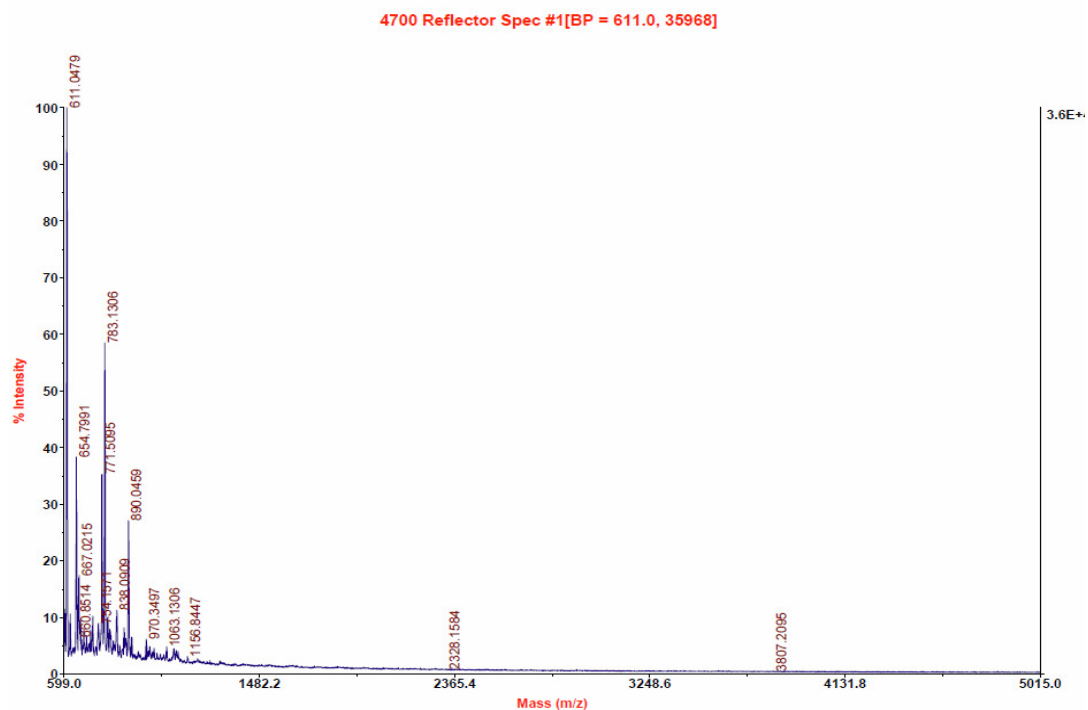


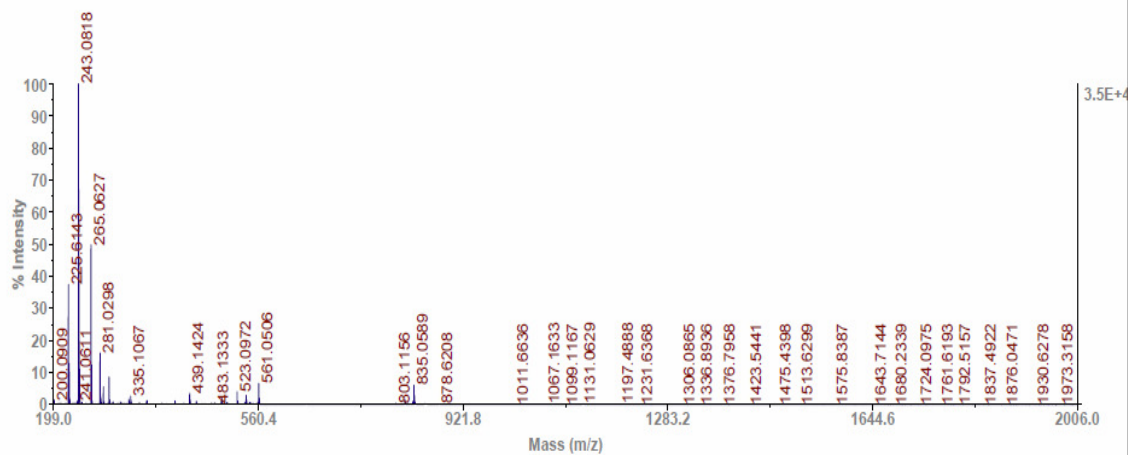
Figure 42: Spectra of dithranol matrix



**HABA matrix**

Applied Biosystems 4700 Proteomics Analyzer 7007

4700 Reflector Spec #1[BP = 243.1, 35042]



4700 Reflector Spec #1[BP = 243.1, 35042]

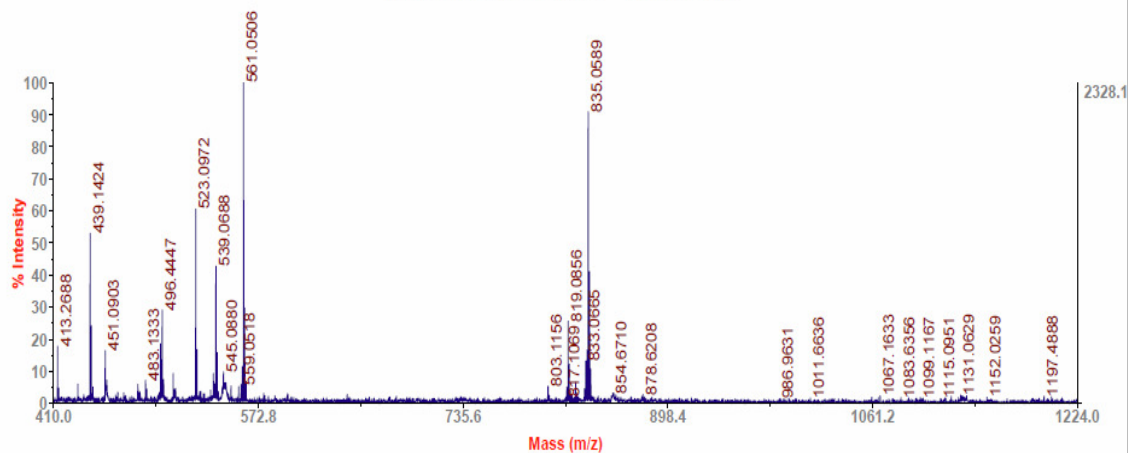


Figure 43: Mass spectra of HABA matrix

**PSf- Dithranol matrix:**

The MALDI was run in reflector positive mode from 600 to 5000 Da. 2000 shots were collected. S/N threshold was 3 and the cluster area S/N optimization was enabled (S/N threshold 10). Figure 44 below shows the spectrum obtained and was determined to have multiple peaks with a difference of 442 Da which is the repeat unit mass.

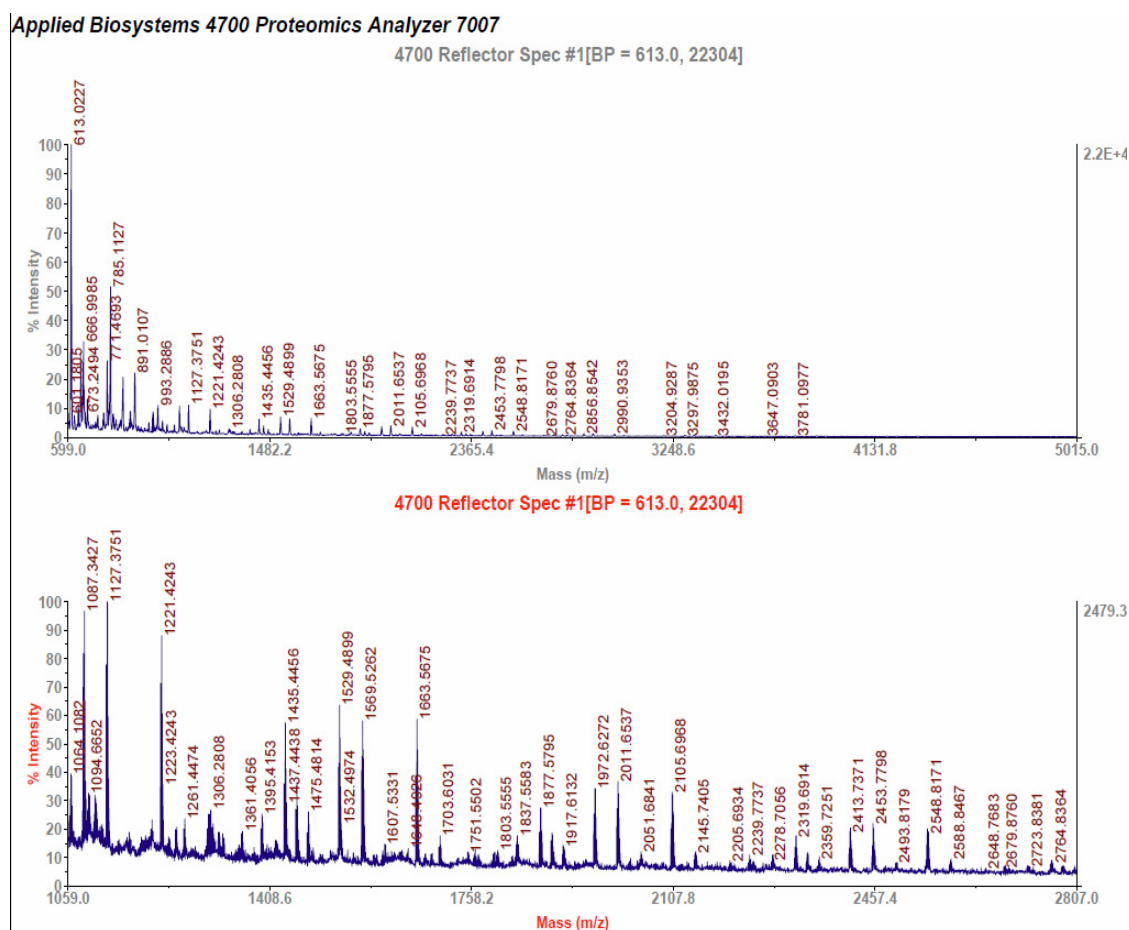


Figure 44: : PSf- tested with dithranol spectra

### PSf- $\alpha$ - cyanocinnamic acid matrix

Polysulfone that was synthesized was also tested by using  $\alpha$ - cyanocinnamic acid as a matrix. Figure 45 and 46 are the spectra at various ranges. It is evident in Figure 45 that at high molecular weight, the spectra has more noise and distinct peaks cannot be seen.

#### Applied Biosystems 4700 Proteomics Analyzer 7007

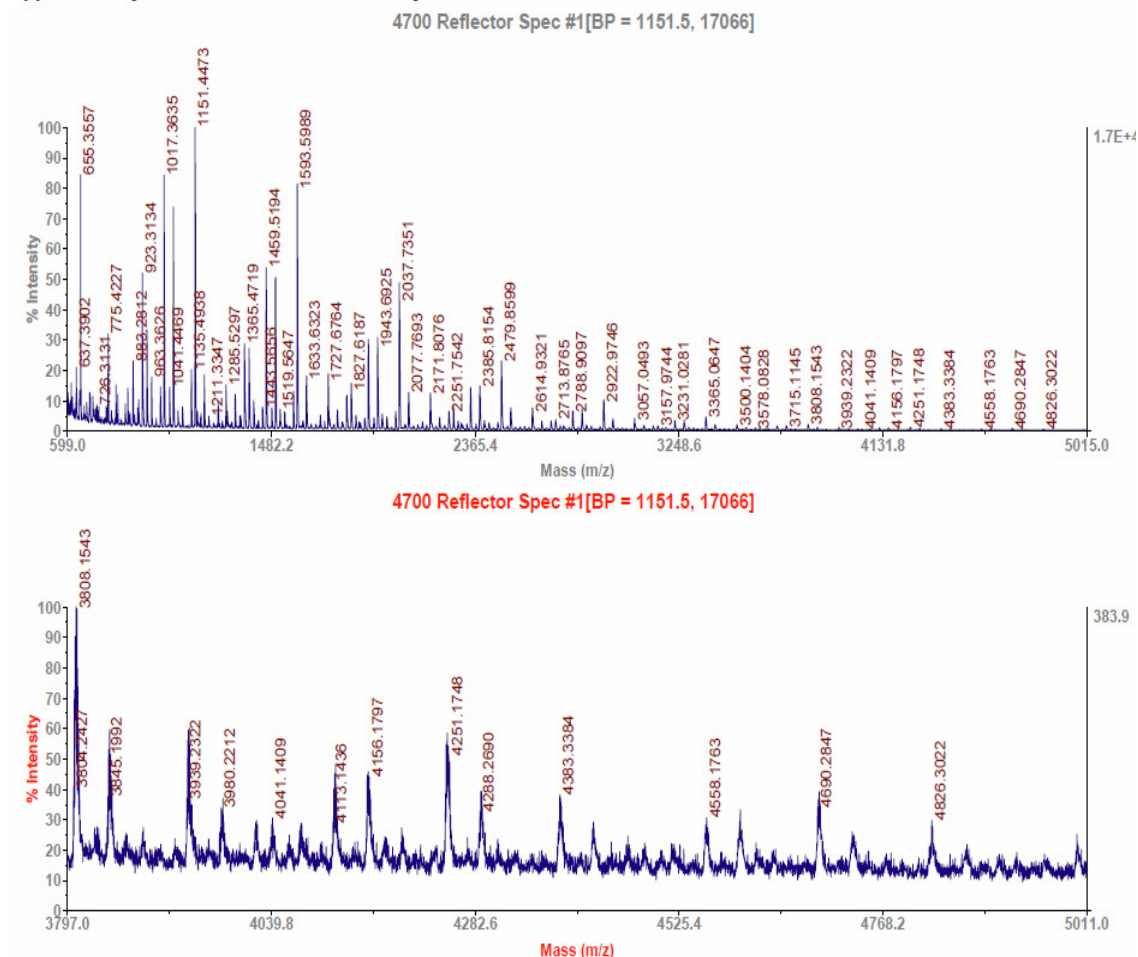


Figure 45: : PSf -  $\alpha$  - cyanocinnamic acid spectra

**PSf-  $\alpha$ -cyanocinnamic acid matrix**

Applied Biosystems 4700 Proteomics Analyzer 7007

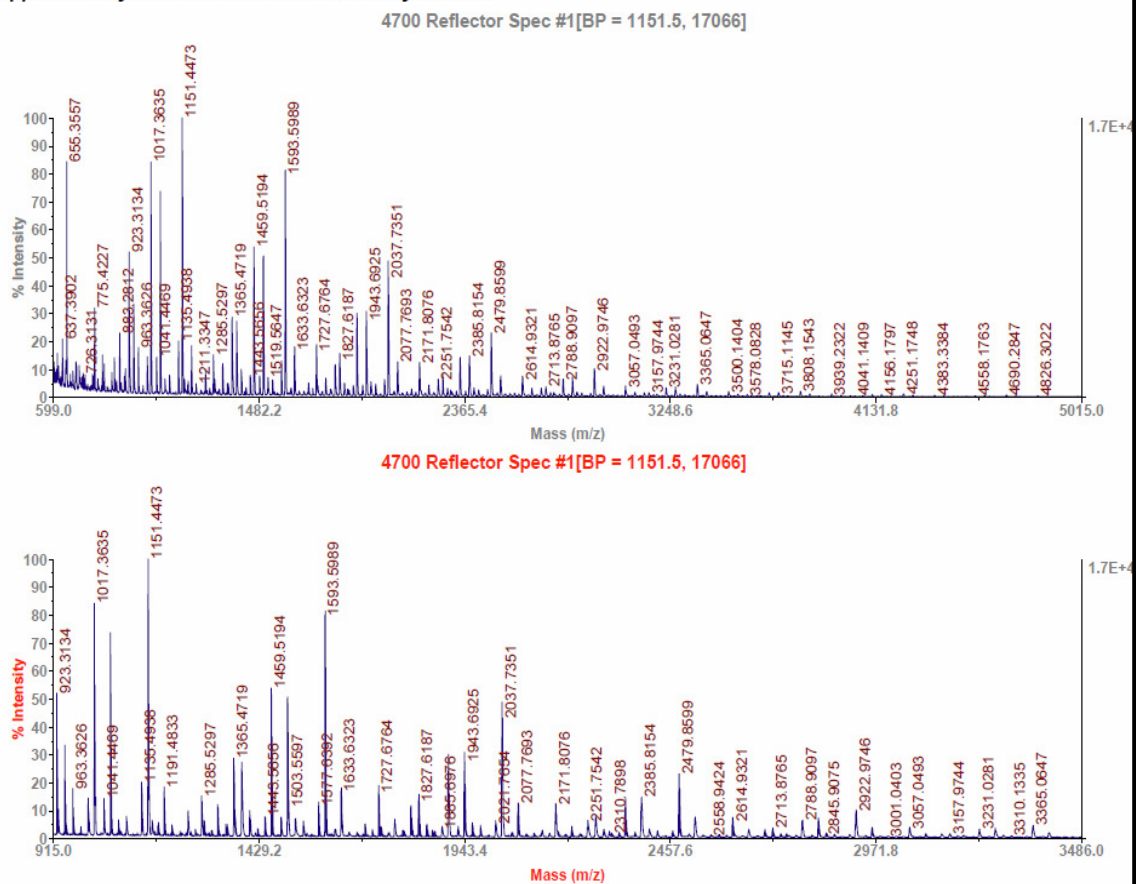


Figure 46: PSf-  $\alpha$ -cinnamic acid spectra

### Commercial PSf:

Polysulfone was obtained from Udel and was tested for its molecular weight. The MALDI-MS of the sample was carried out in positive linear mode. The range was set to be 40,000 to 200,000 Da. 2000 shots were collected and S/N threshold was 50. **Figure 47** shows the structure of commercial PSf and **Figure 48** shows its spectra obtained from MALDI-MS. As was mentioned earlier, higher molecular mass regions resulted in noise.

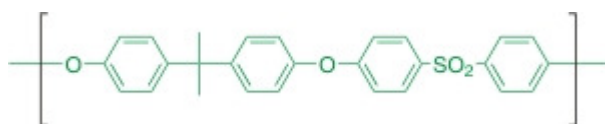


Figure 47: Chemical structure of PSf [13]

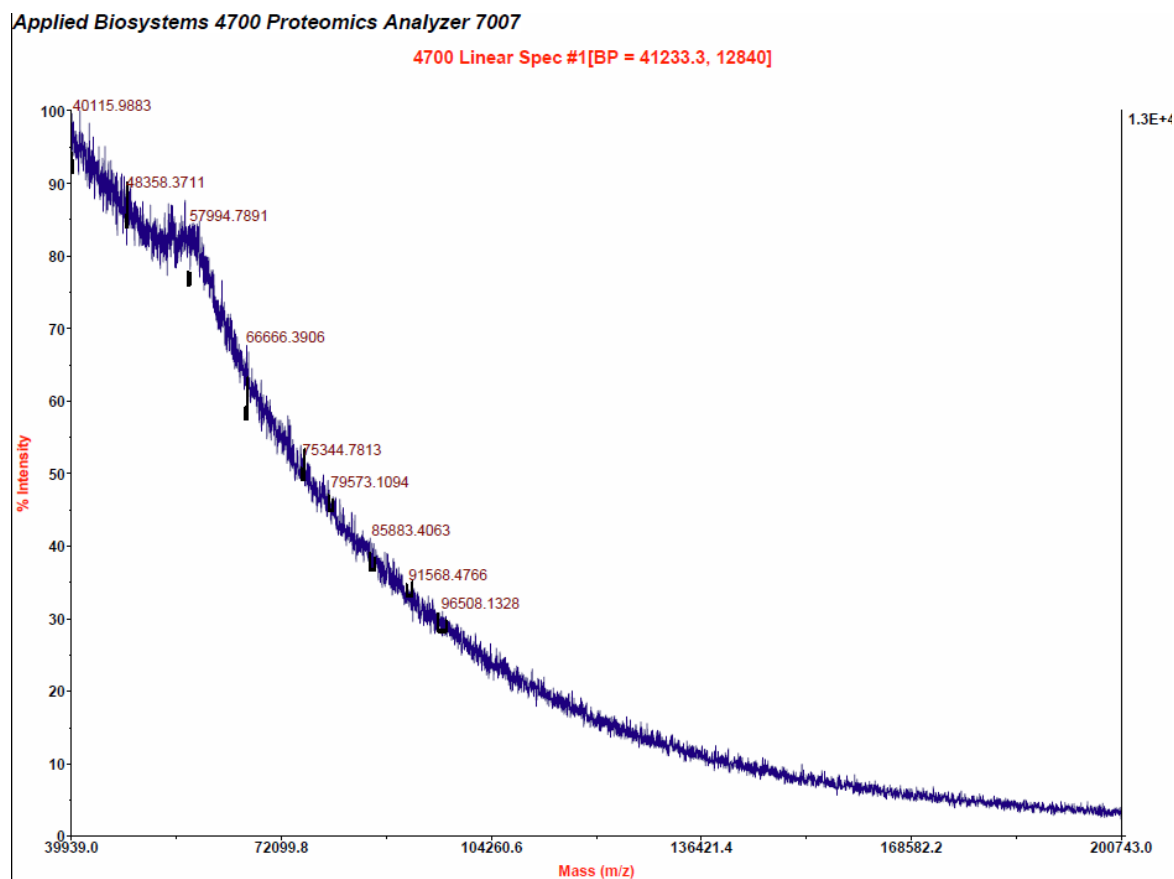


Figure 48: Linear mode spectra of commercial PSf

**Polyquinoxaline based co-polymer with polyether sulfone:** Figure 49 shows the chemical structure of the co-polymer based system and the reaction scheme. The resultant polymer was tested using MALDI-MS and was found to have spectra as shown in **Figure 50**. It is suspected that the molecular weight of the polymer was not much high and might have resulted in oligomers instead of polymers.

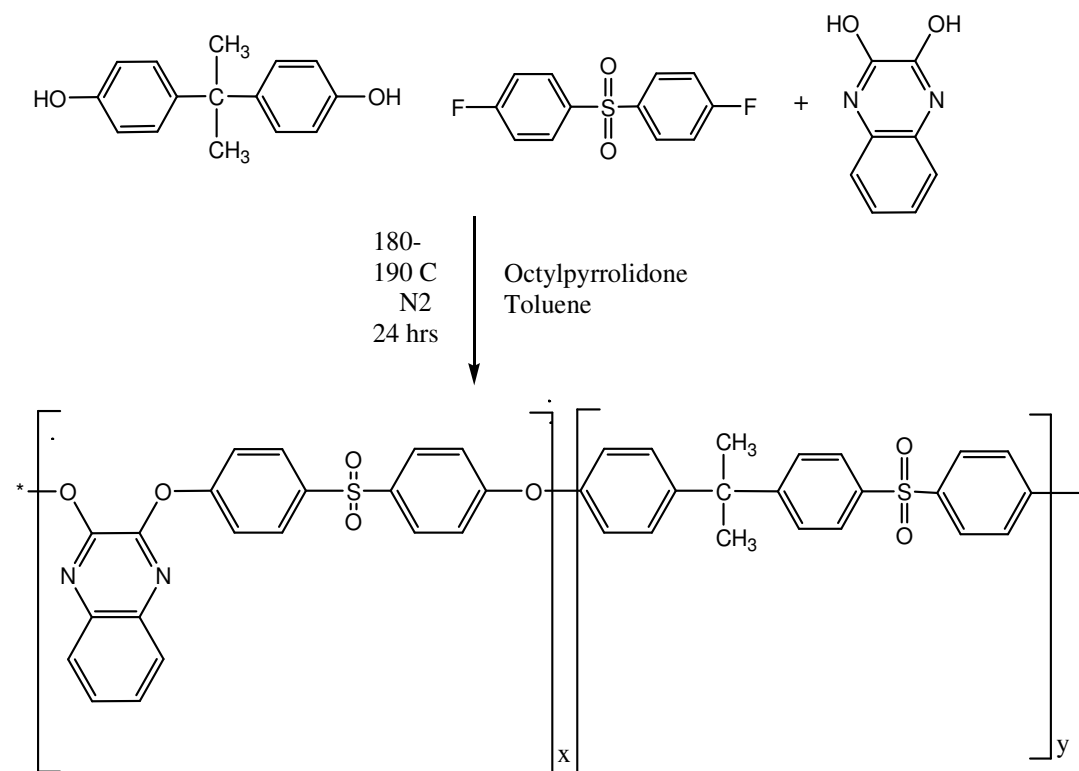


Figure 49: Synthesis of polyether sulfone quinoxaline type I

## Applied Biosystems 4700 Proteomics Analyzer 7007

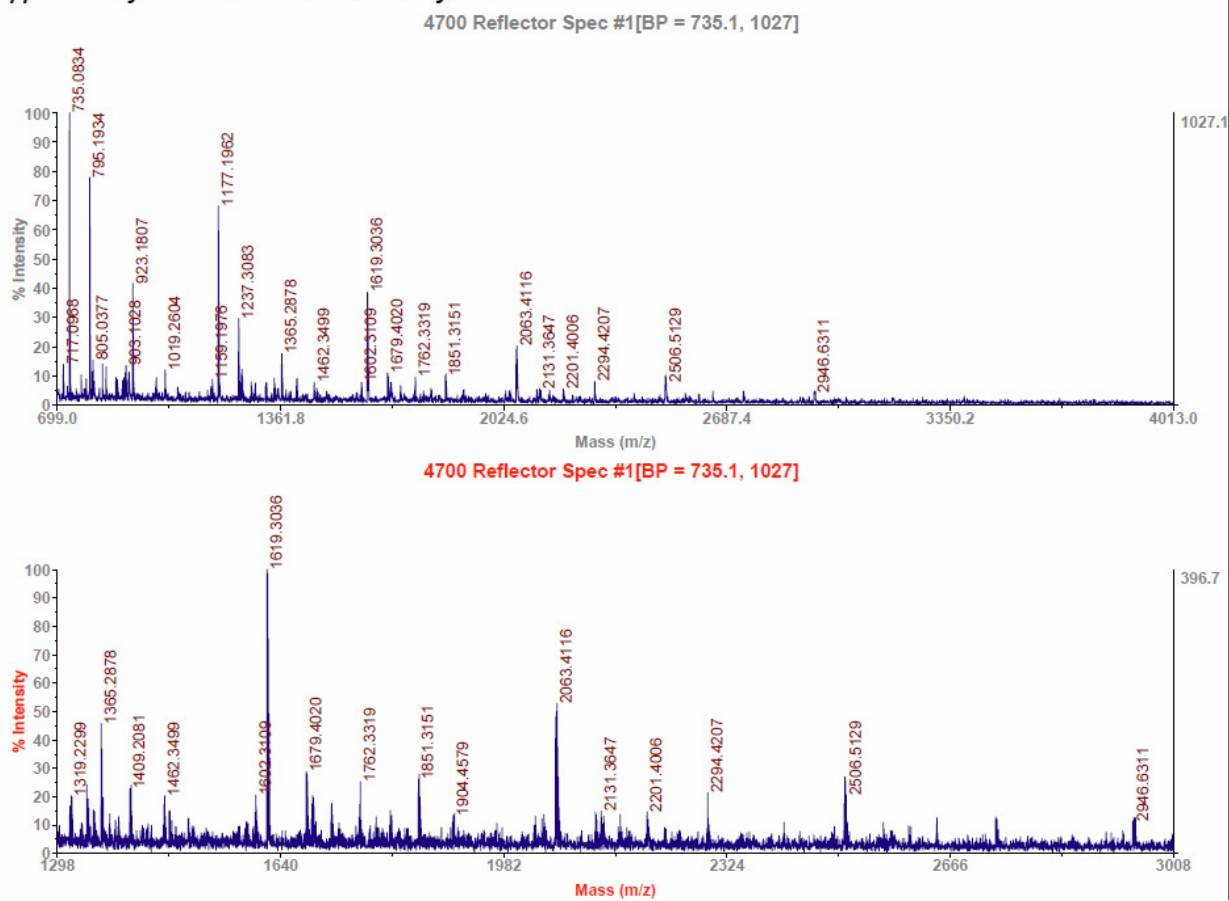


Figure 50: Mass spectra of PESQ Type I

*Polyquinoxaline based polyether sulfone co-polymer*

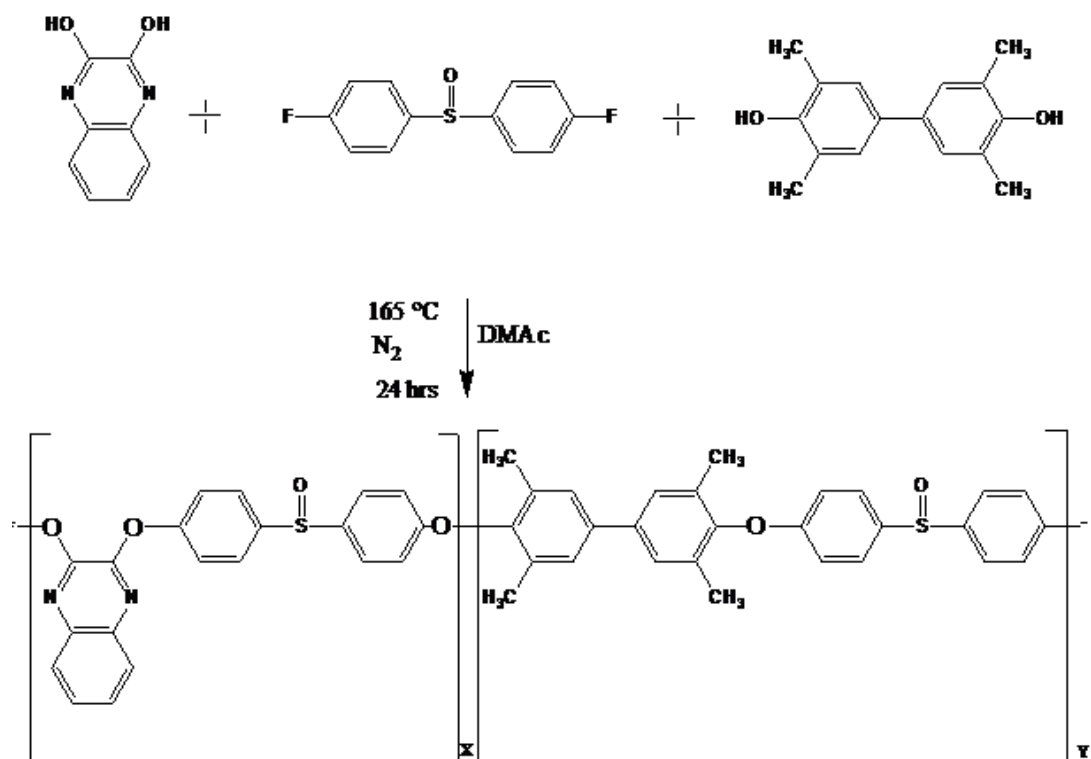


Figure 51: Synthesis of polyether sulfone quinoxaline type II



Applied Biosystems 4700 Proteomics Analyzer 7007

4700 Reflector Spec #1[BP = 735.1, 4478]

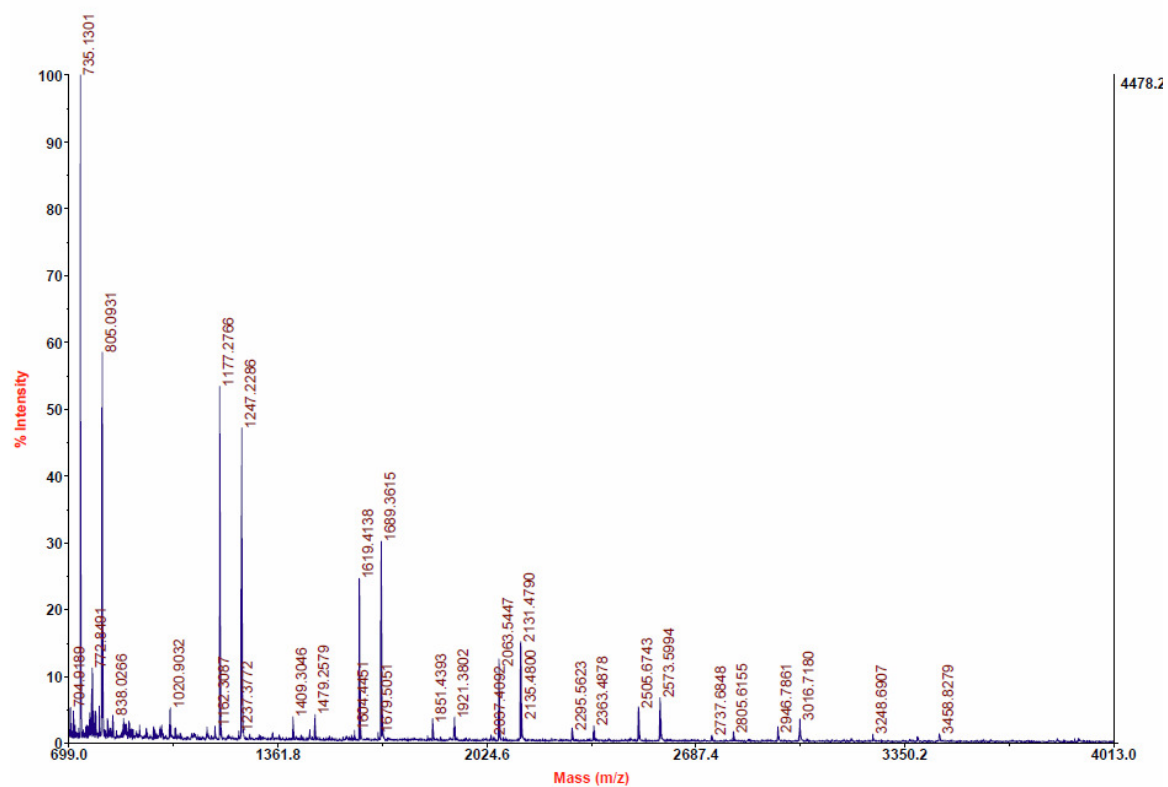
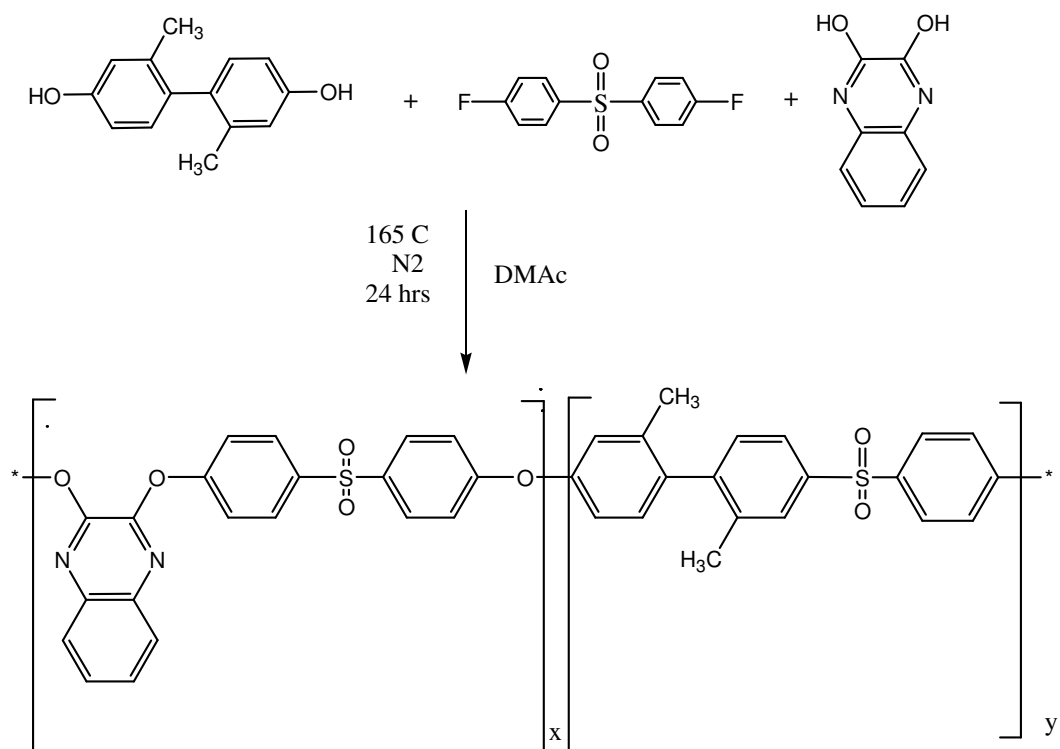


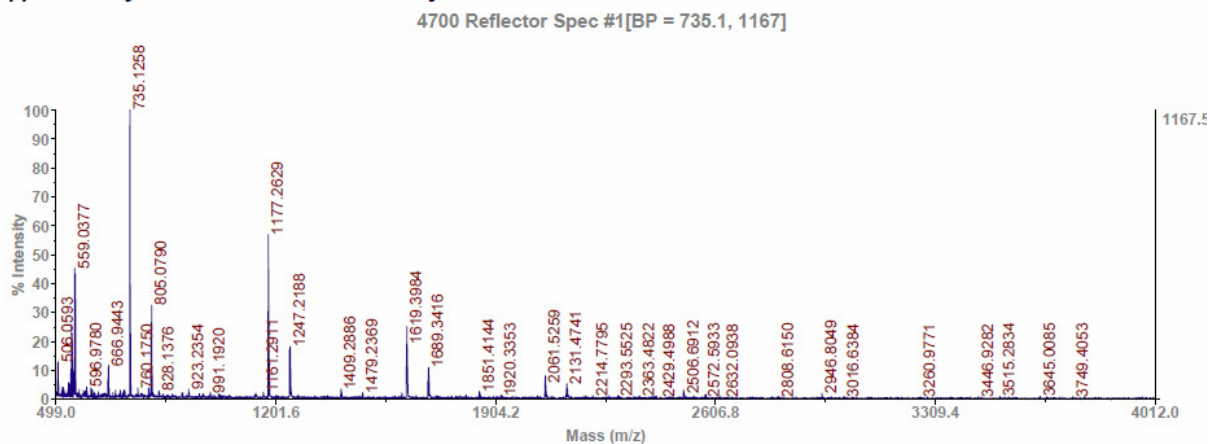
Figure 52: Polyquinoxaline co-polymer in dithranol matrix spectra

**Polyquinoxaline polymer based on polyether sulfone**



**Figure 53: Synthesis of polyether sulfone quinoxaline type III**

## Applied Biosystems 4700 Proteomics Analyzer 7007



4700 Reflector Spec #1[BP = 735.1, 1167]

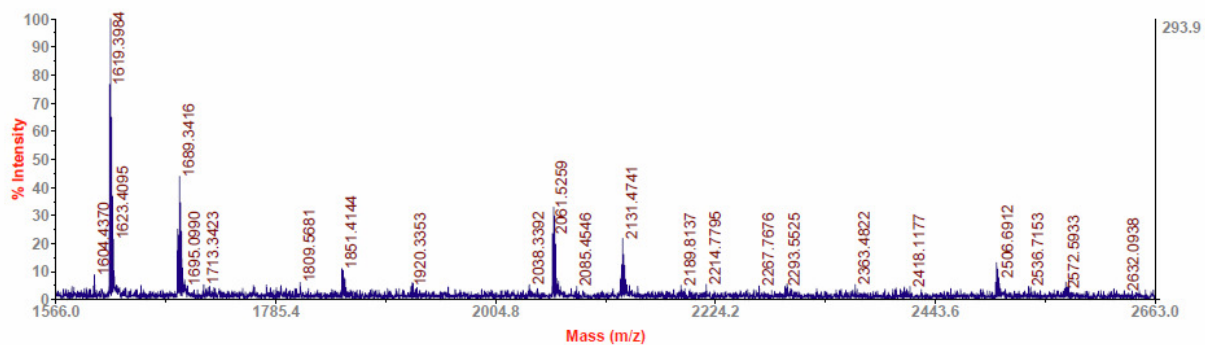
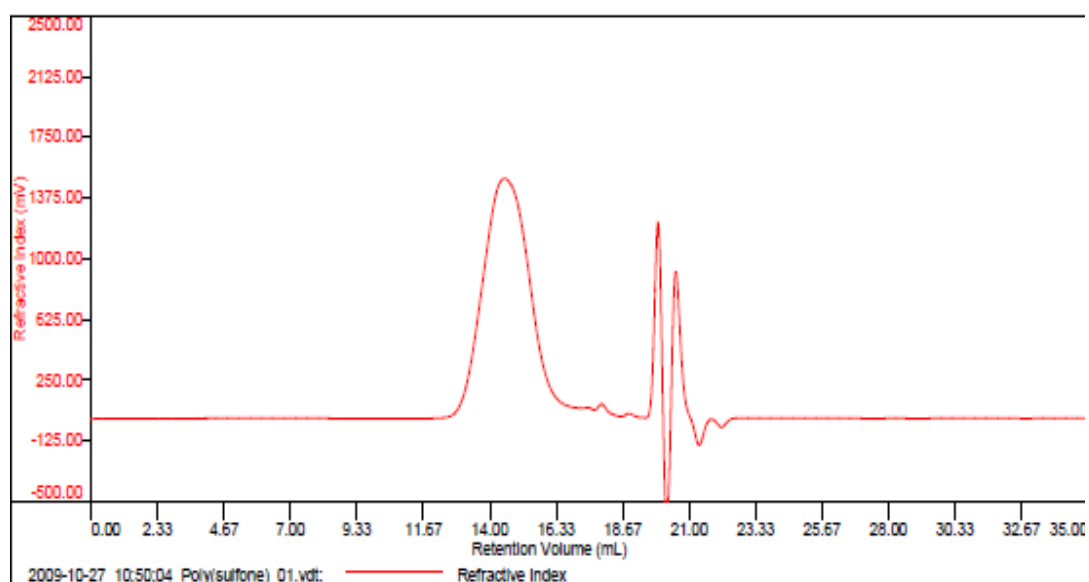


Figure 54: Mass spectra of polyether sulfone quinoxaline type III

#### **4.4 GEL PERMEATION CHROMATOGRAPHY:**

Commercial polysulfone was tested for its molecular weight in a GPC. It was dissolved in THF and was run through the GPC column. The result that was obtained is shown in

**Figure 55.**



**Figure 55: GPC spectra for commercial polysulfone**

The number average molecular weight,  $M_n$  was found to be around 670,000 Da and the mass average molecular weight was found to be around  $2.4 \times 10^6$  Da. The polydispersity index of the polymer was approximately 3.3.

Polyether sulfone quinoxaline was also tested using GPC and the results were compared with the ones obtained for commercial PSf. Depending on the retention volume and after

a comparison is drawn between both, and an approximate analysis is done for the molecular weight.

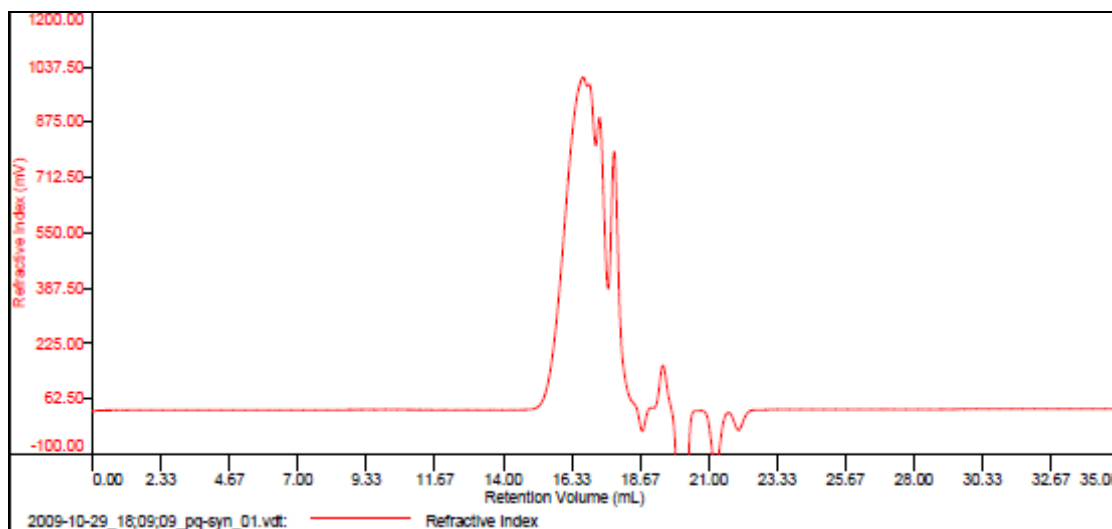


**Figure 56: GPC spectra of polyether sulfone quinoxaline**

The **Figure 56** shows that the number average molecular weight,  $M_n$ , of the polymer is about 21,000 Da and the weight average molecular weight,  $M_w$ , is around 29,000 Da.

The polydispersity index is found to be narrow with 1.3. The results were quantified after standardizing the column with polystyrene standards.

The results for GPC can be summarized in the following **Table 8**:

**Table 8: Results obtained from GPC**

Polymer	Number average molecular weight (Da)	Mass average molecular weight (Da)	Polydispersity index
Polysulfone	670,000	$2.4 \times 10^6$	3.3
Polyether sulfone quinoxaline	21,000	29,000	1.3

#### **4.5 Single Membrane Fuel cell Test:**

Performance of a composite membrane based on SPEEK and 50% HPW was tested. The



**Figure 57: A sample MEA**

membrane electrode assembly was made and hot pressed on the membrane. The MEA was fixed in the fuel cell fixture. An MEA is shown in **Figure 57**. A polarization plot was obtained from a composite membrane that was prepared by SPEEK and 50 wt % PWA.

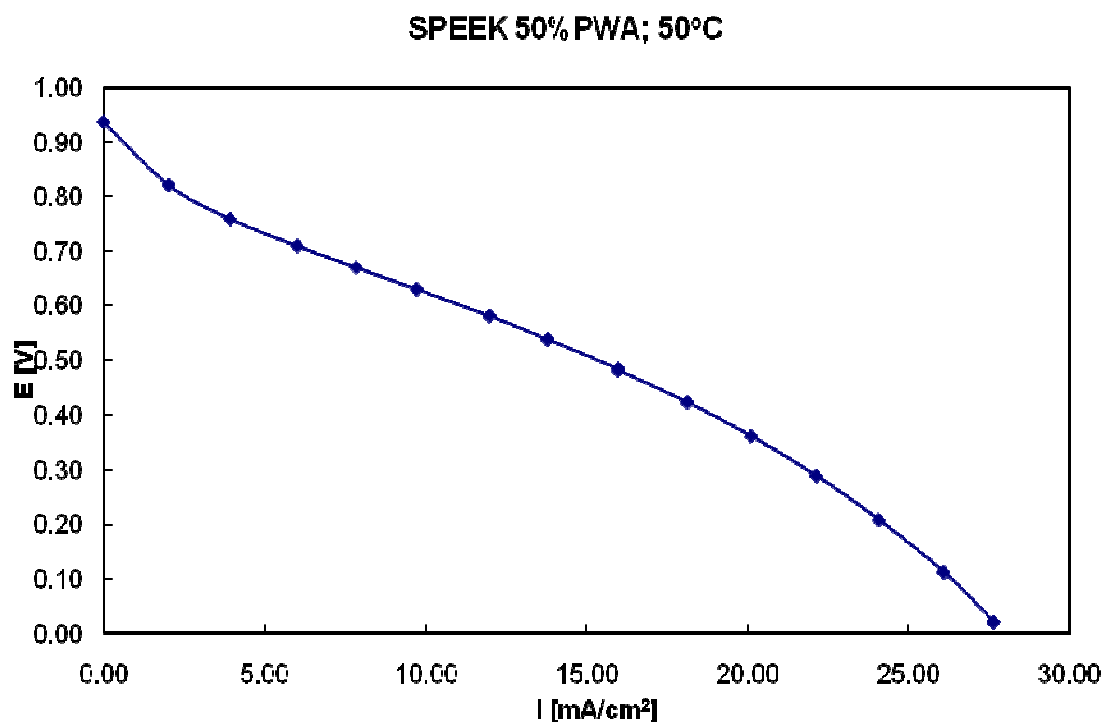
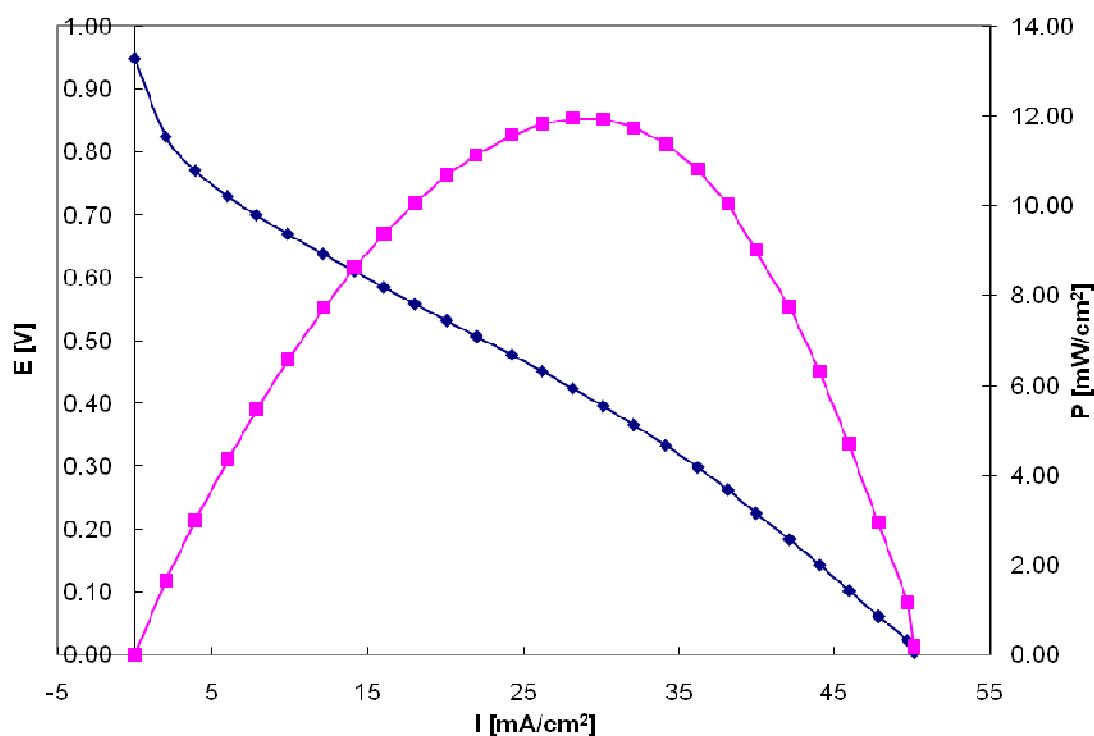


Figure 58: Polarization curve obtained from SPEEK- 50% PWA membrane at 50°C

A current density of almost 28 mA / cm<sup>2</sup> was observed, which is significantly less than Nafion®. In **Figure 58**, it is observed that the ohmic losses are lower since the higher currents are controlled by ohmic losses. On comparing the results with the general polarization plots mentioned in the characterization section, few conclusions can be drawn. At the highest current, the mass transport comes into play, which in this case is lower too. There is no steep decrease in voltage at the mass transport area, indicating that the membrane mass transport is limited. This can be due to low conductivity of membrane and the ohmic losses are due to catalytic layer contact.

SPEEK was blended with 40% PESQ and 48% HPW and was tested for its performance. The overall current density was observed to be higher with the addition of 40 wt %PESQ. This increase can be attributed to an increase in conductivity and better catalyst bonding. The maximum power density was found to be about 12mW/ cm<sup>2</sup>. The ohmic losses are higher in this case which is due to AC impedance that originates from relative humidity dependant resistance to proton conduction through the membrane. The polarization curve of this membrane is shown in **Figure 59**.



**Figure 59: Polarization curve of 40% PESQ- 38% SPEEK and 42% HPW**



#### 4.6 Thermogravetric Analysis (TGA):

TGA is used to analyze the thermal behavior of the polymer and moisture content.

**Figure 60** shows TGA plot of PES. PES shows a slight depression in weight at around 100 C that is because of moisture that leaves the membrane. At around 450<sup>0</sup>C weight loss occurs that continues up till 550<sup>0</sup>C. That can be associated with the degradation of the polymers.

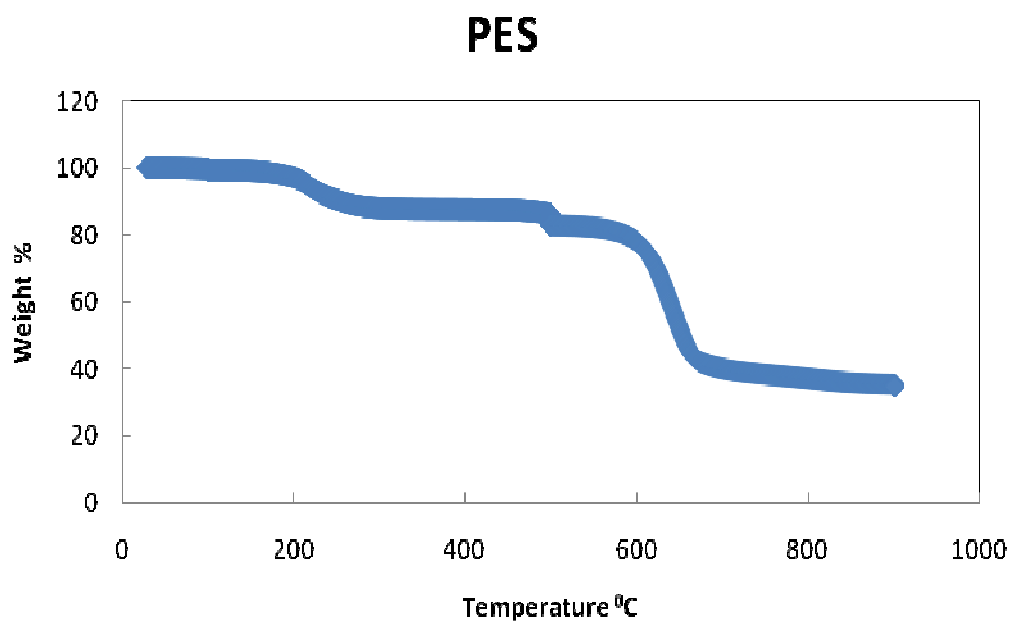


**Figure 60: TGA of pure PES**

For SPES, there is a similar weight loss at around  $100^{\circ}\text{C}$  that is associated to moisture loss. There is not huge quantity of moisture and hence a small loss in weight is observed.

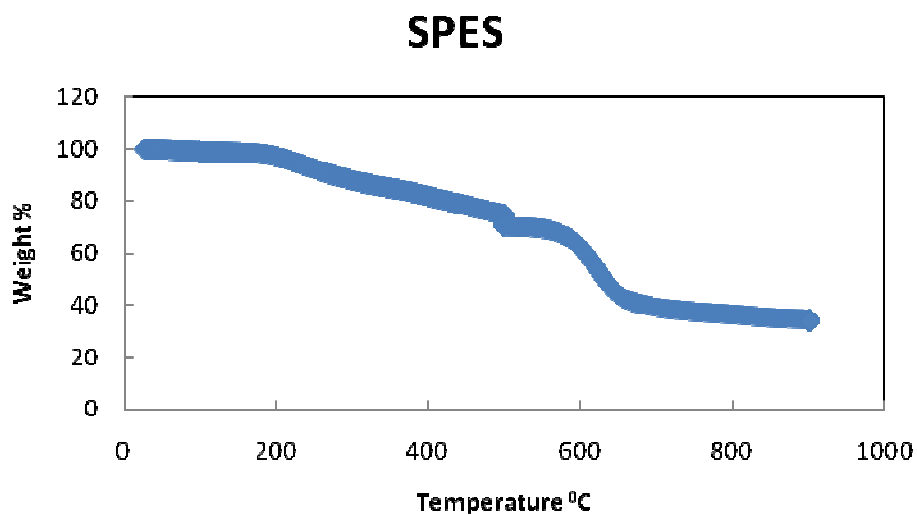


Figure 61: TGA plot of SPES

However, a steady weight loss is observed from  $185^{\circ}\text{C}$ . This steady decrease is due to the loss of sulfonic groups. Finally, the polymer degrades at around  $550^{\circ}\text{C}$ .

For composite membranes, multiple weight loss regions were observed that associated to loss of sulfonic acid group but overall better temperature stability. Major weight loss regions were observed after 350<sup>0</sup>C. A more stable decrease in temperature was observed for SPES- 50% SiWA. The membrane was found to be more thermally stable till 500<sup>0</sup>C. There was a small weight loss at 500<sup>0</sup>C, followed by another sudden weight loss at 555<sup>0</sup>C. This can be associated to the degradation of polymer. This occurs at high temperature of the membrane which is sulfonated and has HPA content in it.

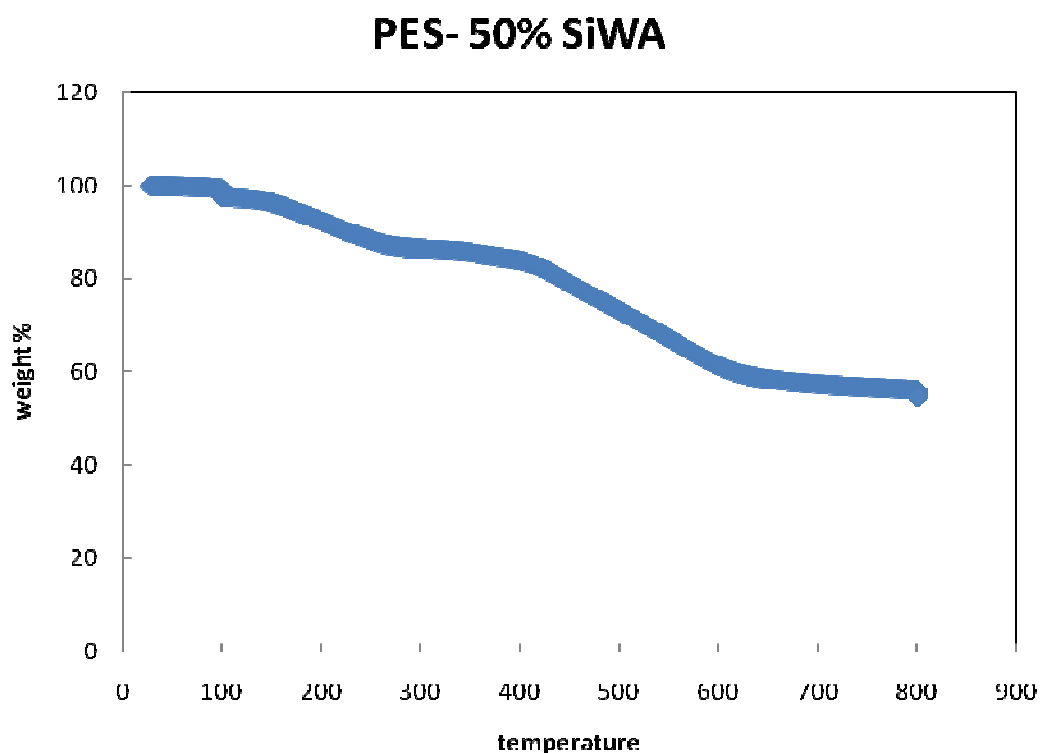
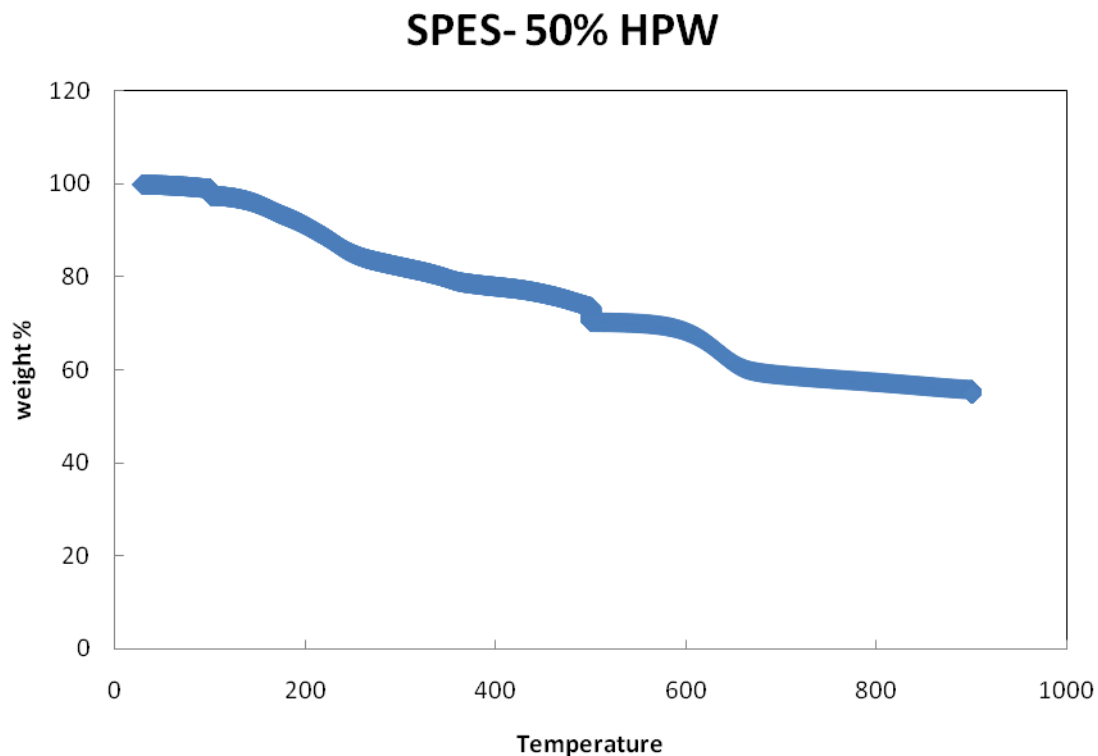


Figure 62: TGA plot of composite PES - 50wt % SiWA



**Figure 63: TGA plot obtained for SPES-50wt% HPA**

Polyethersulfone quinoxaline sample was tested for its thermal stability using TGA.

**Figure 63** shows the TGA plot obtained. There is a weight loss at around 98<sup>0</sup>C. This is associated to the loss of moisture. A major weight loss of about 49% starts at around 450<sup>0</sup>C. It can be due to the polymer chain degradation. Thus, the polyethersulfone quinoxaline is stable thermally till 450<sup>0</sup>C. This is ideal to be used in fuel cells because of the increased conductivity and the thermal stability.

## Polythersulfone quinoxaline

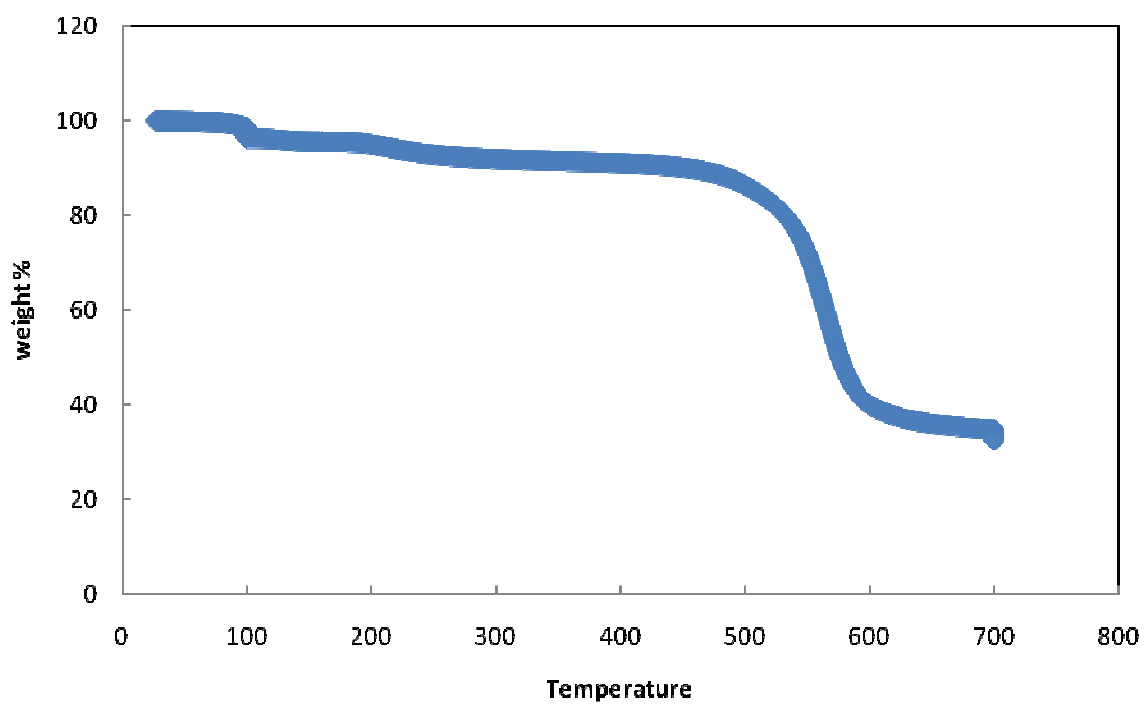


Figure 64: TGA of polyether sulfone quinoxaline type I

## CONCLUSIONS

Various polymers were investigated which are used as proton exchange membranes in fuel cells. Study was carried out on various methods of sulfonation and increasing the proton conductivity of the membrane. Polymers were sulfonated using acetyl sulfate, chlorosulfonic acid and by using fuming sulfuric acid. Doping of the membranes was also performed to increase the overall proton conductivity. However, it was observed that this was a temporary method of sulfonating, since it is subjected to leaching in water.

Sulfonated membranes were synthesized that were a composite with HPAs. Various types of HPAs were tested during the course of the project and compatibility was studied with the base polymer. The membranes were tested and characterized for their properties. Proton conductivity and performance of the membranes were tested and the results were reported. Highest conductivity of  $4.8 \times 10^{-2}$  S/cm was observed for a composite blend membrane.

Synthesis of novel polymers was performed as possible candidates for PEMs. Initial literature review revealed the use of polyquinoxalines in optical applications. Novel polymers based on polyether sulfone and polyquinoxaline were developed. The polymer was tested for its molecular weight and its thermal stability. It was showed that the polymer was stable over  $450^{\circ}\text{C}$ . The polymer was blended with sulfonated polymer and it was found that the performance and the proton conductivity increased by addition polyether sulfone quinoxaline to SPEEK. The current density increased from  $25\text{mA}/\text{cm}^2$

to  $50\text{mA}/\text{cm}^2$ . This is especially of important because the higher temperature membranes are being developed and used for fuel cells lately.

## *FUTURE WORK*

Heteropoly acids are soluble in water. When they are added to a membrane, making a composite, the HPAs leach out in water during the fuel cell operation. This is a major problem for the durability of the membranes and also for uniform power generation from the membrane. Also, the amount of HPAs that can be added to a polymer matrix is limited by the interfacial interactions between the polymer and the inorganic conductors. Surface treatment of HPA particles can result in better interfacial interactions, enabling us to add more HPA to the polymer matrix resulting in better proton conductivity. This will also prevent the loss of HPA to water from PEM during its operation. Nanocomposites membranes can be prepared by using methods to make nano particles of HPA with SPEEK. It is believed that it will give better results in terms of proton composites and membrane homogeneity.

While synthesizing novel polymers for the PEM applications for high temperature operation, various problems were encountered. Nucleophilic polycondensation polymerization methods were used to synthesize novel polymers from their monomers. These reactions are highly moisture dependant and will not proceed to maximum conversion in presence of moisture or impurity. Many reactions were carried out, but high molecular weight polymers were not obtained. In future, work can be carried to understand these systems, with the change in the catalyst and in the reaction conditions high molecular weight polymers can be obtained. The purification of monomers and solvents can be performed to eliminate the possible presence of moisture and impurities.



Also, better solvents and better systems can be studied to understand the reaction mechanism. Yields of the polymer formation can be measured.

Some of the new polymers that can be synthesized are shown in **Figure 65** below.

Sulfonated polymers can be prepared from sulfonated monomers and post sulfonation of these will improve the proton conductivity further.

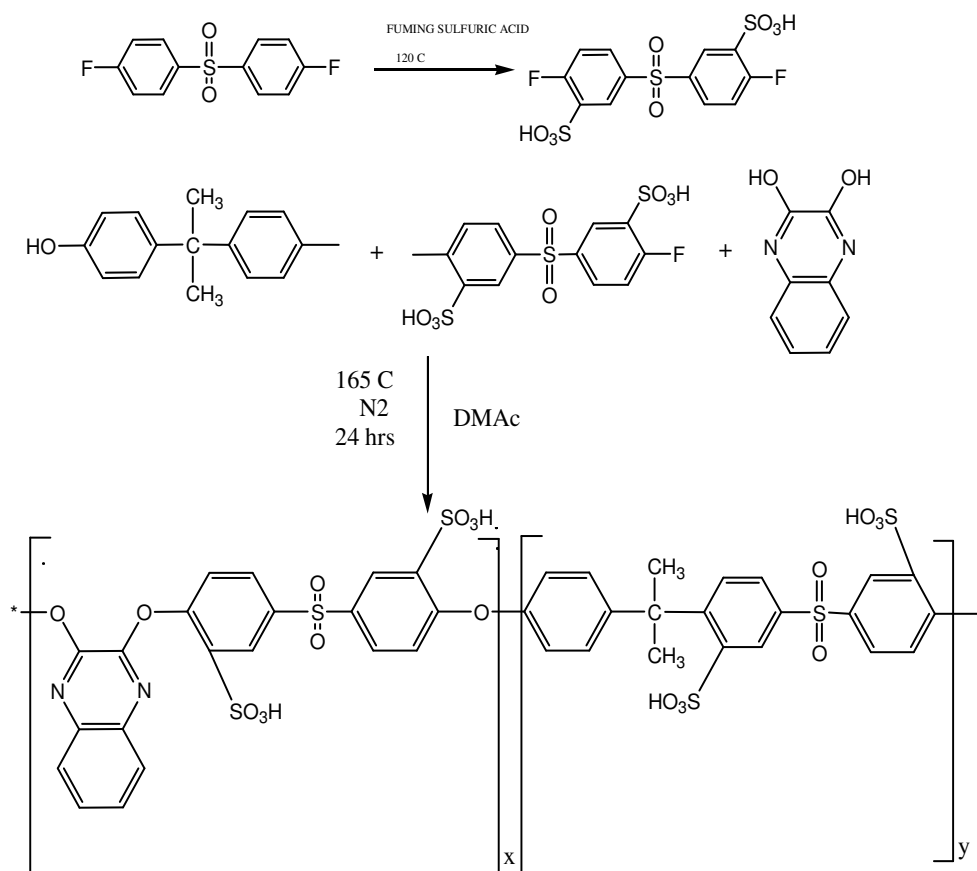


**Figure 65: Sulfonated polyether sulfone quinoxaline**

Sulfonated polysulfone can be synthesized as in shown in **Figure 66**.

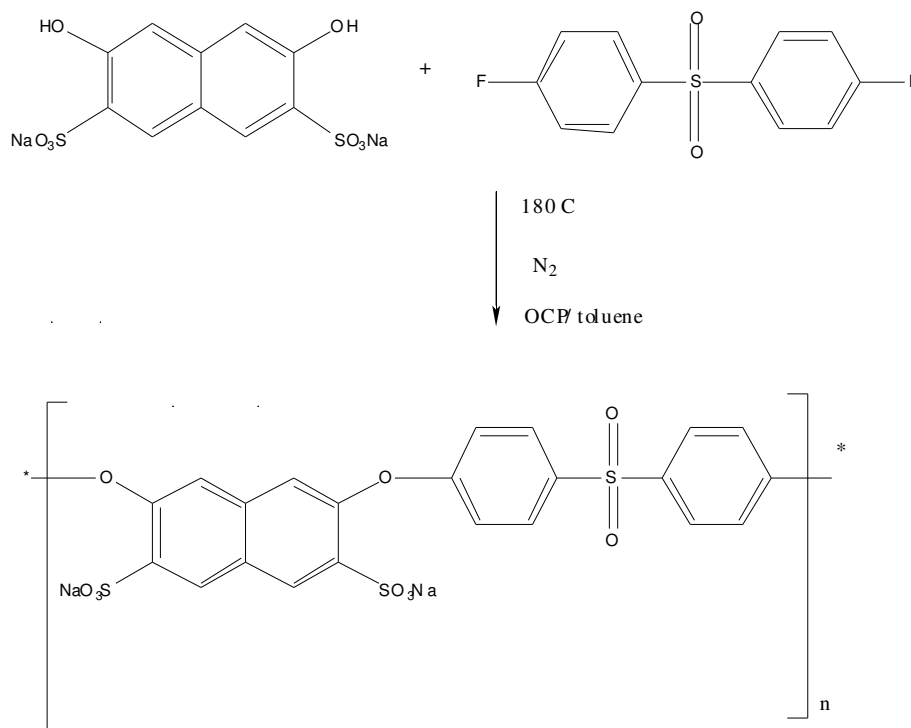


**Figure 66: Sulfonated polysulfone**

Powerful tools like MALDI-MS can be studied better and can be exploited for the present system of polymers. Solvent-free MALDI was performed for low molecular weight PBI; however, MALDI can be used for end group determination as well. The chemical structure and the possible polymers formed from a reaction can be obtained from MALDI. One needs to understand MALDI very well in future that can help better characterization. Also, other characterization methods like NMR and FTIR can be performed in future for novel polymer structure determination and confirmation.

Modeling of the EIS plots can be carried out that will make one understand about the physical behavior of the membranes. This will give not just the proton conductivity data

but also will tell us the electronic circuitry that is associated with the membrane and the interfaces with electrodes.

## References

1. <http://www.nfrcr.uci.edu/EnergyTutorial/pemfc.html>
2. *Fuel cells- Green Power*, information brochure by U.S. Dept. of Energy
3. [http://www.fctec.com/fctec\\_types\\_pem.asp](http://www.fctec.com/fctec_types_pem.asp)
4. <http://en.wikipedia.org/wiki/DMFC>
5. [www1.eere.energy.gov](http://www1.eere.energy.gov)
6. [http://www.fctec.com/fctec\\_types\\_mcfc.asp](http://www.fctec.com/fctec_types_mcfc.asp)
7. Fdkm
8. [www.energi.kemi.dtu.dk/Projekter/fuelcells.aspx](http://www.energi.kemi.dtu.dk/Projekter/fuelcells.aspx)
9. M., Gebert et al., *J. of Fuel Cell Science and Technology*, Vol. 1, pp. 56 – 60, 2004
10. Jansen J.C. et al, *Journal of Membrane Science*, 287 (1), 132, 2007.
11. Li. Q.F et al, *Journal of Membrane Science*, doi:10.1016/j.memsci.2009.10.032
12. [http://www.coleparmer.com/techinfo/images/Zeus\\_Chem\\_Resistance\\_img\\_7.jpg](http://www.coleparmer.com/techinfo/images/Zeus_Chem_Resistance_img_7.jpg)
13. <http://www.solvayadvancedpolymers.com/products>
14. Persson J.C, et al, *Chem mater*, 15, 3044, 2003
15. KreuerK.D, et al, *Chem. Rev.* 2004, 104, 4367
16. Salgado JR, *Electrochimica Acta*, Volume 52, Issue 11, 3766-3778, 2007
17. Viswanathan B et al, *Bulletin of the Catalysis Society of India*, 6, 50, 2007
18. Baglio.V et al, *Journal of Power Sources*, 163, 52, 2006
19. Hara S. et al, *Solic State Ionics*, 168 (1-2), 111, 2004

20. Zhai et al, Journal of membrane Science, 280, 148, 2006
21. Mistry M.K. et al, Chem. Mater. 20, 6857, 2008
22. Zhai.Y. et al, Journal of membrane Science, 169, 2, 259, 2007
23. Mahreni A. et al, Journal of membrane Science, 327, 1-2, 32,2006
24. Herring A.M. Polymer Reviews, 46, 245, 2006
25. Ramani. V. Journal of membrane Science, 232, 31, 2004
26. Limoge R.B. et al, Electrochemical Acta, 50, 5, 1169, 2005
27. Malers, J.L. et al. Journal of Power Sources, 172, 83, 2007
28. A.Noshay et al, Journal of Applied Polymer Science, 20, 1885, 1976
29. Pinto. B.P, et al, Material Letters, 61, 2540, 2007
30. Guan R. et al, European Journal of Polymer Science, 41, 1554 2005
31. Linkous C.A., et al, Int. J. Hydrogen Energy, 23 (7), 525, 1998
32. R Nolte, et al, Journal of Membrane Science, 83, 221, 1993
33. A. Dyck et al, Journal of Applied Polymer Science, 86, 2820, 2002
34. Yamada M, Polymer, 46, 2986, 2005
35. Daletou M.K. et al, Journal of membrane Science, 252, 115, 2005
36. Gourdoupi. N. et al, Chem. Mater., 15 ( 26), 5044, 2003
37. Wang. F. et al, Macromolecules Symposium, 175, 387, 2001
38. Yoshida. S. et al, Macromolecules, 30, 2254, 1997
39. Oh, Y-S. et al, Journal of Membrane Science, 323, 309, 2004.
40. <http://www.colby.edu/chemistry/PChem/lab/DiffScanningCal.pdf>
41. Guan, R., et al, European Polymer Journal, 41, 7, 1554, 2005.

42. B. P. Pinto et al, Materials letters, 2540, (2007).
43. Joko S. Masters' Thesis, UNR, March 2008.
44. Bowen. W.R et al, Journal of Membrane Science, 181 (2), 253, 2001.
45. Odian, G, Principles of polymerization, Wiley- Interscience, c2004.
46. Pasch, H, et al, MALDI-TOF mass spectrometry of synthetic polymers, Springer, c 2003.
47. [www.bekktech.com](http://www.bekktech.com)
48. [http://www.gamry.com/App\\_Notes/EIS\\_Primer/EIS\\_Primer.htm#Impedance%20Definition](http://www.gamry.com/App_Notes/EIS_Primer/EIS_Primer.htm#Impedance%20Definition)
49. [www.wikipedia.com/Gelpermeationchromatography/](http://www.wikipedia.com/Gelpermeationchromatography/)
50. <http://www.ultrac.com/en/methods/analysis/tga.php>
51. [http://www.princetonappliedresearch.com/products/markets/fuel\\_cell.cfm](http://www.princetonappliedresearch.com/products/markets/fuel_cell.cfm)

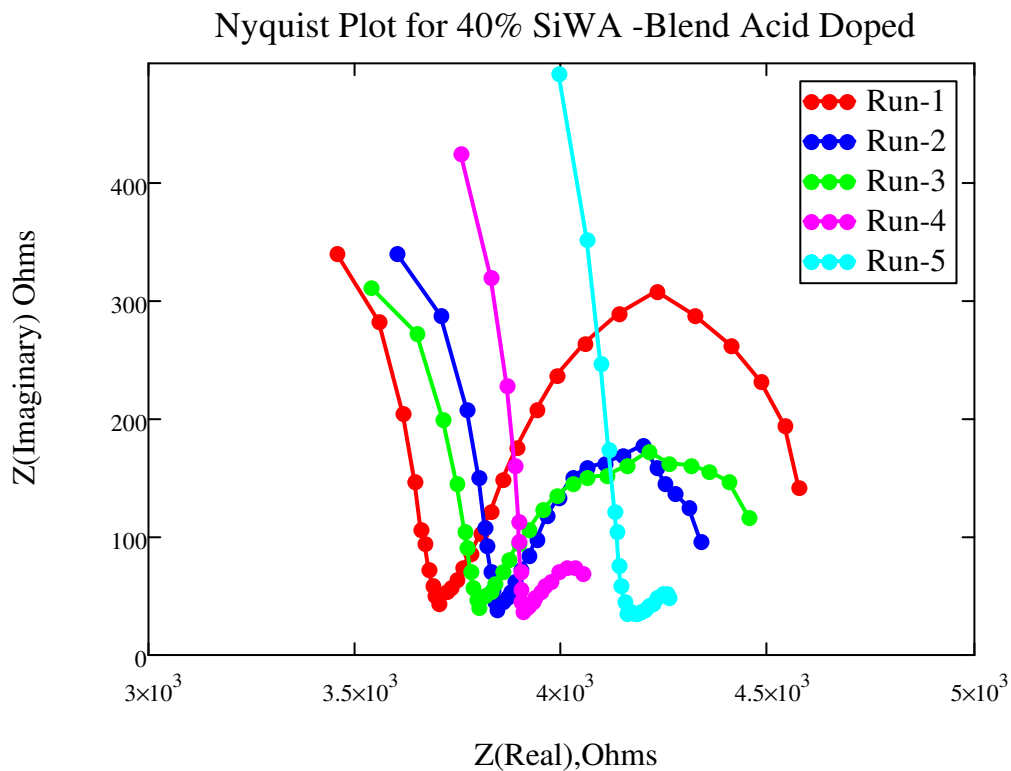
## APPENDIX

### A-1

#### **Random Error Analysis:**

Error analysis was carried out for two membrane values obtained from EIS plots. Nyquist plots were drawn and the minimum value of the imaginary impedance was chosen to calculate for calculation of conductivity. One error analysis is shown in this appendix. This is a 30 wt % SiWA – PBI- PES blend membrane that was acid doped. The runs that were carried out were performed under 100% relative humidity (RH) at room temperature.

The plots are shown in Figure below:



The minimum imaginary values (impedance) are given by:

$$\text{Img\_values} := \begin{pmatrix} 44.319 \\ 38.231 \\ 40.933 \\ 37.314 \\ 35.264 \end{pmatrix}$$

The corresponding real resistance values from the plot are given by:



$$\text{real\_values} := \begin{pmatrix} 3.703 \times 10^3 \\ 3.843 \times 10^3 \\ 3.8 \times 10^3 \\ 3.904 \times 10^3 \\ 4.155 \times 10^3 \end{pmatrix}$$

The standard deviation is given by:

$$\sigma_x = \sqrt{\frac{\sum_{k=1}^N (x_k - x_{\text{mean}})^2}{N \cdot (N - 1)}}$$

The standard error for the values is given by:

$$\text{std\_err} = \frac{\sqrt{\frac{\sum_{k=1}^N (x_k - x_{\text{mean}})^2}{N \cdot (N - 1)}}}{\sqrt{N}}$$

The percent error is calculated by:

$$\varepsilon = \frac{\sigma_x}{x_{\text{mean}}} \cdot 100$$

<b>Mean (ohms)</b>	<b>3.881 x 10<sup>3</sup></b>
<b>Standard deviation (ohms)</b>	169.775
<b>Standard error (ohms)</b>	75.926

<b>Percentage error (%)</b>	4.37 %
-----------------------------	--------

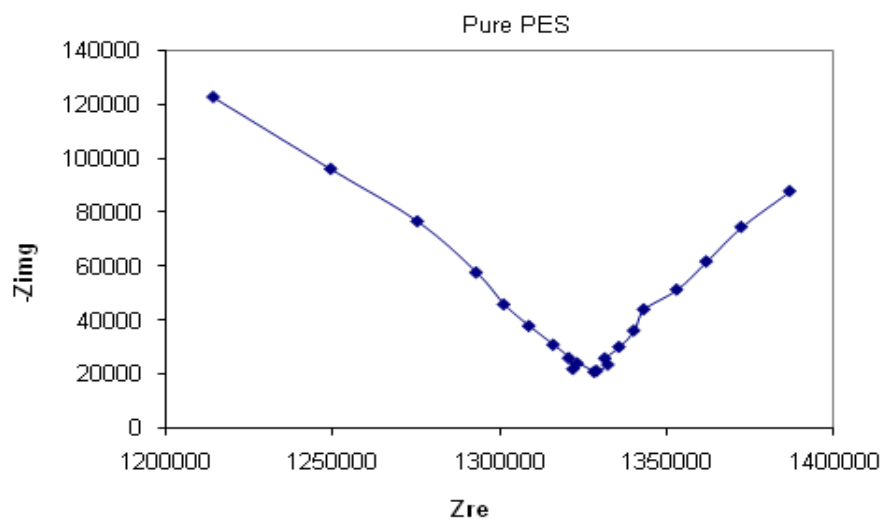
The reason for this error can be justified by the fact that the membrane that was used was acid doped. The acid would leave the membrane in the presence of water since it is only superficially attached to the membrane. Same will be the case when error is measured for a composite membrane with HPA and polymer. HPAs are expected to leave the polymer system and dissolve in water. Homogeneity of the membrane can be improved to reduce the error. The HPA particles have to be more homogeneously distributed over the membrane.

## APPENDIX

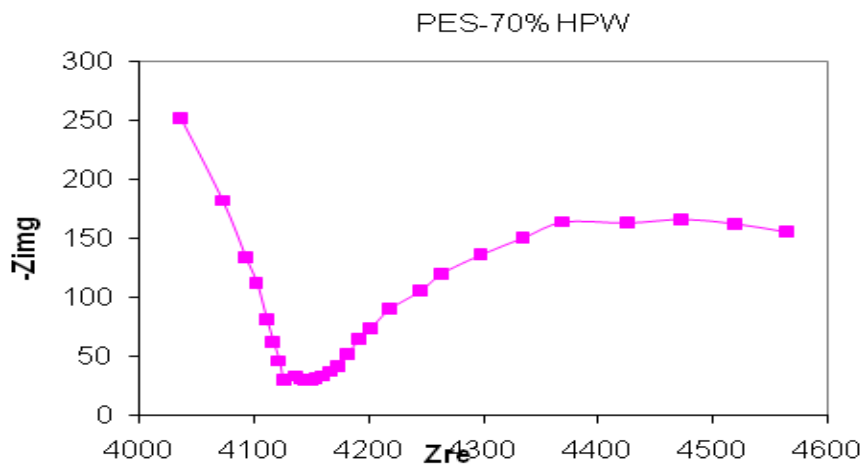
### A-2

#### Additional EIS plots

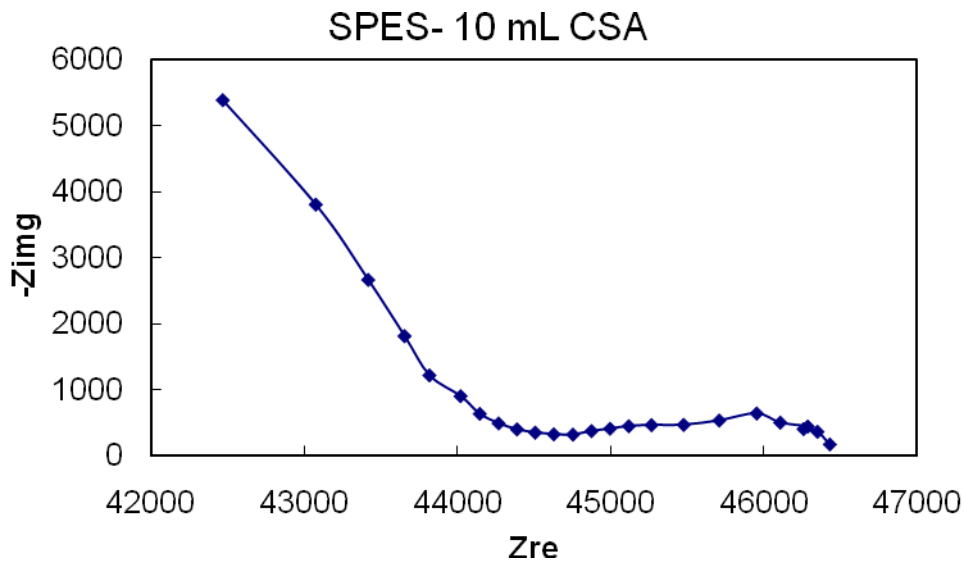
##### 1. Nyquist plot of pure PES



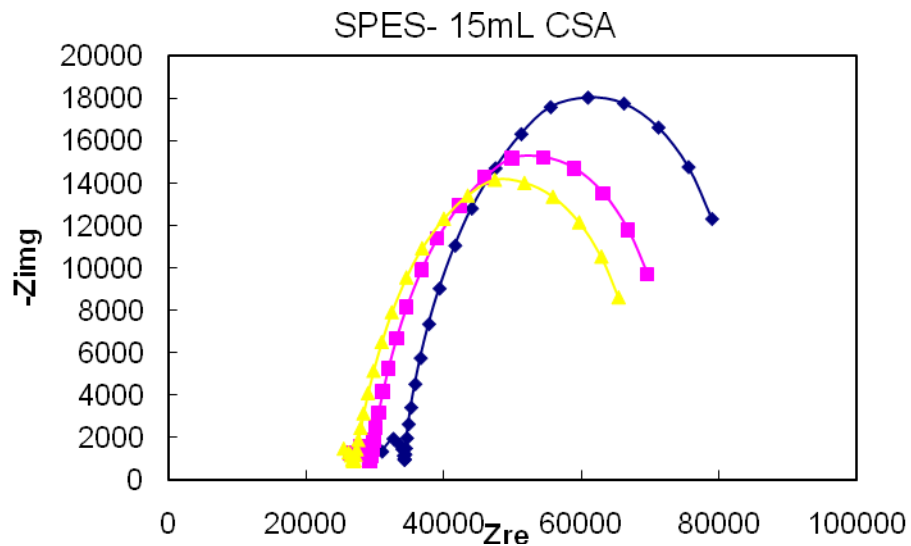
##### 2. Nyquist plot of PES- 70% HPW



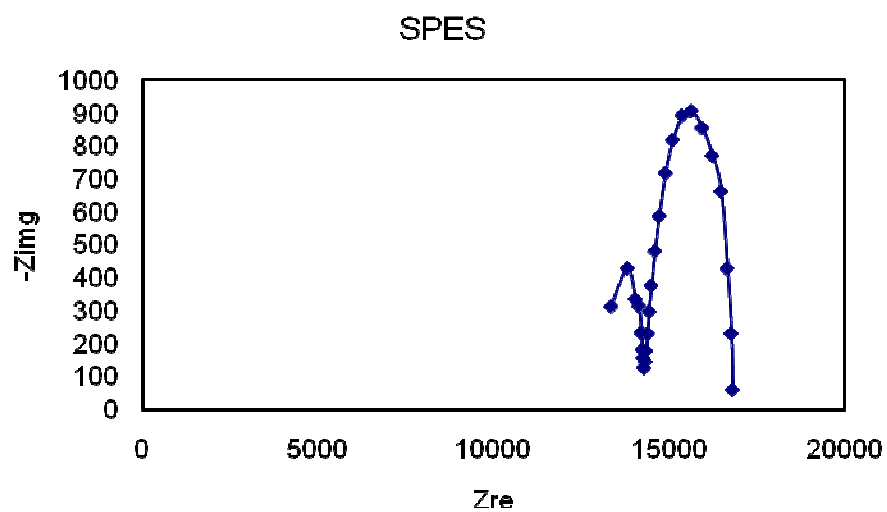
### 3. Nyquist plot of SPES (sulfonated by 10mL of CSA)



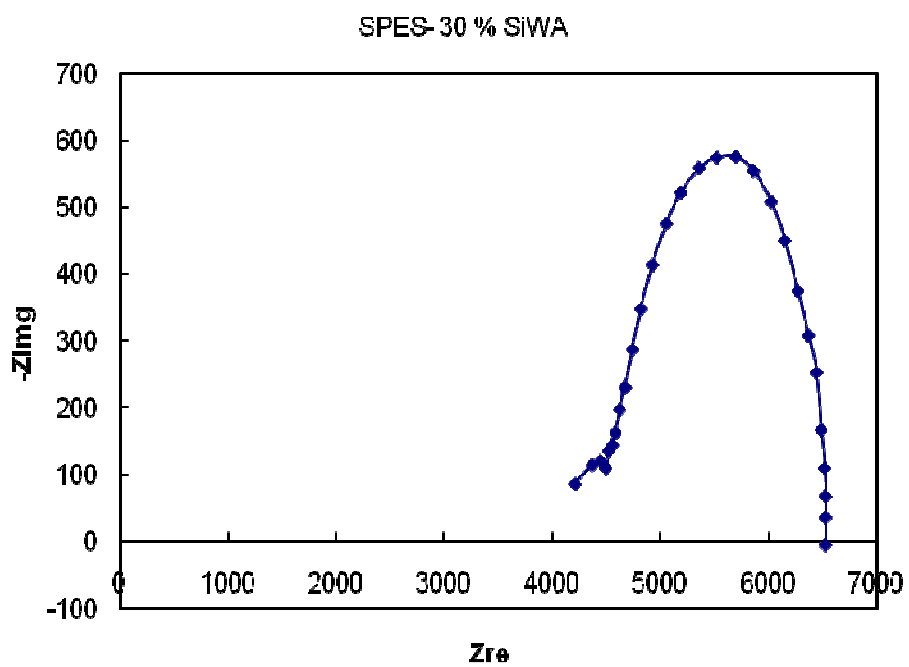
### 4. Nyquist plot of SPES (sulfonated by 15mL CSA)



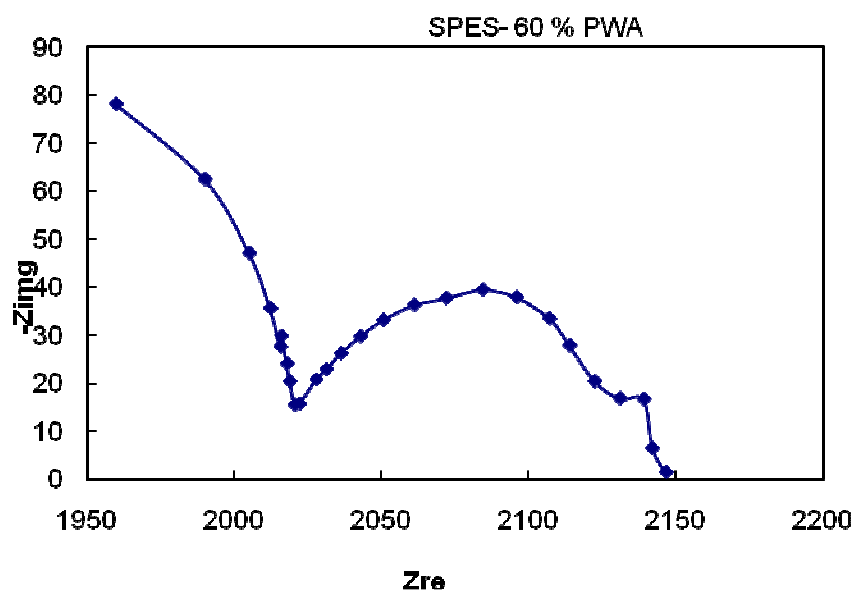
### 5. Nyquist plot of SPES ( IEC – 0.95meq/gm)



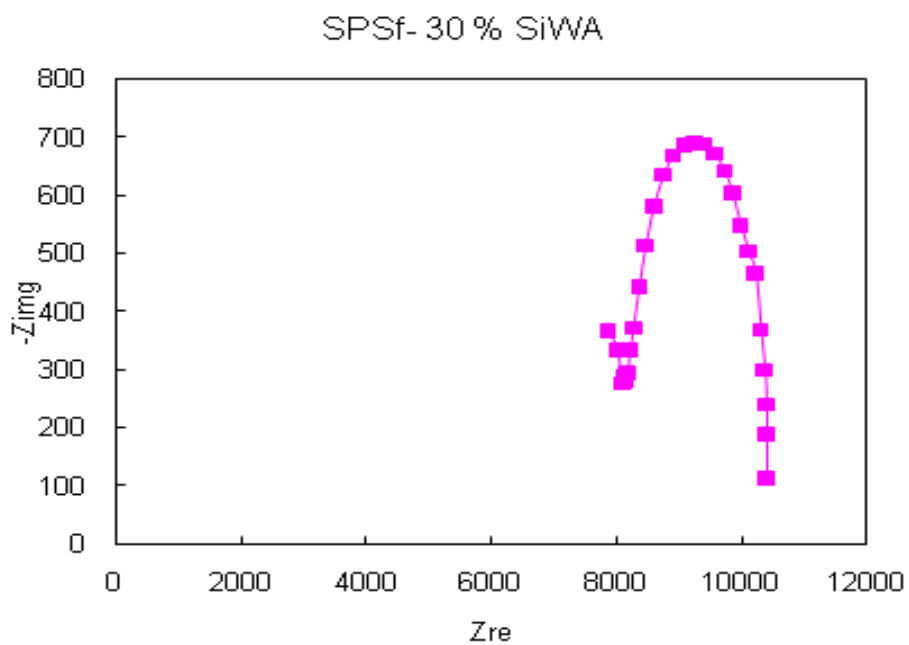
### 6. Nyquist plot of SPES- 30 % SiWA



### 7. Nyquist plot of SPES – 60 % HPW



### 8. Nyquist plot of SPSf- 30% SiWA



**9. Nyquist plot of 40% HSiW- PBI- PES – acid doped**